EDGEWOOD CHEMICAL BIOLOGICAL CENTER
U.S. ARMY RESEARCH, DEVELOPMENT AND ENGINEERING COMMAND
Aberdeen Proving Ground, MD 21010-5424

ECBC-TR-1177

# METABOLOMIC ANALYSIS OF THE SECRETOME OF HUMAN EMBRYONIC STEM CELLS FOLLOWING METHYL PARATHION AND METHYL PARAOXON EXPOSURE, PHASE I: INITIAL NONTARGETED LC-MS

**Jennifer W. Sekowski**
**Vicky L. H. Bevilacqua**
**Janna S. Madren-Whalley**

**RESEARCH AND TECHNOLOGY DIRECTORATE**

**Jessica A. Palmer**
**Elizabeth L. R. Donley**
**Robert E. Burrier**

**STEMINA BIOMARKER DISCOVERY, INC.**
**Madison, WI 53719-1256**

**January 2014**

Disclaimer

The findings in this report are not to be construed as an official Department of the Army position unless so designated by other authorizing documents.

# REPORT DOCUMENTATION PAGE

*Form Approved*
*OMB No. 0704-0188*



| **1. REPORT DATE** *(DD-MM-YYYY)* | **2. REPORT TYPE** | **3. DATES COVERED** *(From - To)* |
|---|---|---|
| XX-01-2014 | Final | Oct 2010–Sept 2011 |

**4. TITLE AND SUBTITLE**
Metabolomic Analysis of the Secretome of Human Embryonic Stem Cells Following Methyl Parathion and Methyl Paraoxon Exposure, Phase I: Initial Nontargeted LC-MS

**5a. CONTRACT NUMBER:**

**5b. GRANT NUMBER**

**5c. PROGRAM ELEMENT NUMBER**

**6. AUTHOR(S):**
Sekowski, Jennifer W.; Bevilacqua, Vicky L. H.; Madren-Whalley, Janna S. (ECBC); Palmer, Jessica A.; Donley, Elizabeth L. R.; Burrier, Robert E. (Stemina)

**5d. PROJECT NUMBER**

**5e. TASK NUMBER**

**5f. WORK UNIT NUMBER**

**7. PERFORMING ORGANIZATION NAME(S) AND ADDRESS(ES)**
Director, ECBC, ATTN: RDCB-DRB, APG, MD 21010-5424
Stemina Biomarker Discovery, Inc., 504 South Rosa Road, Suite 150, Madison, WI 53719-1256

**8. PERFORMING ORGANIZATION REPORT NUMBER**
ECBC-TR-1177

**9. SPONSORING / MONITORING AGENCY NAME(S) AND ADDRESS(ES)**
U.S. Army Edgewood Biological Chemical Center, In-House Laboratory Independent Research Program, Aberdeen Proving Ground, MD 21010-5424

**10. SPONSOR/MONITOR'S ACRONYM(S)**
ECBC ILIR

**11. SPONSOR/MONITOR'S REPORT NUMBER(S)**

**12. DISTRIBUTION / AVAILABILITY STATEMENT**
Approved for public release; distribution is unlimited.

**13. SUPPLEMENTARY NOTES**

**14. ABSTRACT:**
Current literature suggests diverse toxicological consequences for methyl parathion (MP) and its active metabolite, methyl paraoxon (MPO) exposure. These studies, however, have been based on either human epidemiological studies, in vivo animal studies, or in vitro studies using immortal cell lines. Currently, there remains no definitive connection to the molecular events that occur during MP and MPO exposure in normal human cells. Furthermore, chemicals that have certain known effects in adults can have dramatically different toxic effects during embryonic and prenatal development. Since undifferentiated human embryonic stem cells (hESC) maintain the ability to differentiate into any somatic cell in the body, they provide a unique window into the influence of toxicants on the entire early human development. The purpose of this study was to perform initial nontargeted metabolomic analysis on hESC exposed to MP and MPO to identify human metabolites and metabolic pathways which are perturbed following exposure to these chemicals. From this study, two main conclusions were reached: (1) hESC are not able to metabolize MP into MPO, and (2) MPO is much more disruptive to key developmental metabolic pathways at physiologically relevant concentrations than is MP.

**15. SUBJECT TERMS**
Human embryonic stem cells; Methyl parathion; LC-MS; Metabolomics; Methyl paraoxon

| **16. SECURITY CLASSIFICATION OF:** | | | **17. LIMITATION OF ABSTRACT** | **18. NUMBER OF PAGES** | **19a. NAME OF RESPONSIBLE PERSON** |
|---|---|---|---|---|---|
| **a. REPORT** | **b. ABSTRACT** | **c. THIS PAGE** | | | Renu B. Rastogi |
| U | U | U | U | 90 | **19b. TELEPHONE NUMBER** *(include area code)* (410) 436-7545 |

Blank

# PREFACE

The work described in this report was authorized under a U.S. Army Edgewood Chemical Biological Center (ECBC) In-House Laboratory Independent Research (ILIR) program during the 2011 fiscal year. The work was started in October 2010 and completed in September 2011.

The use of either trade or manufacturers' names in this report does not constitute an official endorsement of any commercial products. This report may not be cited for purposes of advertisement.

This report has been approved for public release.


## Acknowledgments

The authors acknowledge the following individuals for their hard work and assistance with the execution of this technical program:

- Way Fountain (ECBC) and Laura Borland (Booz Allen Hamilton, Belcamp, MD) for their support of this project under the ILIR program.
- Kelley Betts (Science Applications International Corporation, McLean, VA) for technical assistance in the preparation of this manuscript.

Blank

CONTENTS

FIGURES



TABLES

# METABOLOMIC ANALYSIS OF THE SECRETOME OF HUMAN EMBRYONIC STEM CELLS FOLLOWING METHYL PARATHION AND METHYL PARAOXON EXPOSURE, PHASE I: INITIAL NONTARGETED LC-MS

## 1. INTRODUCTION

This technical report is the first of three reports from the U.S. Army Edgewood Chemical Biological Center (ECBC) In-House Laboratory Independent Research (ILIR) "Molecular Toxicology of TICs in Human Embryonic Stem Cells". The aim of the study was to provide a better understanding of the basic biological and toxicological mechanisms in human embryonic human cells (hESC) exposed to an organophosphate toxic industrial chemical (TIC). This work has broad implications on many Army goals from developing better toxicant screening tools, including organ-on-a-chip type applications, as well as medical applications including regenerative medicine applications and stem cell based therapies. It also supports U.S. Army Training and Doctrine Command (TRADOC) Pamphlet (Pam) 525-66 (March 08) *Maneuver Sustainment,* Force Operating Capabilities (FOC)-09-07 – "Casualty Prevention", which states the importance of protecting the warfighter from TICs and toxic industrial materials (TIMs) in general.

Chemicals that have certain known effects in adults can have dramatically different toxic effects during embryonic and prenatal development. For example, the successful adult anti-epileptic drug, valproate, has a dramatic toxic effect on embryonic development, leading to neural tube deficits, autism, and cognitive dysfunction. In their 2007 study, Cezar et al. used liquid chromatography-mass spectrometry (LC-MS) to examine the metabolites in spent medium from pluripotent hESC exposed to valproate and found a blockage of the serotonin production pathway. Therefore, an important part of any complete toxicological evaluation must include examination of the compound's effect on human embryonic development. The use of hESC to explore human embryonic molecular toxicological endpoints is a promising development in the field of toxicology. Since pluripotent hESC contain the ability to differentiate into any somatic cell in the body, they provide a unique window into the influence of toxicants on the entire early human development process.

To address the aim of this study, we used a nontargeted LC-MS metabolomic analysis of the secretome of hESC dosed with methyl parathion (MP) and methyl paraoxon (MPO), the active metabolite of MP. In the course of this work, we also confirmed that hESC are not able to convert parathion to paraoxon, thus in order to understand the effect of both the parent compound and its metabolite, the testing of both compounds was necessary. This nontargeted LC-MS approach was able to identify human metabolites and metabolic pathways that were altered as a result of exposure to both chemicals that would be present in vivo.

Overall, MP and MPO were shown to have significant impact on hESC metabolism. Using LC-MS, hundreds of significantly enriched metabolites were identified. These metabolites participate in 13 human metabolic pathways. Although both compounds were suspected to be toxic in human development, these results demonstrate for the first time that MPO, at all physiologically relevant concentrations tested, disrupts specific metabolic pathways in human embryonic development to a much greater degree than does MP. The identity and degree of alteration of these metabolites may equate to potential developmental toxicity in humans.

## 2. METHODS

### 2.1 Cell Viability and Dosing Curves

The general aim of this study was to evaluate the metabolome of hESC exposed to chemicals at physiologically relevant concentrations to which a developing fetus may potentially be exposed. Additionally, doses were chosen which were not likely to reflect metabolic or biochemical injury resulting from cytotoxicity or cell death. Cell viability assays were performed to establish the three concentrations of MP with which to expose the hESC.

Briefly, the WA09 hESC (Wi-Cell Institute, Madison, WI) were plated in 96-well format cell culture plates at a density of 250,000 cells/well and dosed with eight concentrations of MP (0.01, 0.1, 0.5, 1, 10, 50, 100, 200 μM, Appendix A) dissolved in dimethylsulfoxide (DMSO, Figure 1A). These doses were chosen after a literature review of in vitro experiments on MP covering the dose range used in those experiments. Since no dose response was observed in the first set of doses, a second dose curve experiment was performed using higher dose levels. In the second dose curve experiment, the hESC were treated with eight concentrations of MP, from 0-1000 μM (Figure 1B). After 72 h of chemical exposure, cell viability measurements were taken using the MultiTox-Fluor cell based assay (Promega, Madison, WI) and the number of cells/well was determined. Concentration curves were calculated from both experiments to determine the three concentrations which would be used for the metabolomics analysis.

Experiments were also conducted to determine if hESC were metabolizing MP into its active metabolite, MPO. To determine if hESC cells were metabolizing MP to MPO, hESC were treated with eight concentrations (0-500 μM) of MPO and the response was assessed. Following 72 h of chemical exposure, viability was measured using the MultiTox-Fluor cell viability assay and the cells were counted to determine the number of cells/well remaining following treatment.

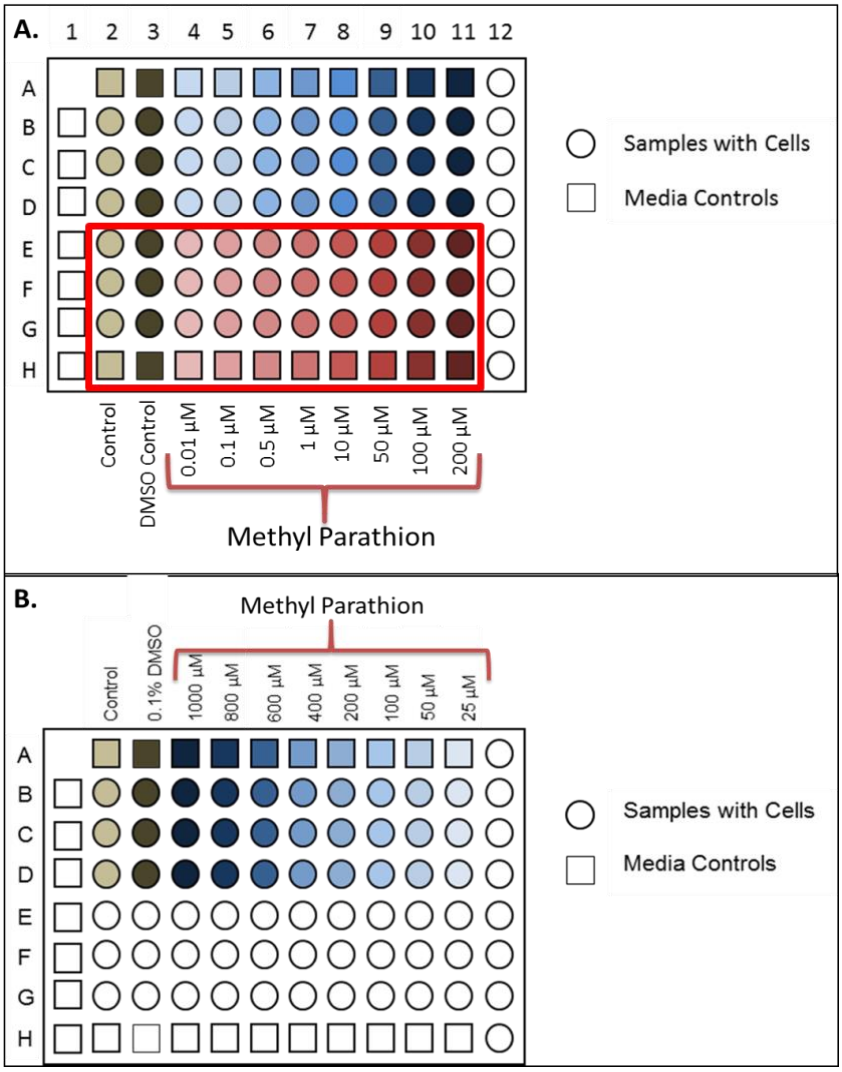


Figure 1. Plate outline for MP dose curve experiments.

## 2.2 Cell Culture for Metabolomic Analysis

For metabolomic analysis, the hESC were dosed at the three concentrations for each chemical based on the cell viability data. Media controls (no cells), dosed media controls (no cells with dosed media), and controls (cells with undosed media) were also included in the experimental design (Figure 2). Additionally, a positive control (i.e, valproate, VPA) and a negative control (i.e., penicillin G) were included on the plate (Figure 2).

In both the viability and metabolomics steps, 96-well plates were seeded with 250,000 cells/well of WA09 hESC. These cells were exposed to each chemical for three days. Each day the spent media was removed and replaced with mTeSR1 media (Stem Cell Technologies, Vancouver, BC) containing the designated compound. Each compound stock solution was made in DMSO and each final solution used to dose hESC contained 0.1% (v/v) DMSO. Spent media samples were collected on the fourth day and quenched with 40% (v/v) acetonitrile. Quenched

samples were stored at –80 °C until they were prepared for metabolomic analysis. Viability was measured after sample collection using the MultiTox-Fluor viability assay.

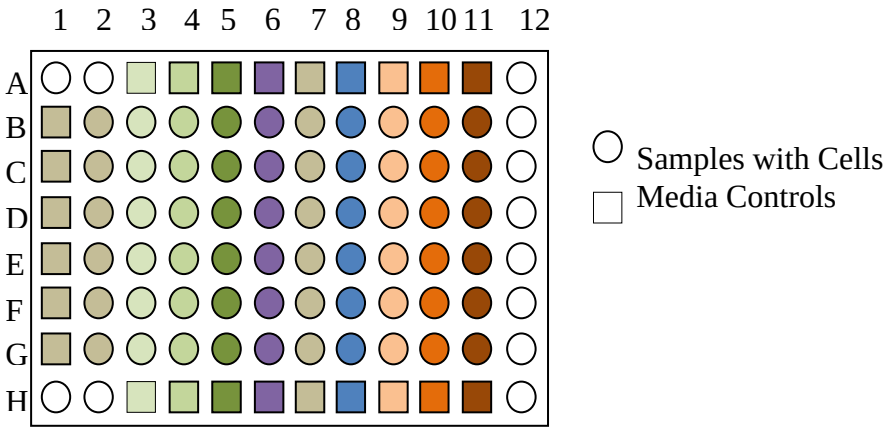


| Symbol | Samples | Sample Name |
|---|---|---|
| | Media Controls | ST010C-57-D112-1B - 1G |
| | Controls | ST010C-57-D112-2B - 2G |
| | 1 µM methyl parathion dosed media control | ST010C-57-D112-3A/3H |
| | 1 µM methyl parathion | ST010C-57-D112-3B - 3G |
| | 50 µM methyl parathion dosed media control | ST010C-57-D112-4A/4H |
| | 50 µM methyl parathion | ST010C-57-D112-4B - 4G |
| | 500 µM methyl parathion dosed media control | ST010C-57-D112-5A/5H |
| | 500 µM methyl parathion | ST010C-57-D112-5B - 5G |
| | 1 mM VPA dosed media control | ST010C-57-D112-6A/6H |
| | 1 mM VPA (166 µg/mL) | ST010C-57-D112-6B - 6G |
| | penicillin G dosed media control | ST010C-57-D112-8A/8H |
| | penicillin G (17 µg/mL) | ST010C-57-D112-8B - 8G |
| | 72 µM methyl paraoxon dosed media control | ST010C-57-D112-9A/9H |
| | 72 µM methyl paraoxon | ST010C-57-D112-9B - 9G |
| | 130 µM methyl paraoxon dosed media control | ST010C-57-D112-10A/10H |
| | 130 µM methyl paraoxon | ST010C-57-D112-10B - 10G |
| | 180 µM methyl paraoxon dosed media control | ST010C-57-D112-11A/11H |
| | 180 µM methyl paraoxon | ST010C-57-D112-11B - 11G |

Figure 2. Plate outline for metabolomics analysis of MP and MPO.

## 2.3 Sample Preparation

### 2.3.1 Data File Creation

Agilent raw data files were converted to the open source mzData file format using Agilent (Santa Clara, CA) MassHunter Qualitative software version 3.0. During the conversion process, deisotoping (+1 charge state only) was performed on the centroid data and peaks with an absolute height less than 400 (approximately double the typical average instrument background level). The resulting mzData files contain centroid data of deisotoped (+1 charge state only) peaks that have an absolute height greater than 400 counts.

### 2.3.2 Mass Feature Creation and Integration

Peak picking and feature creation were performed using the open source software library XCMS. Mass features (peaks) were detected using the centWave algorithm. Following peak picking, deviations in retention times were corrected using the obiwarp algorithm that is based on a nonlinear clustering approach to align LC-MS samples. Mass feature bins or groups were generated using a density based grouping algorithm. After the data had been grouped into mass features, missing features were integrated based on retention time and mass range of a feature bin using iterative peak filling. Feature intensity is based on the Mexican hat integration values of the feature extracted ion chromatograms.

### 2.3.3 Adduct and Higher Charge State Isotope Filter

This algorithm evaluates feature groups and calculates the probability that related features are due to common adducts or isotopes using a correlation based method. The abundance levels for the related features are summed and the redundant features are removed from the XCMS dataset. Features that are the result of the combining isotopes and adducts contain an "_A" or "_I" in the feature identification (ID).

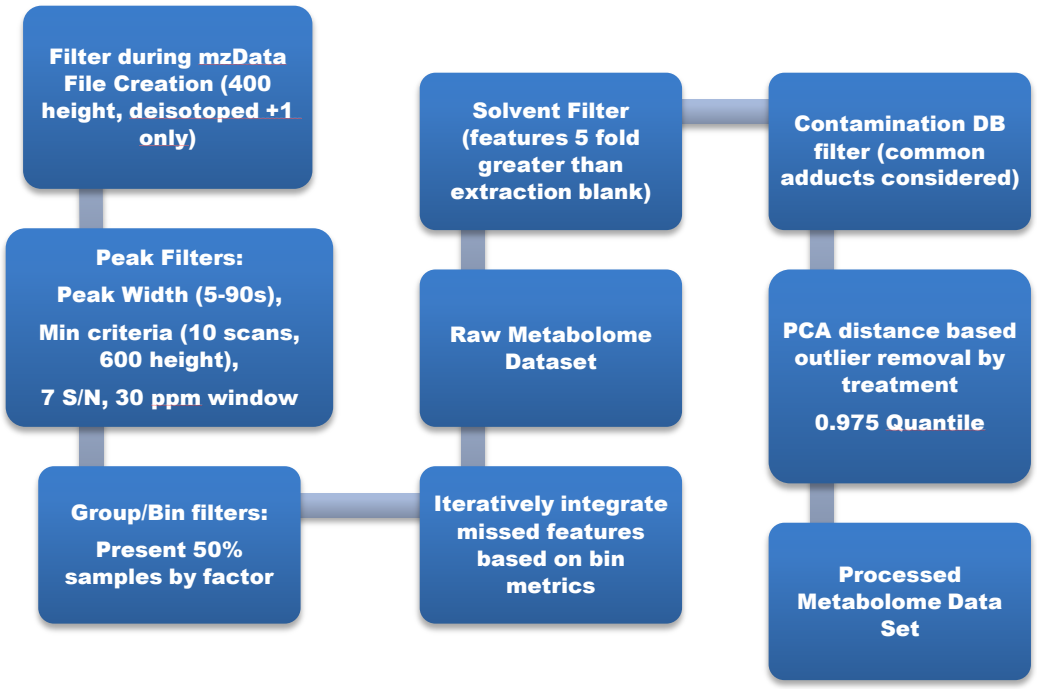


Figure 3. Flow chart for metabolomics analysis of MP and MPO.
PCA, principal component analysis

### 2.3.4 Mass Defect Filter

The mass defect filter combines both linear and polygon based filters to exclude or include mass features. The filter was trained using all of the chemical formulas in the Stemina MetDB (Stemina Biomarker Discovery, Inc., Madison, WI) and creates a conservative filter that

allows many endogenous metabolites, peptides, drugs, and drug metabolites through while removing features of unlikely biological origin.

### 2.3.5 Solvent/Extraction Blank Filter

The extraction blank filter removes ions associated with the sample extraction process and background ions present in the LC-MS system. Features were removed from the metabolomics dataset if the average in the experimental samples was less than five times the average abundance in the extraction blanks.

### 2.3.6 Contamination DB Filter

The contamination DB filter removes features with a mass match within 20 ppm to entries in Stemina's proprietary database which contains a number of contaminants such as plasticizers and polyethylene glycol (PEG), compounds identified in previous studies. Features are removed without respect to retention time if they match a contaminant or a common charge specific adduct of a contaminant.

## 2.4 Statistical Analysis and Identification of Differential Features

### 2.4.1 Abundance and Reproducibility Filter

Prior to statistical analysis, features were filtered by factor (e.g., experimental compound by dose) to remove features that did not exhibit abundance greater than 20,000 in 65% of the LC-MS runs for at least one dose level (e.g., low, medium, or high) of at least one experimental compound (e.g., MP or MPO). This filter selects against spurious low abundance features at the level of detection that are not reproducibly measured, and features that may not have peak shapes amenable to reproducible detection and/or integration. This filter typically removes a large portion of the metabolomics dataset, and focuses the analysis on the most reliable and valuable features. For example, a feature with abundance values greater than 20,000 in 70% of the negative mode LC-MS samples in one dose level of one experimental compound and abundance values greater than 20,000 in none of the other experimental compound by dose combinations would pass the filter because at least one experimental compound by dose factor satisfies the filter criteria. An overview of the MS feature filter process is outlined below in Figure 4.

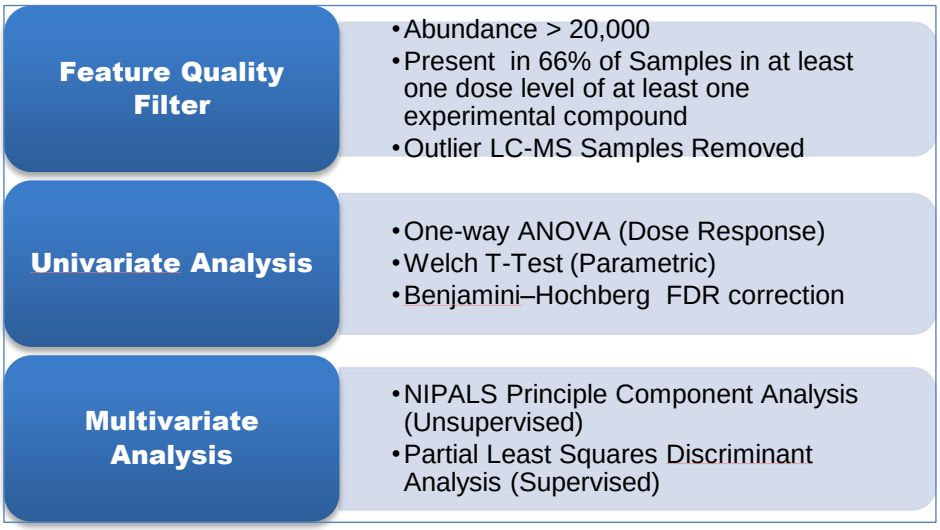


Figure 4. Overview of statistical analysis process.
ANOVA, analysis of variance
FDR, false discovery rates
NIPALS, non-linear iterative partial least squares

### 2.4.2 Data Transformation and Normalization

All data was log base two transformed. Normalization for each factor level was performed by subtracting the column (sample) mean and dividing by the row (feature) standard deviation for each value (autoscaling).

### 2.4.3 Differential Analysis of Mass Features (Univariate)

Mass features were evaluated under the null hypothesis that no difference is present between the means of experimental classes and the alternative hypothesis that there is a difference between experimental classes. Welch two sample T-tests were performed as a parametric method that does not assume equal variances of the experimental classes. False discovery rates were controlled for multiple testing using the Benjamini–Hochberg (1995) method of p-value correction of the ANOVA and Welch T-tests.

### 2.4.4 Analysis of Mass Features (Multivariate)

Multivariate (or chemometric) analysis is the application of statistical/machine learning procedures to identify a group of features that have valuable experimental information. These methods differ from univariate methods in that they consider the importance of a given feature with respect to all of the mass features present in the experimental comparison. This information is typically displayed graphically by separation of groups, but the measure of a given feature's importance to the separation of the experimental classes in multivariate space is evaluated by ranking a feature's contribution. Two different multivariate methods were applied to the data to evaluate the importance of features: a supervised method and an unsupervised method by dose and experimental compound. NIPALS PCA was the unsupervised method used to evaluate the contribution of a feature by ranking the loadings values of features over three principle components. The supervised linear classifier method partial least squares-discriminant analysis (PLS-DA) was

used to rank the importance of features based on their ability to discern experimental classes. The PLS-DA scored mass features based on the variable importance in projection (VIP) scores.

### 2.4.5 Identification of Mass Features

Annotation of mass features was carried out by comparing the m/z mass values of the mass features to Stemina's internal metabolite database containing records from multiple public databases such as human metabolome data base (HMDB), Kyoto Encyclopedia of Genes and Genomes (KEGG), PubChem Compound, and metabolomics database resource (METLIN) and company-specific metabolite data. The features were annotated with respect to the appropriate adducts for each electrospray ionization (ESI) mode. The identities of all mass features were not validated, and therefore all annotations are putative.

### 2.4.6 Pathways Analysis

Pathway enrichment analysis was performed by mapping annotated mass features for each experimental compound to human metabolic pathways using KEGG compound identities. Hyper geometric p-values and FDR were used to assign a quantitative measure of statistical significance to each pathway. Features derived from ESI negative and positive mode for each experimental compound were pooled for this analysis. False positive results can be generated by isobaric compounds that generate multiple "hits" in a pathway from the same mass, so unique masses instead of unique compound identities were used for these calculations. The relevant parameters used to calculate hypergeometric p-values for each pathway were: (1) the number of unique mass "hits", (2) the number of unique masses in the pathway, and (3) the total number of unique masses in all of the human pathways in the KEGG database. For each experimental compound, the p-values for the derived pathways were converted to FDR using the Benjamini and Hochberg (1995) correction.

### 2.4.7 Selection of Interesting Features

Feature selection was performed on a chemical by dose basis using Welch T-tests and fold changes. Features were selected for further evaluation if they had a Welch FDR <0.05 with at least a 75% fold change. If a feature was selected as interesting in a dose level comparison it was then evaluated experiment wide for fold changes. Following feature selection, only significant features putatively annotated as human in origin and present on KEGG pathway diagrams were further evaluated. Pathway enrichment analysis was then performed on the selected features and features in pathways exhibiting a statistically significant enrichment were further evaluated for fold changes. These selection criteria focused the analysis on biochemical pathways.

## 3. RESULTS AND DISCUSSION

### 3.1 Dose Response Curves

After chemical exposure, cell number and viability were determined. The Multitox-Fluor assay was used to determine the viability and cytotoxicity present after treating the cells for 72 h with MP or MPO. The relative fluorescence units (RFU) for viability (live cell protease) are normalized to the 0.1% DMSO control readout by dividing the viability RFU of each well by the

average 0.1% DMSO viability RFU. To determine the average number of cells/well, the three wells for each treatment were trypsinized and pooled. An aliquot was taken from this sample and added to trypan blue to determine the number of viable cells/well. Cell counts were performed on each treatment sample using an automated cell counter (Cellometer Auto T4, Nexcelom Bioscience, Lawrence, MA).

Treatment of hESC with 0-200 µM MP did not identify a decrease in cell viability or cell number (Figure 5). In the next set of experiments, hESC were treated with 0-1000 µM MP (Figure 6). A decrease in cell viability was seen at starting at 100 µM. The data from these two experiments were combined to determine the effective concentrations ($EC_{30}$, $EC_{10}$ and $EC_0$) to be used for the metabolomics experiments (Table 1).

Table 1. Summary of Doses Chosen for LC-MS Evaluation

| Response | Methyl Parathion (µM) | Methyl Paraoxon (µM) |
|---|---|---|
| **$EC_{30}$** | 500 | 180 |
| **$EC_{10}$** | 50 | 130 |
| **$EC_0$** | 1 | 72 |

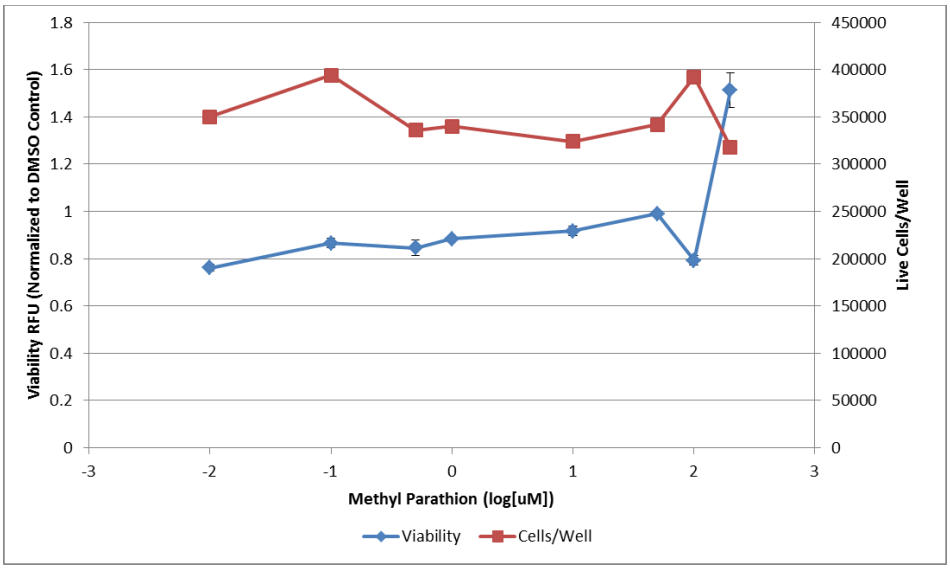


Figure 5. Viability and number of cells/well of hESC following 72 h of exposure to 0-200 µM MP.

In the third set of viability experiments, hESC were treated with MPO, the active metabolite of MP. As expected, MPO was found to be more cytotoxic than its parent compound (Figure 7). A sharp decrease in cell viability was seen between 125 and 250 µM. Very few

(~14000) cells survived treatment with 500 µM MPO. These results suggest that hESC do not efficiently metabolize MP into its active metabolite.

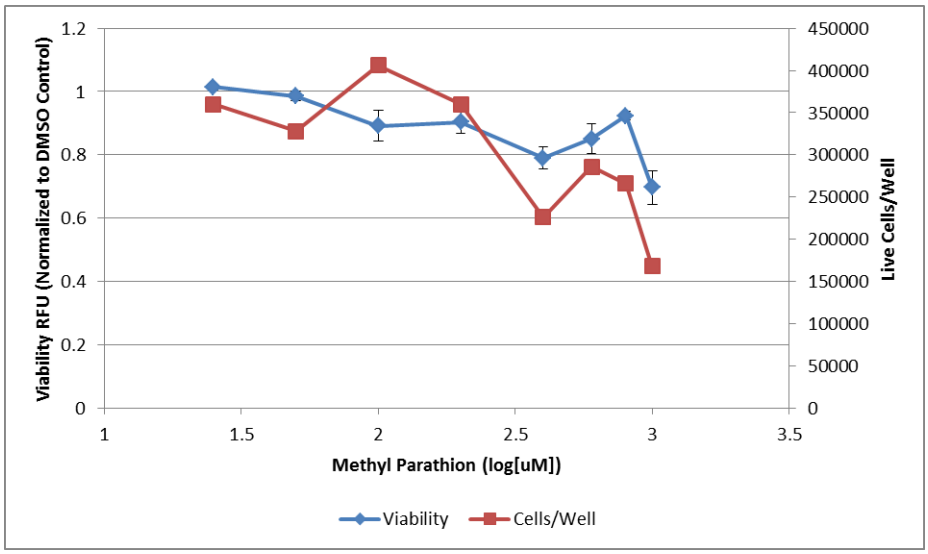


Figure 6. Viability and number of cells/well of hESC following 72 h of exposure to 0–1000 µM MP.

After treatment with the $EC_{30}$, $EC_{10}$ and $EC_0$ of each compound, viability was measured using the MultiTox-Fluor assay. A decrease in hESC viability was seen following MPO treatment, but not MP treatment (Figure 8). This is consistent with the results seen in the previous viability assays.

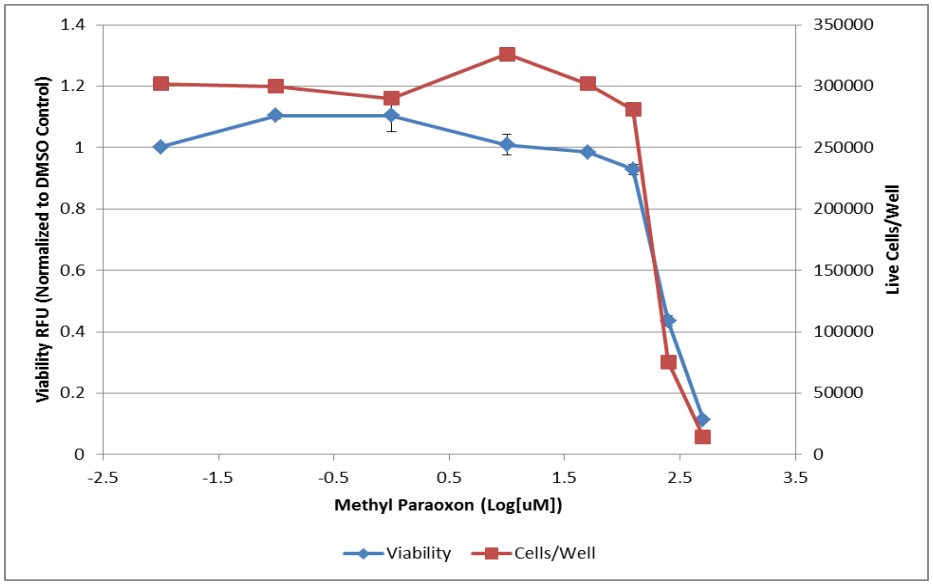


Figure 7. Viability and number of cells/well of hESC following 72 h of exposure to 0–500 µM MPO.

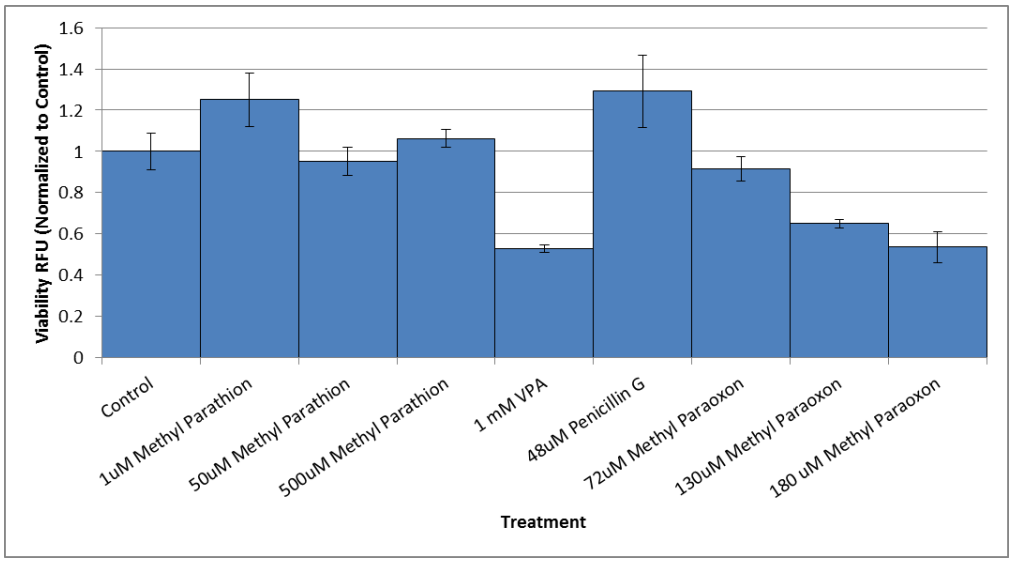


Figure 8. Viability of hESC following exposure to the $EC_{30}$, $EC_{10}$ and $EC_0$ of MP or MPO. VPA was used as the positive control and penicillin G was used as the negative control.

## 3.2 LC-MS Evaluation of MP and MPO

We plotted the m/z values for MP and MPO to determine if hESC are indeed converting parathion to the active paraoxon form. Based on extracted ion chromatograms (EIC)s for the high and low doses of parathion and paraoxon in plate D112 (refer to Figure 2), corresponding to M+H, M+Na and M-H peak values, there was a chromatographic peak at 4 min that is consistent with paraoxon (M-H) and present in only the paraoxon high dose samples. This peak was not present in any dose of parathion. Parathion was not detected in any sample under these LC-MS conditions. These results are consistent with the hypothesis that hESC cannot convert parathion to paraoxon.

## 3.3 Feature Selection and Pathway Interpretation

The raw metabolome dataset had 13,932 features in positive mode and 2,182 features in negative mode, as is shown in Table 2. After filtering in the data processing pipeline, the number of features in positive and negative mode was 6,853 and 1,363, respectively.

Table 2. Number of Features in Raw Metabolome Dataset

| | ESIpos | ESIneg |
|---|---|---|
| Raw metabolome data set | 13932 | 2182 |
| Isotope/adduct filter | 13227 | 2056 |
| Mass defect filter | 9443 | 1635 |
| Contaminant filter | 8932 | 1571 |
| Extraction blank filter | 6853 | 1363 |

Filtering on a 65% reproducible abundance threshold of 20,000 and selection of statistically significant features (Welch FDR<0.05 and > 75% fold change) yielded a set of 1,483 features in ESI positive mode and 345 features in ESI negative mode. These results are shown in Table 3.

Table 3. Number of Features by Drug and Dose Level

| Drug | | Number of Features | |
|---|---|---|---|
| | Dose Level | ESIpos | ESIneg |
| Methyl paraoxon | L | 637 | 130 |
| Methyl paraoxon | M | 431 | 104 |
| Methyl paraoxon | H | 390 | 101 |
| Methyl parathion | L | 209 | 65 |
| Methyl parathion | M | 246 | 58 |
| Methyl parathion | H | 93 | 86 |
| | Total | 1483 | 345 |

After statistical selection, features were putatively mapped to compounds present in KEGG human pathways. These features were passed through a quality control evaluation of EIC review to confirm the validity of individual mass features. The number of features passing these criteria are shown in Table 4. Several features with putative annotations that exhibit statistically significant fold changes are highlighted in Figure 9.

Table 4. Number of Features Mapped to KEGG Pathways and Passed EIC Reviews

| | Number of Features | |
|---|---|---|
| | ESIpos | ESIneg |
| Mapped to KEGG human pathways | 170 | 61 |
| Passed EIC review | 118 | 48 |

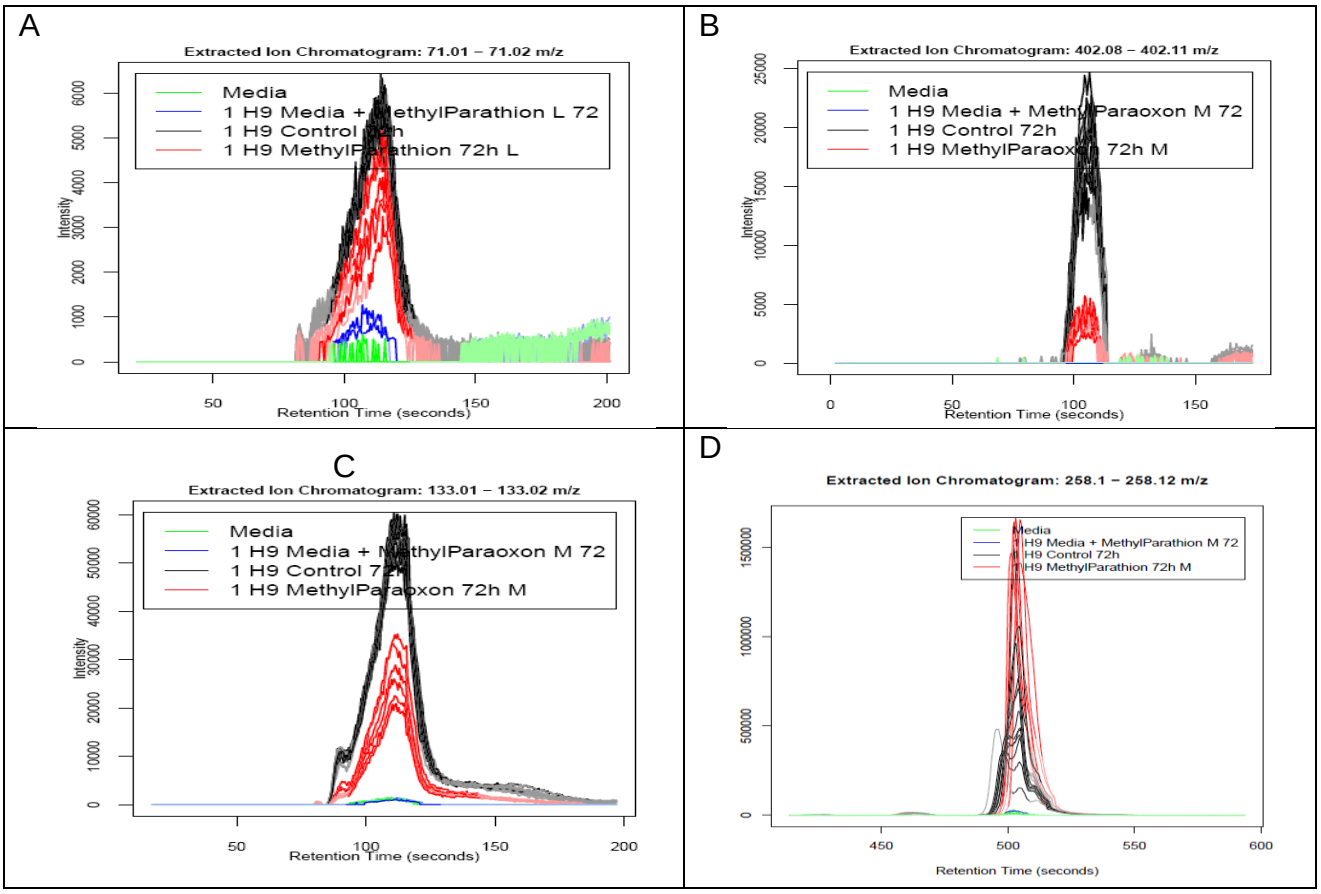


Figure 9. EICs of several mass features exhibiting a statistically significant response to treatment that have putative annotations.
A: Methylglyoxal
B: Lactoyl-glutathione
C: Malate (RT match to standard)
D: Glycerophosphocholine

ESI positive and ESI negative mode features were then combined into a unified dataset for evaluation of pathway enrichment by drug treatment and dose level. These mass features mapped to 69 different KEGG pathways of which 13 exhibited a statistically significant (FDR <0.1) enrichment of annotated features in at least one treatment by dose level (Table 5).

Table 5. Pathways Exhibiting a Statistically Significant Enrichment as Evaluated for Each MP and MPO Exposure Concentration

| Treatment | Dose | Kegg Pathway | Pathway Description | Hits | # in Path | P value | FDR |
|---|---|---|---|---|---|---|---|
| **MP** | L | hsa00020 | Citrate cycle (TCA cycle) | 3 | 15 | 0.002165 | 0.02 |
| **MP** | L | hsa00030 | Pentose phosphate pathway | 3 | 23 | 0.007362 | 0.05 |
| **MP** | L | hsa00053 | Ascorbate and aldarate metabolism | 3 | 25 | 0.009242 | 0.05 |
| **MPO** | H | hsa00260 | Glycine, serine and threonine metabolism | 6 | 40 | 0.006188 | 0.10 |
| **MP** | H | hsa00260 | Glycine, serine and threonine metabolism | 3 | 40 | 0.010283 | 0.07 |
| **MP** | H | hsa00280 | Valine, leucine and isoleucine degradation | 3 | 24 | 0.002486 | 0.02 |
| **MPO** | H | hsa00290 | Valine, leucine and isoleucine biosynthesis | 5 | 18 | 0.000802 | 0.02 |
| **MPO** | M | hsa00290 | Valine, leucine and isoleucine biosynthesis | 6 | 18 | 0.00015 | 0.01 |
| **MP** | H | hsa00290 | Valine, leucine and isoleucine biosynthesis | 3 | 18 | 0.001066 | 0.02 |
| **MP** | L | hsa00410 | beta-Alanine metabolism | 3 | 31 | 0.016307 | 0.07 |
| **MP** | L | hsa00561 | Glycerolipid metabolism | 3 | 13 | 0.001408 | 0.02 |
| **MPO** | H | hsa00620 | Pyruvate metabolism | 6 | 24 | 0.000431 | 0.01 |
| **MPO** | M | hsa00620 | Pyruvate metabolism | 5 | 24 | 0.005066 | 0.07 |
| **MP** | L | hsa00620 | Pyruvate metabolism | 4 | 24 | 0.000743 | 0.02 |
| **MP** | L | hsa00640 | Propanoate metabolism | 3 | 28 | 0.012509 | 0.06 |
| **MP** | L | hsa00650 | Butanoate metabolism | 4 | 31 | 0.001964 | 0.02 |
| **MPO** | H | hsa00760 | Nicotinate and nicotinamide metabolism | 8 | 37 | 0.000134 | 0.01 |
| **MPO** | M | hsa00760 | Nicotinate and nicotinamide metabolism | 7 | 37 | 0.001661 | 0.04 |
| **MP** | L | hsa00760 | Nicotinate and nicotinamide metabolism | 4 | 37 | 0.003737 | 0.03 |
| **MPO** | M | hsa00770 | Pantothenate and CoA biosynthesis | 5 | 24 | 0.005066 | 0.07 |
| **MP** | M | hsa04142 | Lysosome | 2 | 4 | 0.002426 | 0.10 |
| **MPO** | M | hsa04930 | Type II diabetes mellitus | 3 | 5 | 0.001157 | 0.04 |
| **MPO** | M | hsa05211 | Renal cell carcinoma | 2 | 3 | 0.007339 | 0.08 |
| **MP** | L | hsa05211 | Renal cell carcinoma | 2 | 3 | 0.000993 | 0.02 |

Note: FDR values are based on pathway enrichment analysis of the individual chemical by dose level evaluation.
CoA, coenzyme A
TCA, tricarboxylic acid cycle

A number of these pathways were of particular interest because they contained clusters of metabolites with significant fold changes that are closely adjacent to each other and linked by reactions catalyzed by enzymes that are known to be active in humans. KEGG diagrams for these pathways are shown in Appendix E.

EICs for all metabolites, in 5 pathways that exhibited significant enrichment in at least two dose levels of a chemical exposure or contain the acetylcholinesterase (AChE) enzyme, were plotted and evaluated for feature quality. The glycerophospholipid metabolism pathway was also included in this review because it includes the AChE enzyme inhibited by MPO. Features that passed EIC review were used to plot the KEGG pathway diagrams with color coding for fold change by chemical and dose level (Appendix E). The analysis of the 5 pathways was expanded to evaluate the fold change of features with putative annotations within a given pathway. The 5 targeted pathways were also further mined for features missed by the centWave peak picking algorithm and added to the fold change analysis. Features exhibiting abundance greater than 50% ($x > 0.5$) of the control are colored red, features between 50% and –50% ($0.5 < x > -0.5$) are colored yellow and features with an abundance less than 50% ($x < -0.5$) of the control are colored green. Features which are present but did not exhibit a fold change of at least 50% are yellow.

Metabolites which were not represented by mass features in the dataset are white. If a metabolite mapped to more than one feature and the features exhibited different orientation and magnitude, the fold change with the highest absolute value was used. In general, perturbation of the pathways was more pronounced after exposure to MPO than MP. Another view of the significance of the metabolite fold changes by chemical and dose level is shown in Appendix F. The metabolites in the KEGG diagrams of Appendix F are color coded according to the combination of dose levels where a statistically significant fold change was observed. For example, a feature or metabolite exhibiting a statistically significant fold change at all does levels (e.g., L, M, H) is colored black, at only the highest dose colored blue, at both medium and high is colored green, at medium only is colored yellow, and at the lowest dose only is magenta.

The organophosphorus (OP) insecticides have been known for many years to cause cholinergic crisis in humans as a result of the inhibition of the critical enzyme AChE. The interactions of the activated, toxic insecticide metabolites like paraoxon with AChE have been studied extensively for decades. Interestingly, studies have also suggested that the interactions of certain anticholinesterase organophosphates with AChE are more complex than previously thought since their inhibitory capacity has been noted to change as a function of inhibitor concentration (Sultatos, 2007). These data were interpreted to suggest secondary binding sites and interactions. Since these oxons are chemically reactive and contain functionality that allow potential strong protein interactions, it remains possible that the choline binding sites on other proteins and enzymes may also have functions that are modulated by oxons resulting in the significant metabolomic changes in related molecules we observed in this study.

Choline levels were reduced after exposure to all three dose levels of MPO and increased after exposure to all three dose levels of MP. The glycine, serine and threonine metabolism pathway is of interest because choline and a number of closely related metabolites were consistently decreased at all three dose levels of MPO. The primary mechanism of action for OP insecticides, including parathion, is to inhibit AChE by their oxygenated metabolites (paraoxons), due to the phosphorylation of the serine hydroxyl group located in the active site of the molecule. There are also additional studies suggesting the potential importance of a secondary peripheral binding site associated with AChE kinetics, particularly at low, environmentally relevant concentrations (Kousba et al., 2004).

In the pyruvate metabolism pathway, a subnetwork of six closely related metabolites was perturbed after exposure to both experimental compounds. Perturbation of this network was more pronounced after exposure to MPO than MP. Interestingly, for MP, the largest number of metabolites with fold changes was noted at the lowest dose level. However, for MPO, the number of metabolites that showed fold changes increased with increasing dose levels. Both MP and MPO are nontarget organism toxicants, where studies have shown MP affecting the pyruvate metabolism pathway (Moorthy et al., 1985). The pyruvate metabolism pathway plays a vital role in virtually every living cell, and any perturbation can have adverse negative effects on a cell's metabolism. Pyruvate metabolism directly intersects with aerobic and anaerobic respiration, and poisoning from paraoxon will lead to a disruption in these processes and inevitable cell death.

In the glycerolipid metabolism pathway a small cluster of metabolites closely related to glycerol were increased in response to both MP and MPO. These effects were most pronounced at the lowest dose level. Glycerolipid metabolism produces many signaling molecules which regulate biological processes (Prentki and Madiraju, 2008). Glycerol is a major component of

phospholipids and is involved in energy processes. Changes in lipid homeostasis have been implicated in the pathogenesis of numerous diseases, including neurodegeneration, cancer, type 2 diabetes, and obesity (Brisson et al., 2001; Casida et al., 2008; Prentki and Madiraju, 2008). The majority of glycerol was likely converted to glycerol-3-phosphate, since the level of glycerol-3-phosphate was increased by MP and paraoxon exposure in this study.

This report outlines many metabolites and pathways of interest and highlights several areas for further study. These include investigating fold changes of statistically significant unannotated small molecules by MS-MS fragmentation and analytical chemistry, validation of small molecules of interest by running chemical standards, further pathway analysis, evaluation of metabolites present in orphaned reactions, and generation of toxicity based metabolic networks.

## 4. CONCLUSIONS

Several hundred statistically significant differences were observed between treated and untreated controls that indicate MP and MPO have significant impact on hESC metabolism. Putative annotations of these small molecules have been identified in Stemina's database of human metabolites. These exhibited statistically significant enrichment in 13 human metabolic pathways, 5 of which are highlighted in this report. Of particular interest, we identified alterations in glycerophosphocholine metabolism consistent with MPO's mechanism of action. MP was not cytotoxic in hESC at dose levels below 500 μM. However, the active form, MPO was observed to be cytotoxic at doses greater than 100 μM. Evaluation of the MPO m/z EIC showed that the paraoxon form was not present in MP treated cells. From these results, we conclude that hESC do not metabolize MP into the active metabolite MPO. However, concentrations of MPO which could result from hepatic metabolism of MP in an intact normal human system appear to disrupt several key metabolic pathways in hESC required for normal development at much lower concentrations than does MP.

## LITERATURE CITED


Brisson, D.; Vohl, M.C.; St-Pierre, J.; Hudson, T.J.; Gaudet, D. Glycerol: a neglected variable in metabolic processes? *BioEssays* **2001**, *23*(6), 534−42.

Casida, J.E.; Nomura, D.K.; Vose, S.C.; Fujioka, K. Organophosphate-sensitive lipases modulate brain lysophospholipids, ether lipids and endocannabinoids. *Chem.-Biol. Interact.* **2008**, *175*(1−3), 355−64.

Cezar, G.G.; Quam, J.A.; Smith, A.M.; Guilherme, J.M.R.; Piekarczyk, M.S.; Brown, J.F.; Gage, F.H.; Muotri, A.R. Identification of small molecules from human embryonic stem cells using metabolomics. *Stem Cells Dev.* **2007**, *16*(6), 869−892.

Kousba, A.A.; Sultatos, L.G.; Poet, T.S.; Timchalk, C. Comparison of chlorpyrifos-oxon and paraoxon acetylcholinesterase inhibition dynamics: potential role of a peripheral binding site. *Toxicol. Sci.* **2004**, *80*(2), 239−248.

Moorthy, K.S.; Kasi, Reddy B.; Swami, K.S.; Chetty, C.S. Glucose metabolism in hepatopancreas and gill of Lamellidens marginallis during methyl parathion toxicity. *Pestic. Biochem. Physiol*. **1985**, *24*(1), 40−44.

Prentki, M.; Madiraju, S.R. Glycerolipid metabolism and signaling in health and disease. *Endocr. Rev*. **2008**, *29*(6), 647−676.

Sultatos, L.G. Concentration-dependent binding of chlorpyrifos oxon to acetylcholinesterase. *Toxicol., Sci*. **2007**, *100*(1), 128−135.

Blank

ACRONYMS AND ABBREVIATIONS

| | |
|---|---|
| AchE | acetylcholinesterase |
| ADMA | asymmetric dimethylarginine |
| APG | Aberdeen Proving Ground |
| ANOVA | analysis of variance |
| CoA | coenzyme A |
| DMSO | dimethylsulfoxide |
| DB | data base |
| $EC_{10}$ | concentration at which the effect was observed in 10% of the test population |
| $EC_{30}$ | concentration at which the effect was observed in 30% of the test population |
| $EC_{50}$ | concentration at which the effect was observed in 50% of the test population |
| ECBC | U.S. Army Edgewood Chemical Biological Center |
| EIC | extracted ion chromatographs |
| ESI | electrospray ionization |
| FDR | false discovery rate |
| FOC | Force Operating Capabilities |
| hESC | human embryonic stem cell |
| HILIC | hydrophilic interactive liquid chromatography |
| HMDB | human metabolome data base, freely available metabolomics data base |
| ID | identification |
| ILIR | in-house laboratory independent research |
| KEGG | Kyoto Encyclopedia of Genes and Genomes |
| LC-MS | liquid chromatography-mass spectrometry |
| LC/MS/MS | liquid chromatography/mass spectrometer/mass spectrometer |
| METLIN | metabolomics database resource managed by Scripps Research Institute |
| MP | methyl parathion |
| MPO | methyl paraoxon |
| m/z | mass over charge ratio |
| NIPALS | nonlinear iterative partial least squares |
| NIPALS PCA | nonlinear iterative partial least squares principal component analysis |
| OP | organophosphorus |
| Pam | pamphlet |
| PCA | principal components analysis |
| PEG | polyethylene glycol |
| PLS-DA | partial least-squares–discriminant analysis |
| PPM | parts per million |
| Q-TOF | quantitative time of flight |
| RF | random forest |
| RFU | relative fluorescence units |
| TIC | toxic industrial chemicals |
| TIM | toxic industrial materials |
| TRADOC | U.S. Army Training and Doctrine Command |
| VIP | variable importance in projection |
| VPA | valproate |

Blank

# APPENDIX A

## Dilutions for Dose-Response No. 1: Methyl Parathion (MP)

METHYL PARATHION (ST010B-36-A)
MW: 263.21

- Prepared a 200 mM stock solution in dimethylsulfoxide (DMSO)
  (1) Added 2.6 mg compound to 50 µL DMSO

- Prepared serial dilutions in DMSO using the stock solution
  (2) 100 mM dilution: Added 25 µL of stock solution (1) to 25 µL DMSO
  (3) 50 mM dilution: Added 25 µL dilution (2) to 25 µL DMSO
  (4) 10 mM dilution: Added 10 µL of dilution (3) to 40 µL DMSO
  (5) 1 mM dilution: Added 5 µL of dilution (4) to 45 µL DMSO
  (6) 500 µM dilution: Added 25 µL of dilution (5) to 25 µL DMSO µL
  (7) 100 µM dilution: Added 10 µL of dilution (6) to 40 µL DMSO
  (8) 10 µM dilution: Added 5 µL of dilution (7) to 45 µL DMSO

- Prepared solutions of compounds in mTeSR1 containing 0.1% DMSO
  A. 200 µM solution: Added 5 µL of (1) to 5 mL mTeSR1
  B. 100 µM solution: Added 5 µL of (2) to 5 mL mTeSR1
  C. 50 µM solution: Added 5 µL of (3) to 5 mL mTeSR1
  D. 10 µM solution: Added 5 µL of (4) to 5 mL mTeSR1
  E. 1 µM solution: Added 5 µL of (5) to 5 mL mTeSR1
  F. 0.5 µM solution: Added 5 µL of (6) to 5 mL mTeSR1
  G. 0.1 µM solution: Added 5 µL of (7) to 5 mL mTeSR1
  H. 0.01 µM solution: Added 5 µL of (8) to 5 mL mTeSR1

Blank

# APPENDIX B

## Dilutions for Dose-Response No. 2: Methyl Parathion (MP)

- Prepared a 1 M stock solution in dimethylsulfoxide (DMSO)
  (1) Added 5.2 mg compound to 19.76 µL DMSO

- Prepared serial dilutions in DMSO using the stock solution (1)
  (2) 800 mM dilution: Added 8 µL of stock solution (1) to 2 µL DMSO
  (3) 600 mM dilution: Added 4.5 µL stock solution (1) to 3 µL DMSO
  (4) 400 mM dilution: Added 3.75 µL of dilution 2 to 3.75 µL DMSO
  (5) 200 mM dilution: Added 1.875 µL of dilution 2 to 5.625 µL DMSO
  (6) 100 mM dilution: Added 3.75 µL of dilution 5 to 3.75 µL DMSO
  (7) 0.5 mM dilution: : Added 3.75 µL of dilution 6 to 3.75 µL DMSO
  (8) 0.25 mM dilution: Added 3.75 µL of dilution 7 to 3.75 µL DMSO

- Prepared solutions of compounds in mTeSR1 containing 0.1% DMSO
  I. 1000 µM solution: Added 2 µL of (1) to 3 mL mTeSR1
  J. 800 µM solution: Added 3 µL of (2) to 3 mL mTeSR1
  K. 600 µM solution: Added 3 µL of (3) to 3 mL mTeSR1
  L. 400 µM solution: Added 3 µL of (4) to 3 mL mTeSR1
  M. 200 µM solution: Added 3 µL of (5) to 3 mL mTeSR1
  N. 100 µM solution: Added 3 µL of (6) to 3 mL mTeSR1
  O. 50 µM solution: Added 3 µL of (7) to 3 mL mTeSR1
  P. 25 µM solution: Added 3 µL of (8) to 3 mL mTeSR1

Blank

APPENDIX C

Dilutions for Methyl Paraoxon (MPO)

METHYL PARAOXON (ST010C-45-B)
Sigma no. 46192
Lot no. SZE9113X
Exp. April 23, 2015
MW: 247.14

- Prepared a 500 mM stock solution in dimethylsulfoxide (DMSO)
  (1) Added 6.2 mg compound to 50 µL DMSO

- Prepared serial dilutions in DMSO using the stock solution (1)
  (2) 250 mM dilution: Added 25 µL of stock solution (1) to 25 µL DMSO
  (3) 125 mM dilution: Added 25 µL dilution 2 to 25 µL DMSO
  (4) 50 mM dilution: Added 20 µL of dilution 3 to 30 µL DMSO
  (5) 10 mM dilution: Added 10 µL of dilution 4 to 40 µL DMSO
  (6) 1 mM dilution: Added 5 µL of dilution 5 to 45 µL DMSO
  (7) 0.1 mM dilution: Added 5 µL of dilution 6 to 45 µL DMSO
  (8) 0.01 mM dilution: Added 5 µL of dilution 7 to 45 µL DMSO

- Prepared solutions of compounds in mTeSR1 containing 0.1% DMSO
  A. 500 µM solution: Added 5 µL of (1) to 5 mL mTeSR1
  B. 250 µM solution: Added 5 µL of (2) to 5 mL mTeSR1
  C. 125 µM solution: Added 5 µL of (3) to 5 mL mTeSR1
  D. 50 µM solution: Added 5 µL of (4) to 5 mL mTeSR1
  E. 10 µM solution: Added 5 µL of (5) to 5 mL mTeSR1
  F. 1 µM solution: Added 5 µL of (6) to 5 mL mTeSR1
  G. 0.1 µM solution: Added 5 µL of (7) to 5 mL mTeSR1
  H. 0.01 µM solution: Added 5 µL of (8) to 5 mL mTeSR1

Blank

APPENDIX D

LC-MS Data Acquisition Method Information

MethodName: ESI_Luna_HILIC12_95to70ACN_12min_1mlEQ_1MinJD_EQD_LM_IsoRamp.m

Method Path: D:\MassHunter\Data\ArmyProject\H9_Army_PlateD112_SS473_2011-06-08\ST010C_57_D112_1B_2011-06-08.d\AcqData\ESI_Luna_ HILIC12_95to70ACN_12min_1mlEQ_1MinJD_EQD_LM_IsoRamp.m

Method Description: Column: Phenomenex Luna HILIC #12; 100x3mm;S/N 512587-1 B/N 5540-15

Device List
1290 Sampler
1290 BinPump
1260 IsoPump
1290 TCC
MS Q-TOF

TOF/Q-TOF Mass Spectrometer

Ion Source: Dual ESI
Tune File: AutoTune.tun
Stop Mode: No Limit/As Pump
Stop Time
Fast Polarity: N/A

| Time Segment # | Start Time | Diverter Valve State | Storage Mode | Mode/Ion Mode |
|---|---|---|---|---|
| 1 | 0 | Waste | Centroid | Dual ESI/ Pos |
| 2 | 1.0 | MS | | Dual ESI |
| 3 | 17 | Waste | | Dual ESI |

<u>Time Segment 1</u>
Acquisition Mode: MS1
Min Range: 70
Max Range: 1600
Scan Rate: 2

*Source Parameters*
Gas Temp: 325 °C
Gas Flow: 10 L/min
Nebulizer: 30 psi

| Scan Segment No. | Ion Polarity |
|---|---|
| 1 | Positive |

Scan Segment 1
*Scan Source Parameters*
VCap: 3500
Fragmentor: 170
Skimmer: 166
OctopoleRFPeak: 750

Scan Segment 2
Scan Segment 3

Time Segment 2

Acquisition Mode: MS1
Min Range: 70
Max Range: 1600
Scan Rate: 2

*Source Parameters*
Gas Temp: 325 °C
Gas Flow: 10 L/min
Nebulizer: 30 psi

| Scan Segment No. | Ion Polarity |
|---|---|
| 1 | Positive |
| 2 | Positive |

Scan Segment 1

VCap: 3500
Fragmentor: 170
Skimmer1: 66
OctopoleRFPeak: 750

Scan Segment 2

VCap: 3500
Fragmentor: 170
Skimmer1: 66
OctopoleRFPeak: 750

Scan Segment 3

*Scan Source Parameters*
Time Segment: 3
Acquisition Mode: MS1
Min Range: 70
Max Range: 1600
Scan Rate: 2

*Source Parameters*
Gas Temp: 325 °C
Gas Flow: 10 L/min
Nebulizer: 30 psi

| Scan Segment No. | Ion Polarity |
|---|---|
| 1 | Positive |
| 2 | |
| 3 | |

Scan Segment 1

*Scan Source Parameters*
VCap: 3500
Fragmentor: 170
Skimmer: 166
OctopoleRFPeak: 750

Scan Segment 2

VCap: 3500
Fragmentor: 170
Skimmer: 166
OctopoleRFPeak: 750

Scan Segment 3

*Chromatograms*

| Chromatogram Type | Label | Offset | Y-Range |
|---|---|---|---|
| TIC | TIC | 15 | 10000000 |

Reference Mass Enabled
Use Bottle A: FALSE
Ref Nebulizer: 16

AutoRecalibration
AverageScans: 1
DetectionWindow: 25
MinHeight: 1000
Reference Masses

<Positive>
121.050873
922.009798

Wellplate Sampler
Name: 1290-ALS
Model: G4226A
Ordinal no.: 1
Options: THM

Stop Time (min) As Pump Post Time (min) Off

Injection Type: Needle Wash
Injection Volume: 5
Overlap Time: Disable Overlapped Injection
Draw Position: –2.5
Draw Position Detection: 0
Draw Speed: 200
Eject Speed: 200
Flush Out Factor: 5
Automatic Delay Volume Reduction: No
Equilibration Time: 0
Wash Vessel: N/A
Wash Location: FlushPort
Wash Time: 3
Wash Cycles: N/A
Ready Temperature Range
Temperature

Contact 1: 0
Contact 2: 0
Contact 3: 0
Contact 4: 0

*Injector Program*
*Signals Selected*
*Contacts Time Table*

Binary Pump
Name: 1290-Bin Pump
Model: G4220A
Ordinal no.: 1
Options: SSV

Stop Time (min): 22
Post Time (min): Off

Flow: 0.5 mL/min

Pressure Min: 5 bar
Pressure Max: 340 bar
Max Flow Gradient: 100 mL/min

Solvent A: 0.1% Formic acid
Solvent B: 0.1% Formic acid in ACN
Solvent Ratio A: 5
Solvent Ratio B: 95

Solvent Type A1: Aqueous
Solvent Type A2: -----
Solvent Type B1: Organic
Solvent Type B2: -----

Compress. A (*10–6/bar): 46
Compress. B (*10–6/bar): 115
Stroke A: Auto
Stroke B: Auto

Stroke Synchronization: Yes

Contact 1: 0
Contact 2: 0
Contact 3: 0
Contact 4: 0

*Pump Time Table*

| Time | Flow | Pressure | Solv Ratio B |
|---|---|---|---|
| 0 | 0.5 | 320 | 95 |
| 1.5 | 0.5 | | 95 |
| 12 | 0.5 | | 69.7 |
| 13 | 0.5 | | 5 |
| 17 | 0.5 | | 5 |
| 18 | 1 | | 95 |
| 22 | 1 | | 95 |

*Signals Selected*
Description
Solvent% A
Solvent% B
Direction of piston A
Direction of piston B

Isocratic Pump
Name: Iso Pump
Model: G1310A
Ordinal no.: 1
Stop Time: 22 min
Post Time (min): Off
Flow: 1.5 mL/min
Pressure Min: 0 bar
Pressure Max: 400 bar
Max Flow Gradient: 100 mL/min
Solvent A: Agilent *m/z* 121 and 922 reference
Solvent Ratio A: 100
Compress. A (*10–6/bar): 120
Stroke A: Auto
Contact 1: 0
Contact 2: 0
Contact 3: 0
Contact 4: 0

*Pump Time Table*

| Time | Flow | Pressure |
|---|---|---|
| 0 | 1.5 | No Change |
| 0.99 | 1.5 | |
| 1 | 2.5 | |
| 4.5 | 3 | |
| 17 | 2.5 | |
| 22 | 1.5 | |

*Signals Selected*
*Contacts Time Table*
Thermostated Column Compartment
Name: 1290-Column
Model: G1316C
Ordinal no.: 1
Options: CSV

Stop Time (min): As Pump
Post Time (min): Off
Left Temp.: 30
Right Temp.: Same as left
Left Ready: When Temp Within Set Point ±1.5
Right Ready: When Temp Within Set Point ±1.5
Valve Position: 1
Contact 1: 0
Contact 2: 0
Contact 3: 0
Contact 4: 0

APPENDIX E

Enriched Pathway Maps Colored by Fold Change

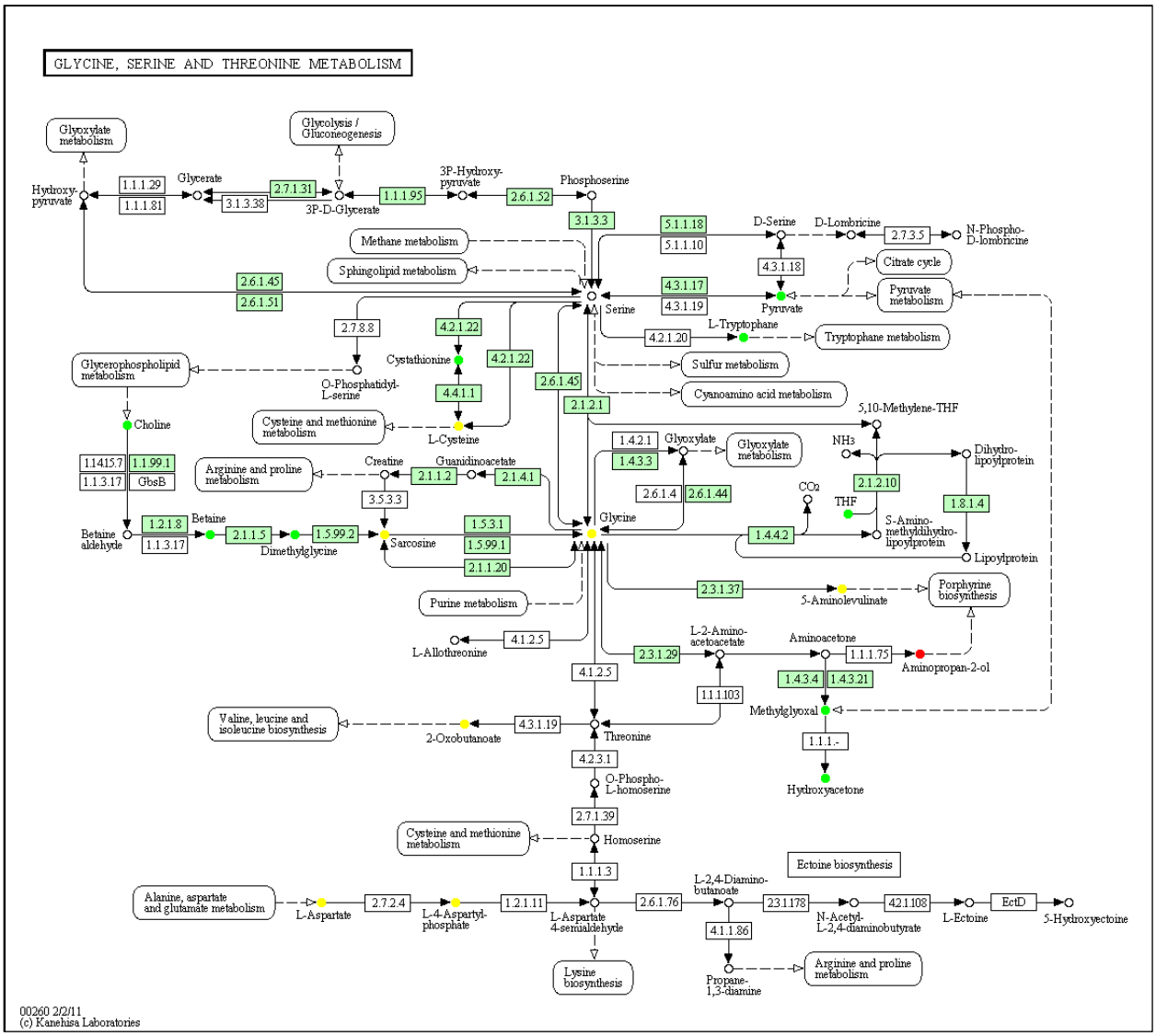


Figure E-1. Further evaluation of the glycine, serine and threonine metabolism pathway of the high dose of methyl paraoxon (MPO) colored by fold change (treatment vs. control) of high quality features identified with putative annotations within the pathway.

Features exhibiting abundance greater than 50% (x >0.5) of the control are colored red, features between 50% and -50% (0.5 < x > -0.5) are colored yellow and features with an abundance less than 50% (x < -0.5) of the control are colored green. Enzymes or enzymatic activity observed in humans are represented by green colored boxes. Putative metabolites observed in this study are represented with colored circles. Arrows represent direction of enzymatic activity.

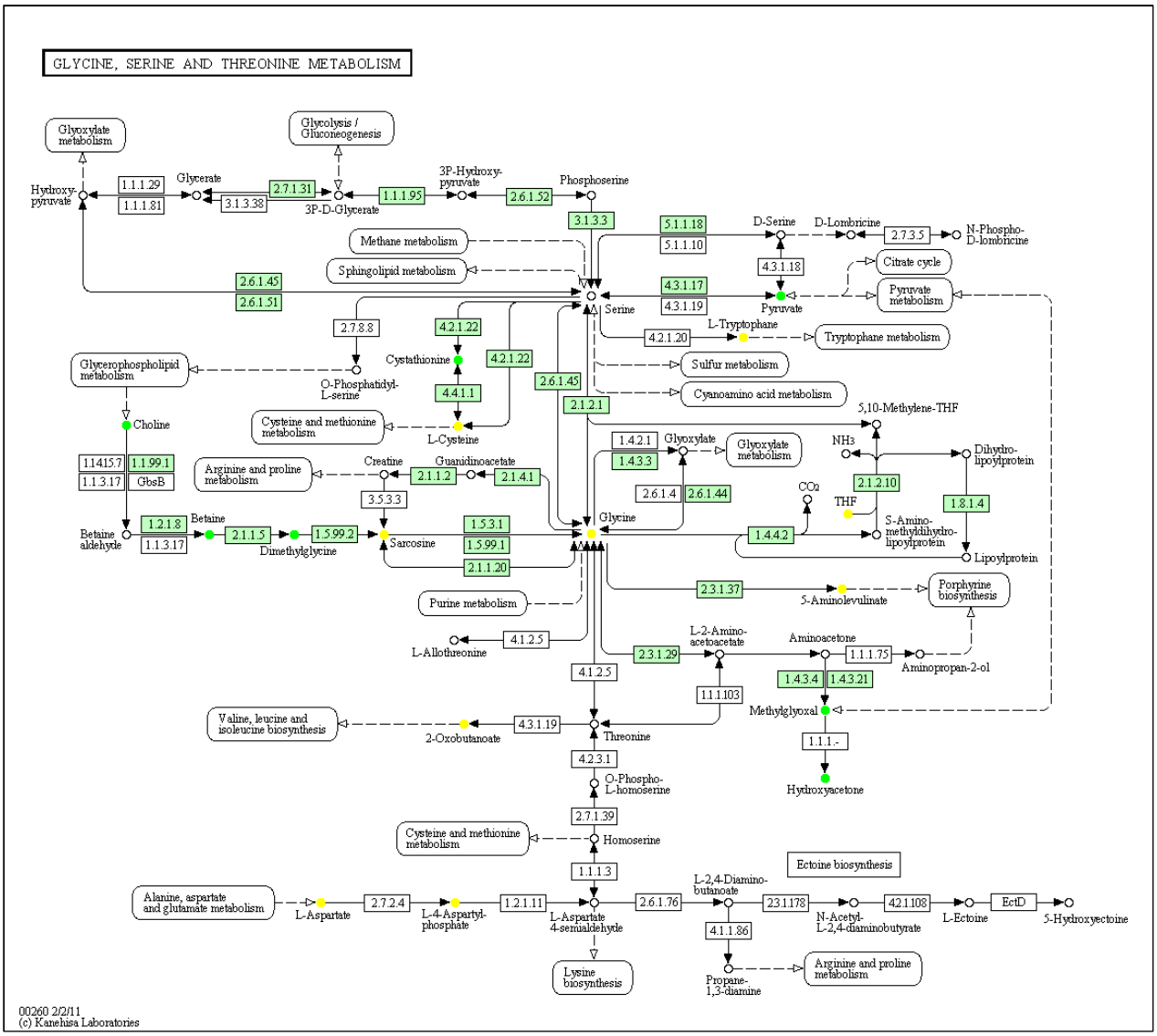


Figure E-2. Further evaluation of the glycine, serine and threonine metabolism pathway of the middle dose of MPO colored by fold change (treatment vs. control) of high quality features identified with putative annotations within the pathway.

Features exhibiting abundance greater than 50% (x >0.5) of the control are colored red, features between 50% and -50% (0.5 < x > -0.5) are colored yellow and features with an abundance less than 50% (x < -0.5) of the control are colored green. Enzymes or enzymatic activity observed in humans are represented by green colored boxes. Putative metabolites observed in this study are represented with colored circles. Arrows represent direction of enzymatic activity.

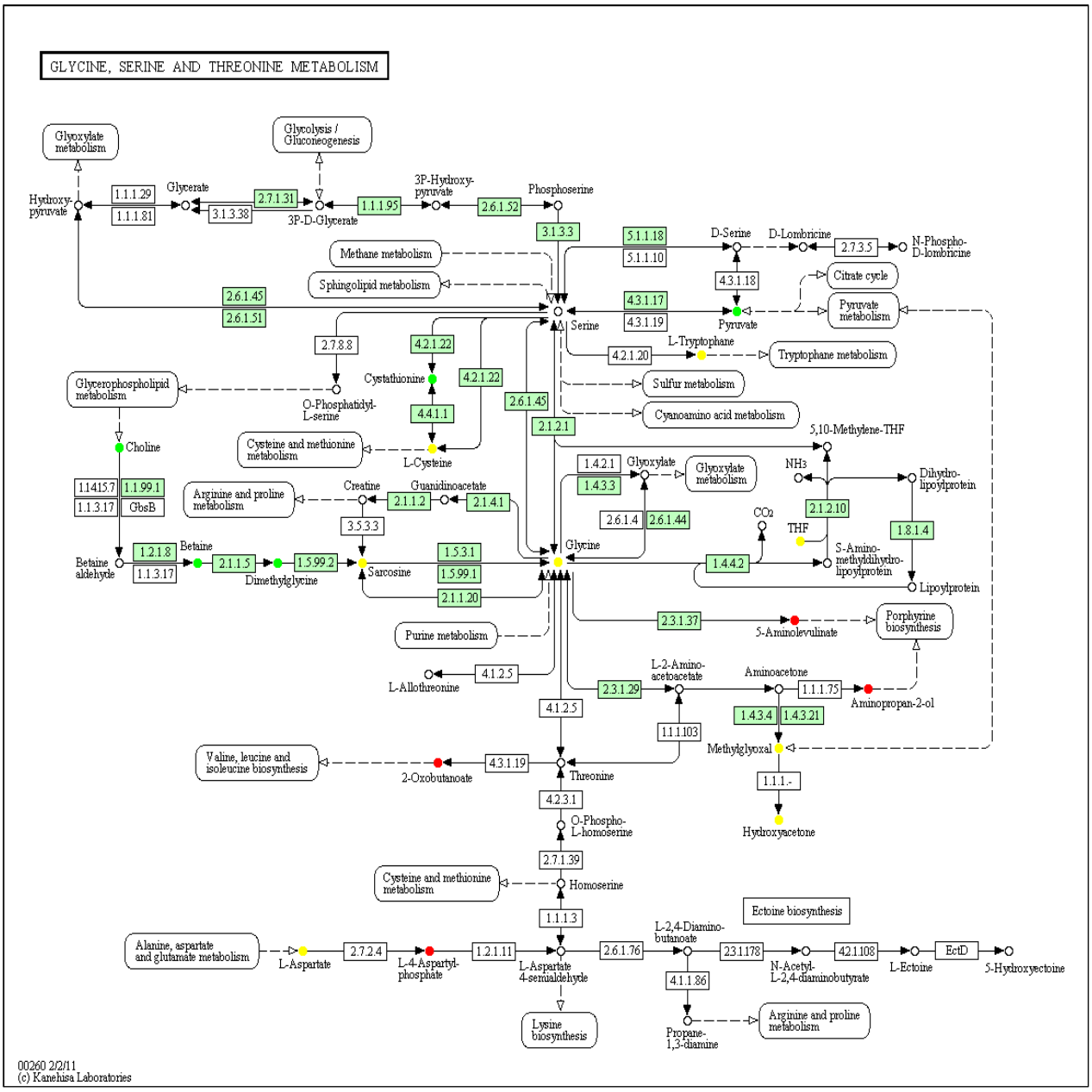


Figure E-3. Further evaluation of the glycine, serine and threonine metabolism pathway of the low dose of MPO colored by fold change (treatment vs. control) of high quality features identified with putative annotations within the pathway.

Features exhibiting abundance greater than 50% (x >0.5) of the control are colored red, features between 50% and -50% (0.5 < x > -0.5) are colored yellow and features with an abundance less than 50% (x < -0.5) of the control are colored green. Enzymes or enzymatic activity observed in humans are represented by green colored boxes. Putative metabolites observed in this study are represented with colored circles. Arrows represent direction of enzymatic activity.

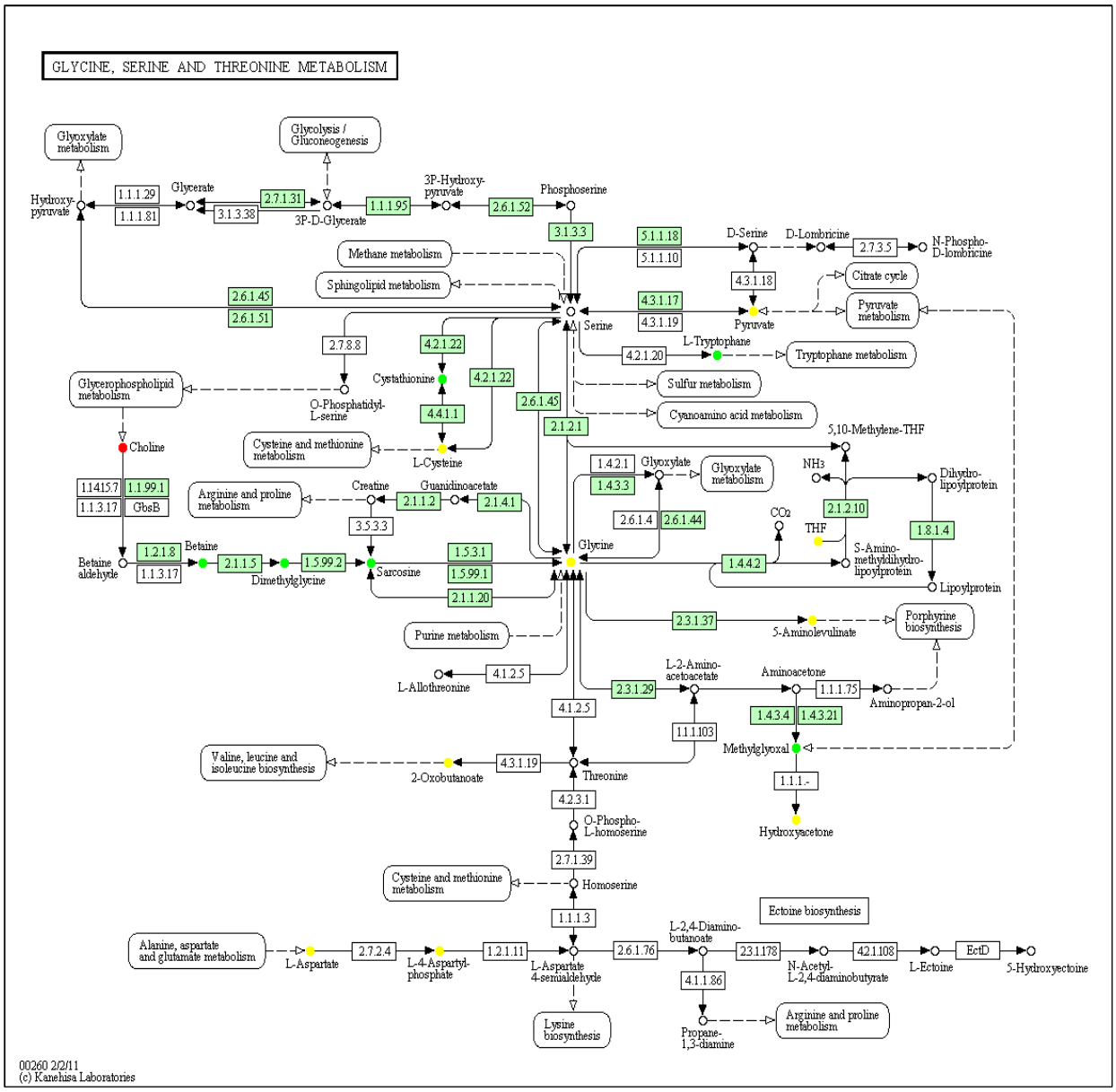


Figure E-4. Further evaluation of the glycine, serine and threonine metabolism pathway of the high dose of MP colored by fold change (treatment vs. control) of high quality features identified with putative annotations within the pathway.

Features exhibiting abundance greater than 50% (x >0.5) of the control are colored red, features between 50% and -50% (0.5 < x > -0.5) are colored yellow and features with an abundance less than 50% (x < -0.5) of the control are colored green. Enzymes or enzymatic activity observed in humans are represented by green colored boxes. Putative metabolites observed in this study are represented with colored circles. Arrows represent direction of enzymatic activity.

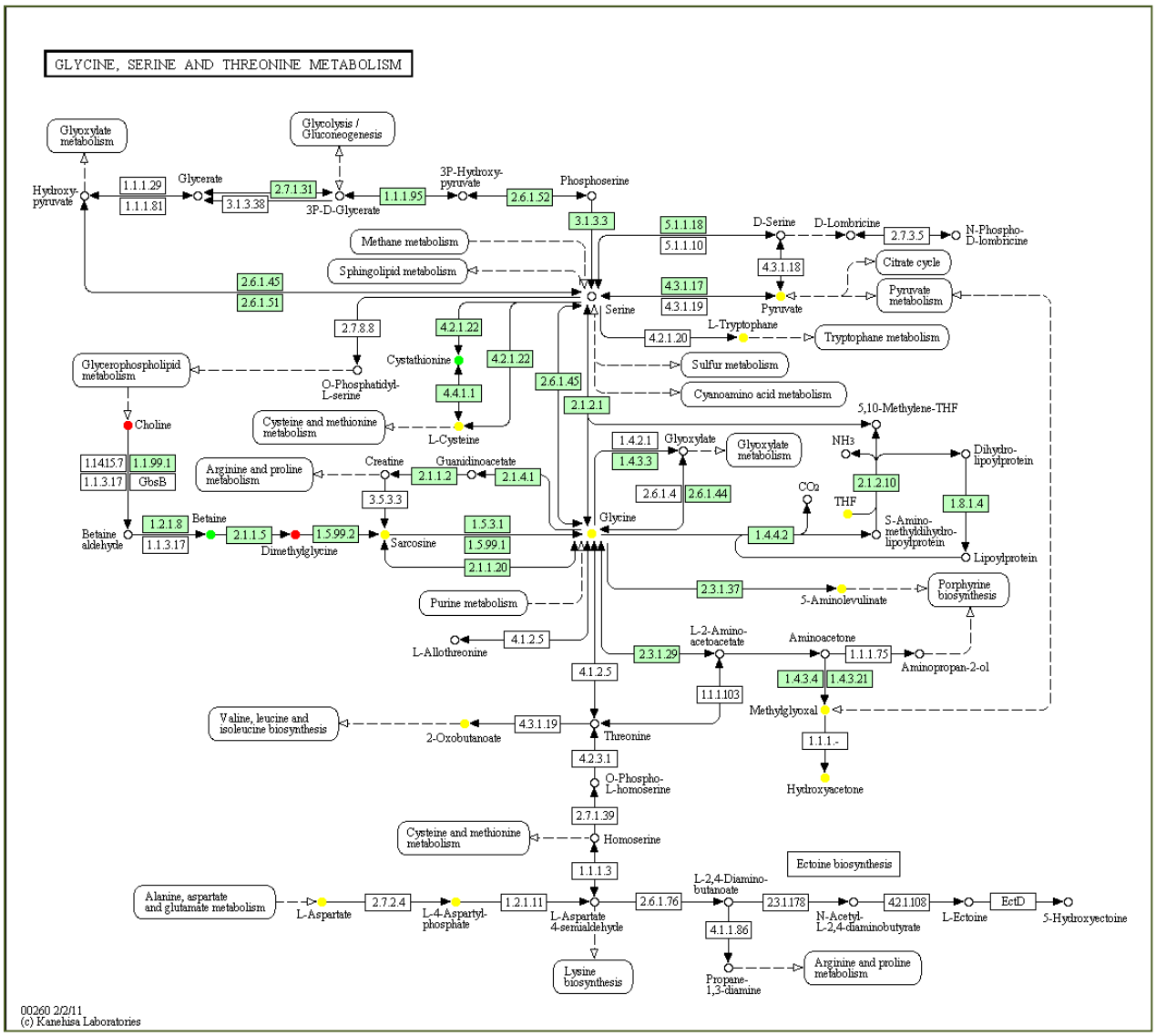


Figure E-5. Further evaluation of the glycine, serine and threonine metabolism pathway of the middle dose of MP colored by fold change (treatment vs. control) of high quality features identified with putative annotations within the pathway.

Features exhibiting abundance greater than 50% (x >0.5) of the control are colored red, features between 50% and -50% (0.5 < x > -0.5) are colored yellow and features with an abundance less than 50% (x < -0.5) of the control are colored green. Enzymes or enzymatic activity observed in humans are represented by green colored boxes. Putative metabolites observed in this study are represented with colored circles. Arrows represent direction of enzymatic activity.

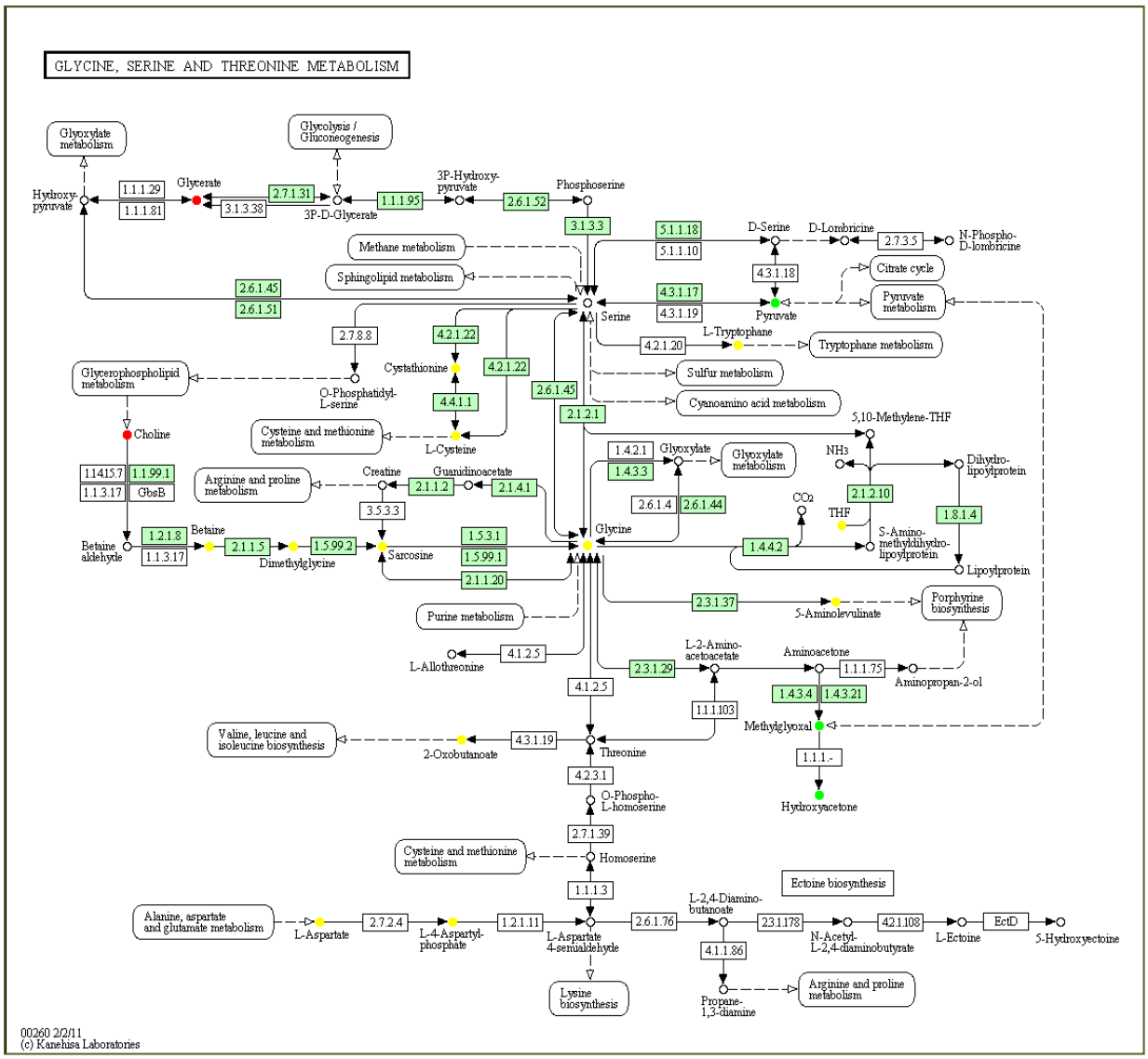


Figure E-6. Further evaluation of the glycine, serine and threonine metabolism pathway of the low dose of MP colored by fold change (treatment vs. control) of high quality features identified with putative annotations within the pathway.

Features exhibiting abundance greater than 50% (x >0.5) of the control are colored red, features between 50% and -50% (0.5 < x > -0.5) are colored yellow and features with an abundance less than 50% (x < -0.5) of the control are colored green. Enzymes or enzymatic activity observed in humans are represented by green colored boxes. Putative metabolites observed in this study are represented with colored circles. Arrows represent direction of enzymatic activity.

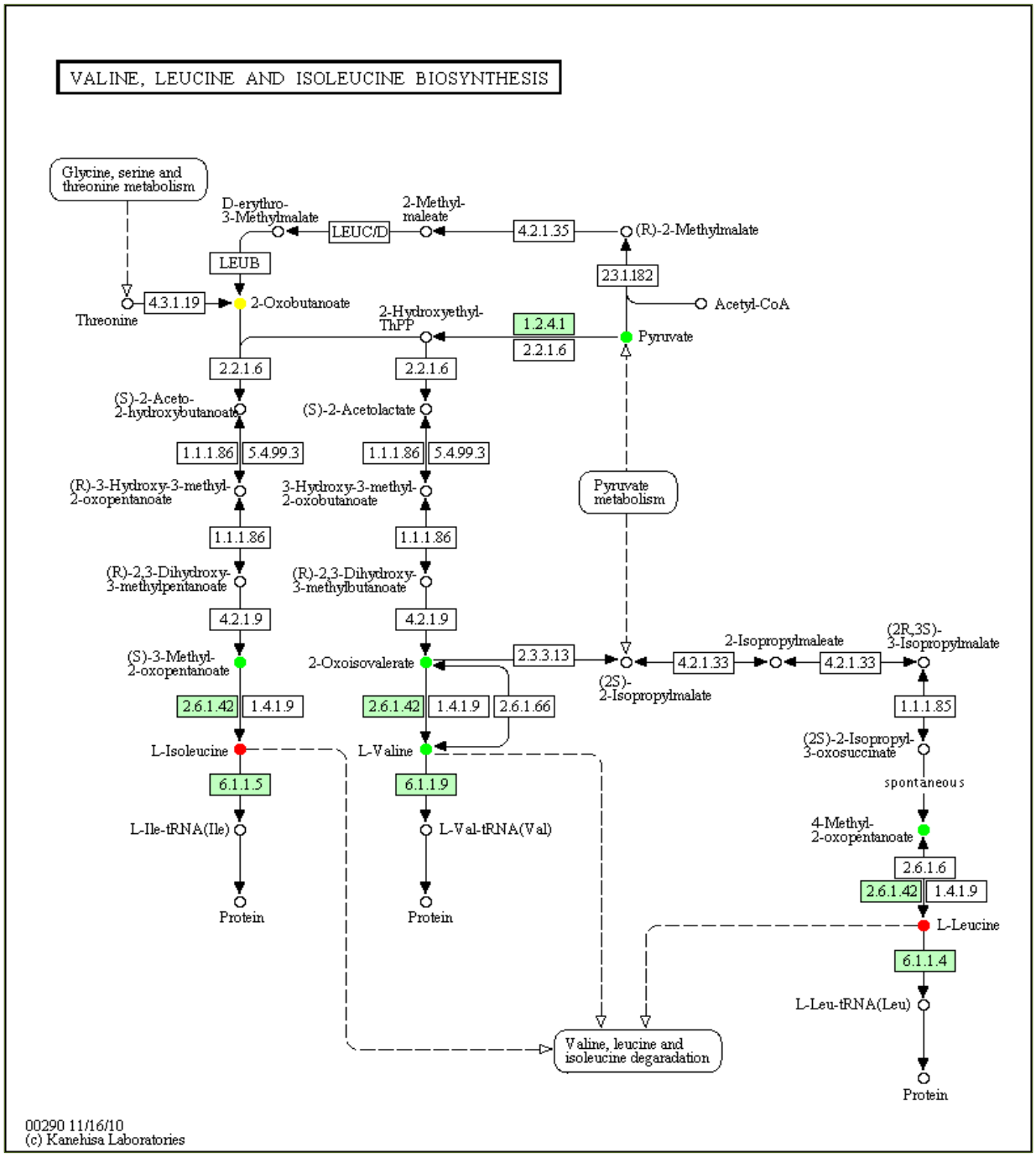


Figure E-7. Further evaluation of the valine, leucine and isoleucine biosynthesis pathway of the high dose of MPO colored by fold change (treatment vs. control) of high quality features identified with putative annotations within the pathway.

Features exhibiting abundance greater than 50% (x >0.5) of the control are colored red, features between 50% and -50% (0.5 < x > -0.5) are colored yellow and features with an abundance less than 50% (x < -0.5) of the control are colored green. Enzymes or enzymatic activity observed in humans are represented by green colored boxes. Putative metabolites observed in this study are represented with colored circles. Arrows represent direction of enzymatic activity.

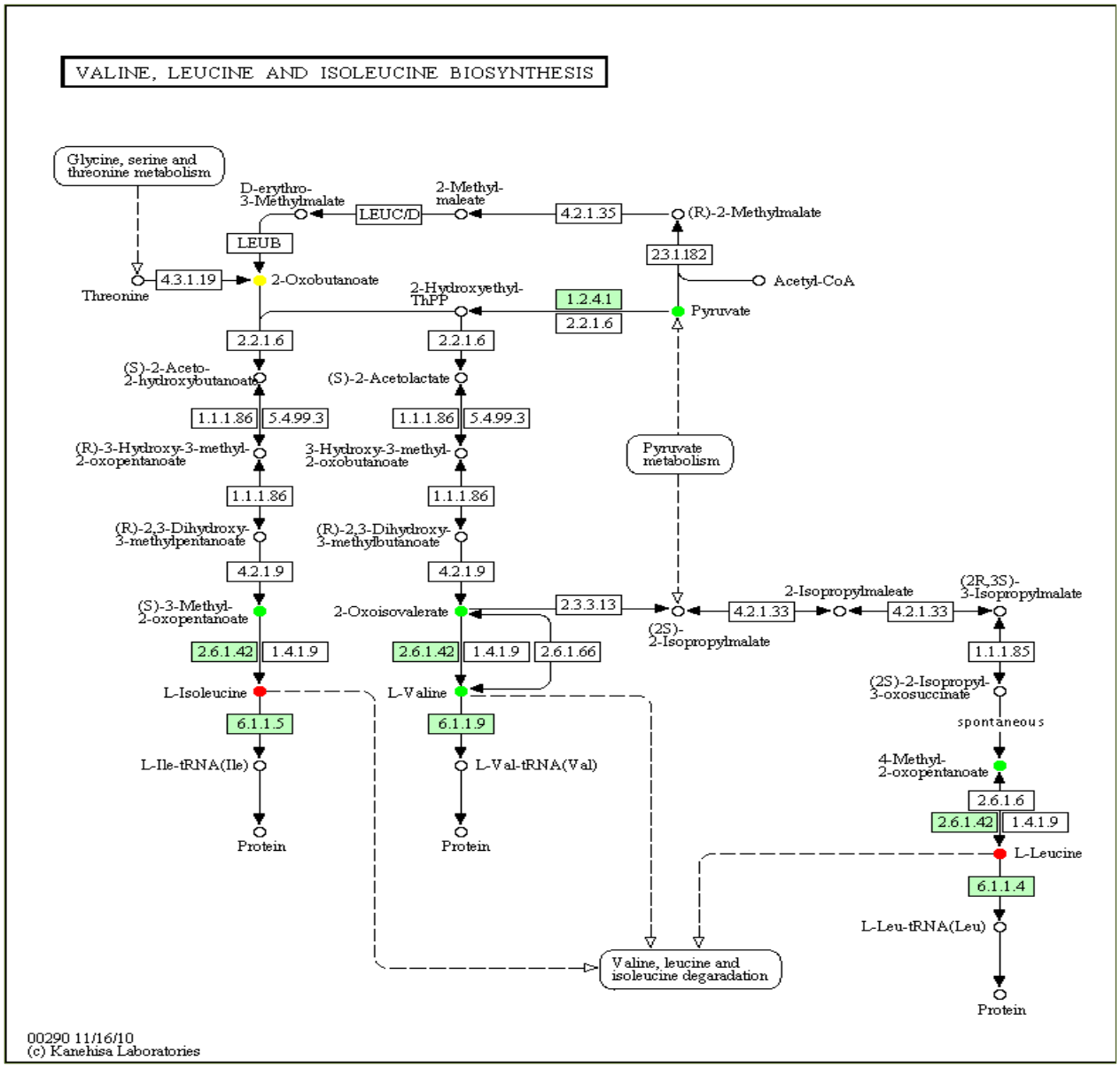


Figure E-8. Further evaluation of the valine, leucine and isoleucine biosynthesis pathway of the middle dose of MPO colored by fold change (treatment vs. control) of high quality features identified with putative annotations within the pathway.

Features exhibiting abundance greater than 50% (x >0.5) of the control are colored red, features between 50% and -50% (0.5 < x > -0.5) are colored yellow and features with an abundance less than 50% (x < -0.5) of the control are colored green. Enzymes or enzymatic activity observed in humans are represented by green colored boxes. Putative metabolites observed in this study are represented with colored circles. Arrows represent direction of enzymatic activity.

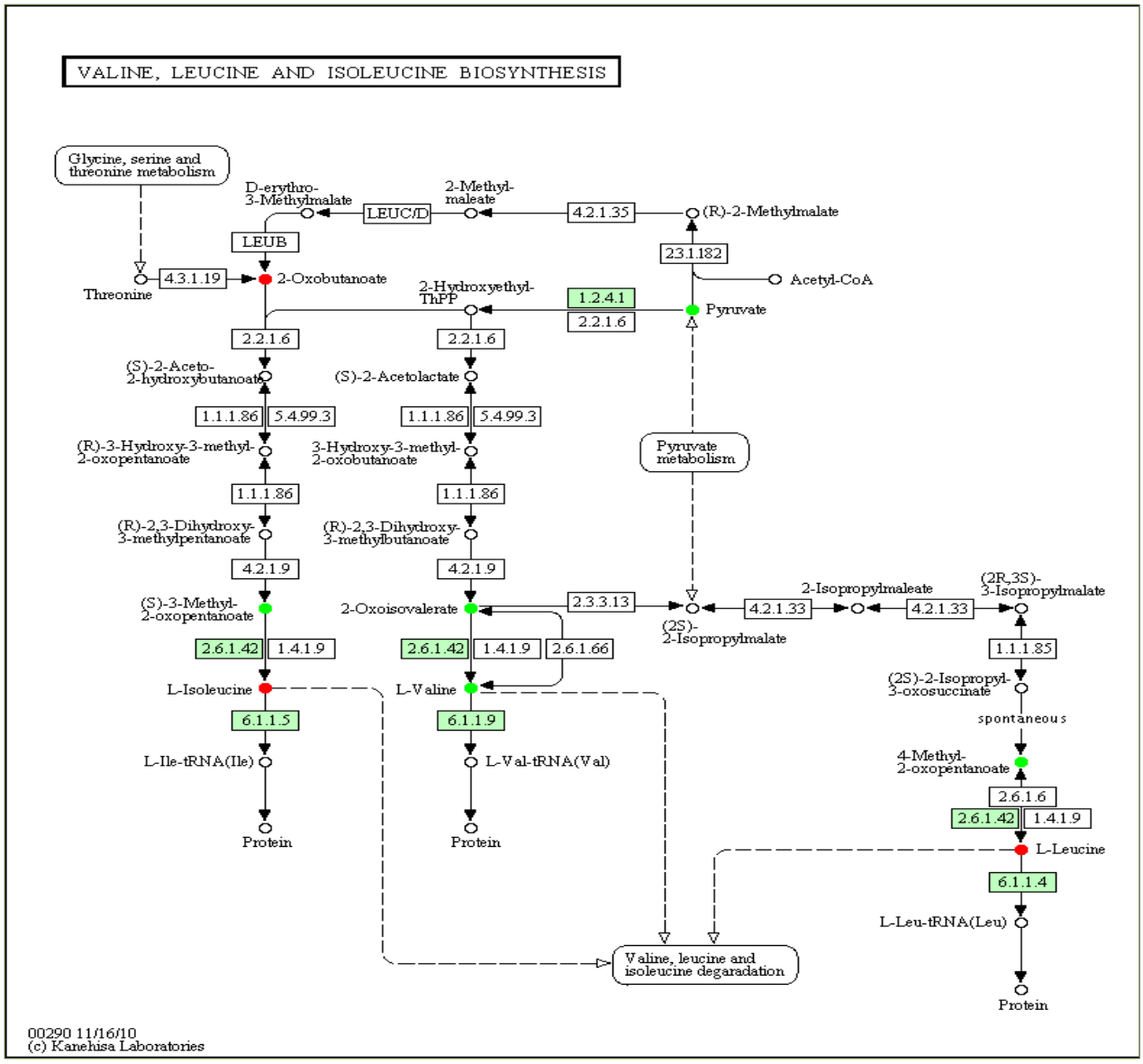


Figure E-9. Further evaluation of the valine, leucine and isoleucine biosynthesis pathway of the low dose of MPO colored by fold change (treatment vs. control) of high quality features identified with putative annotations within the pathway.

Features exhibiting abundance greater than 50% (x >0.5) of the control are colored red, features between 50% and -50% (0.5 < x > -0.5) are colored yellow and features with an abundance less than 50% (x < -0.5) of the control are colored green. Enzymes or enzymatic activity observed in humans are represented by green colored boxes. Putative metabolites observed in this study are represented with colored circles. Arrows represent direction of enzymatic activity.

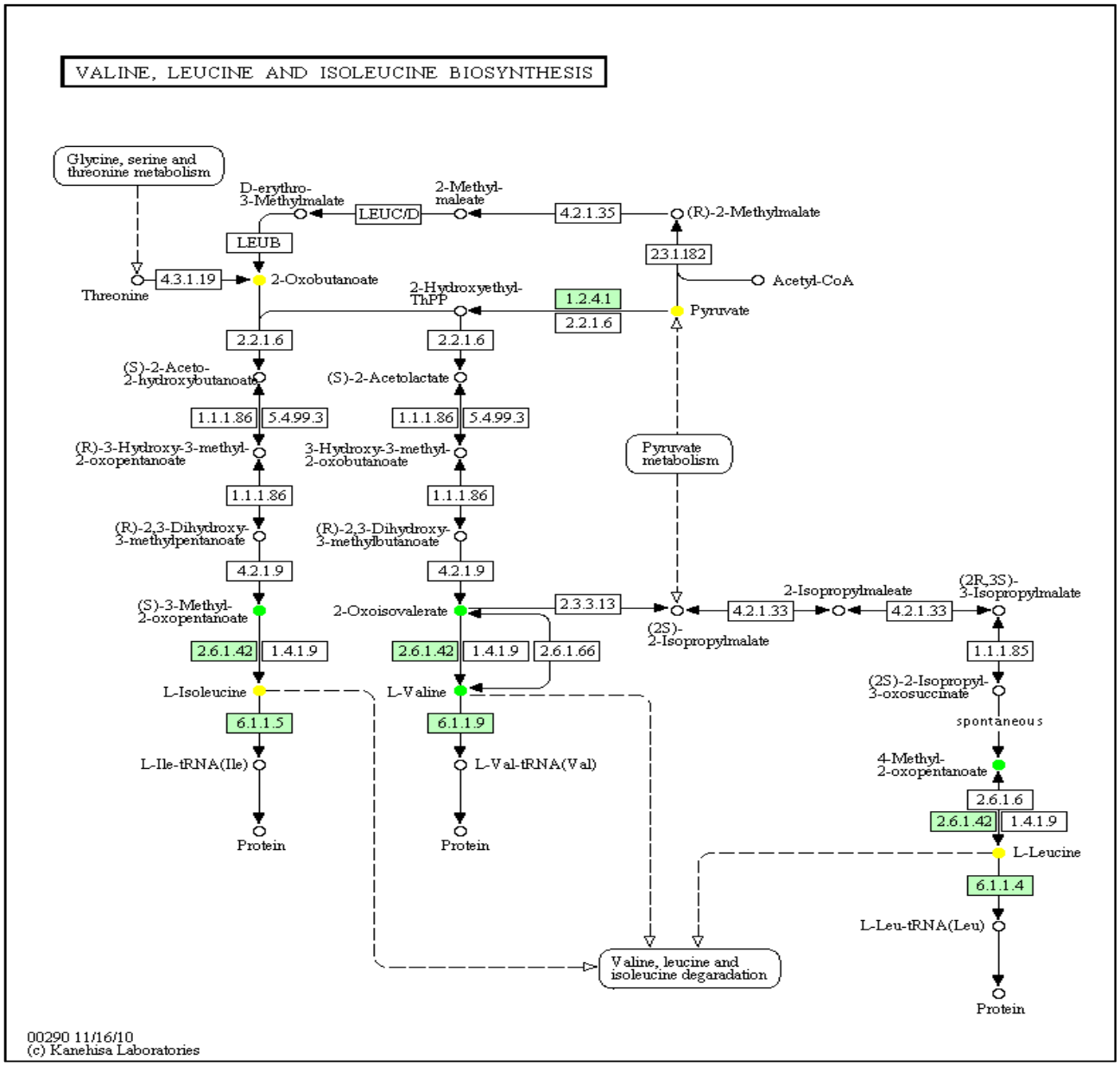


Figure E-10. Further evaluation of the valine, leucine and isoleucine biosynthesis pathway of the high dose of MP colored by fold change (treatment vs. control) of high quality features identified with putative annotations within the pathway.

Features exhibiting abundance greater than 50% (x >0.5) of the control are colored red, features between 50% and -50% (0.5 < x > -0.5) are colored yellow and features with an abundance less than 50% (x < -0.5) of the control are colored green. Enzymes or enzymatic activity observed in humans are represented by green colored boxes. Putative metabolites observed in this study are represented with colored circles. Arrows represent direction of enzymatic activity.

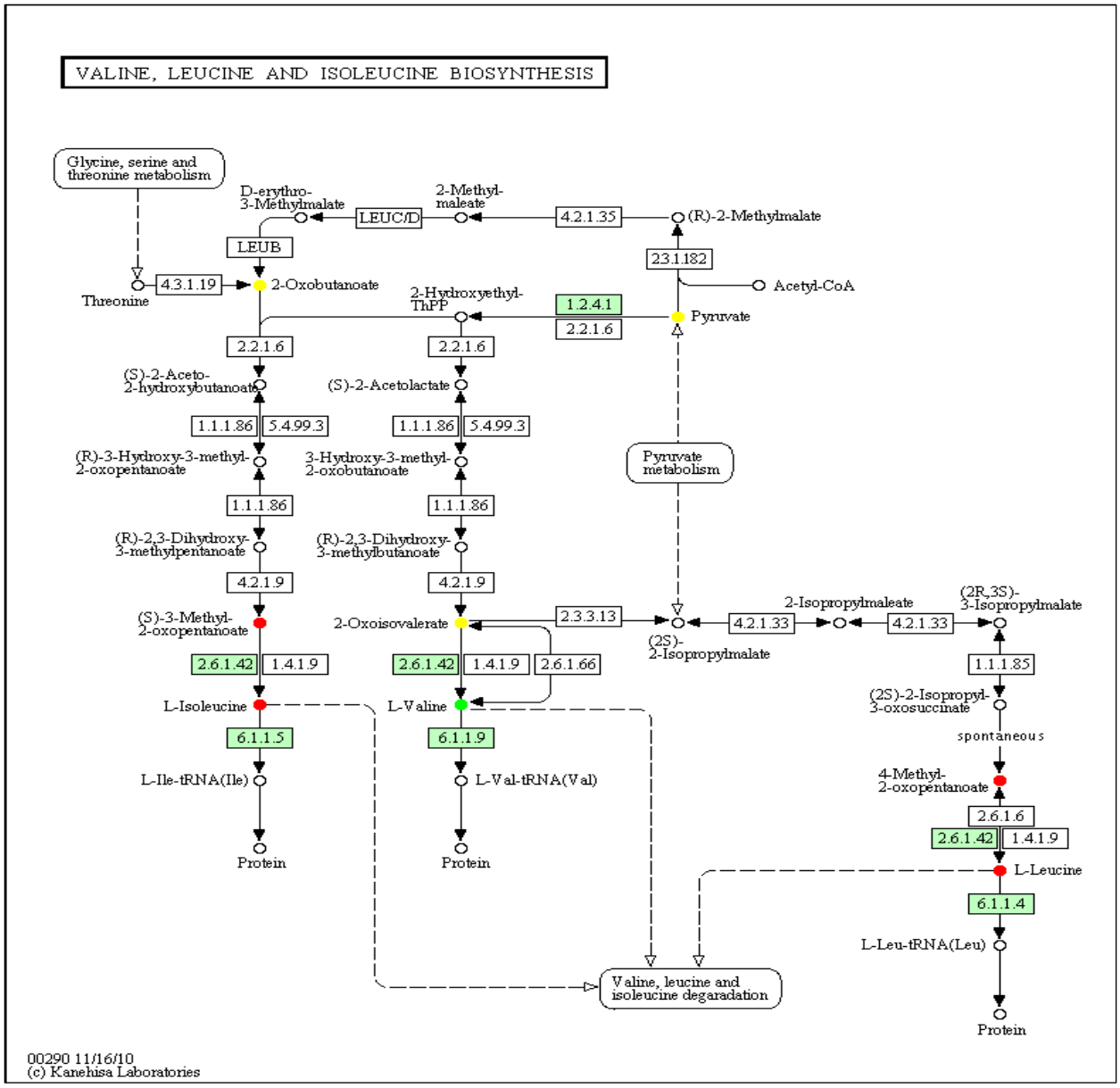


Figure E-11. Further evaluation of the valine, leucine and isoleucine biosynthesis pathway of the middle dose of MP colored by fold change (treatment vs. control) of high quality features identified with putative annotations within the pathway.

Features exhibiting abundance greater than 50% (x >0.5) of the control are colored red, features between 50% and -50% (0.5 < x > -0.5) are colored yellow and features with an abundance less than 50% (x < -0.5) of the control are colored green. Enzymes or enzymatic activity observed in humans are represented by green colored boxes. Putative metabolites observed in this study are represented with colored circles. Arrows represent direction of enzymatic activity.

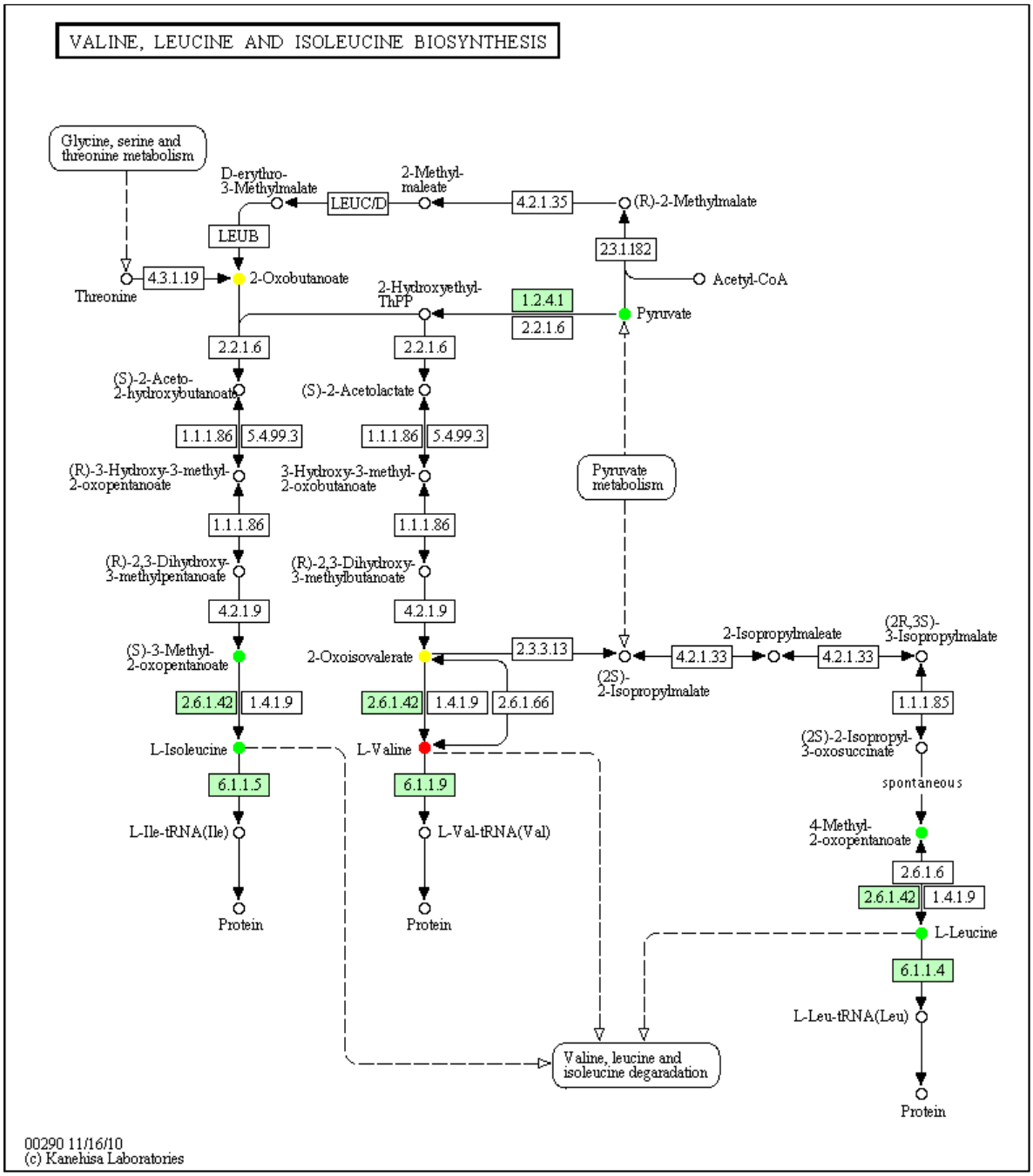


Figure E-12. Further evaluation of the valine, leucine and isoleucine biosynthesis pathway of the low dose of MP colored by fold change (treatment vs. control) of high quality features identified with putative annotations within the pathway.

Features exhibiting abundance greater than 50% ($x > 0.5$) of the control are colored red, features between 50% and -50% ($0.5 < x > -0.5$) are colored yellow and features with an abundance less than 50% ($x < -0.5$) of the control are colored green. Enzymes or enzymatic activity observed in humans are represented by green colored boxes. Putative metabolites observed in this study are represented with colored circles. Arrows represent direction of enzymatic activity.

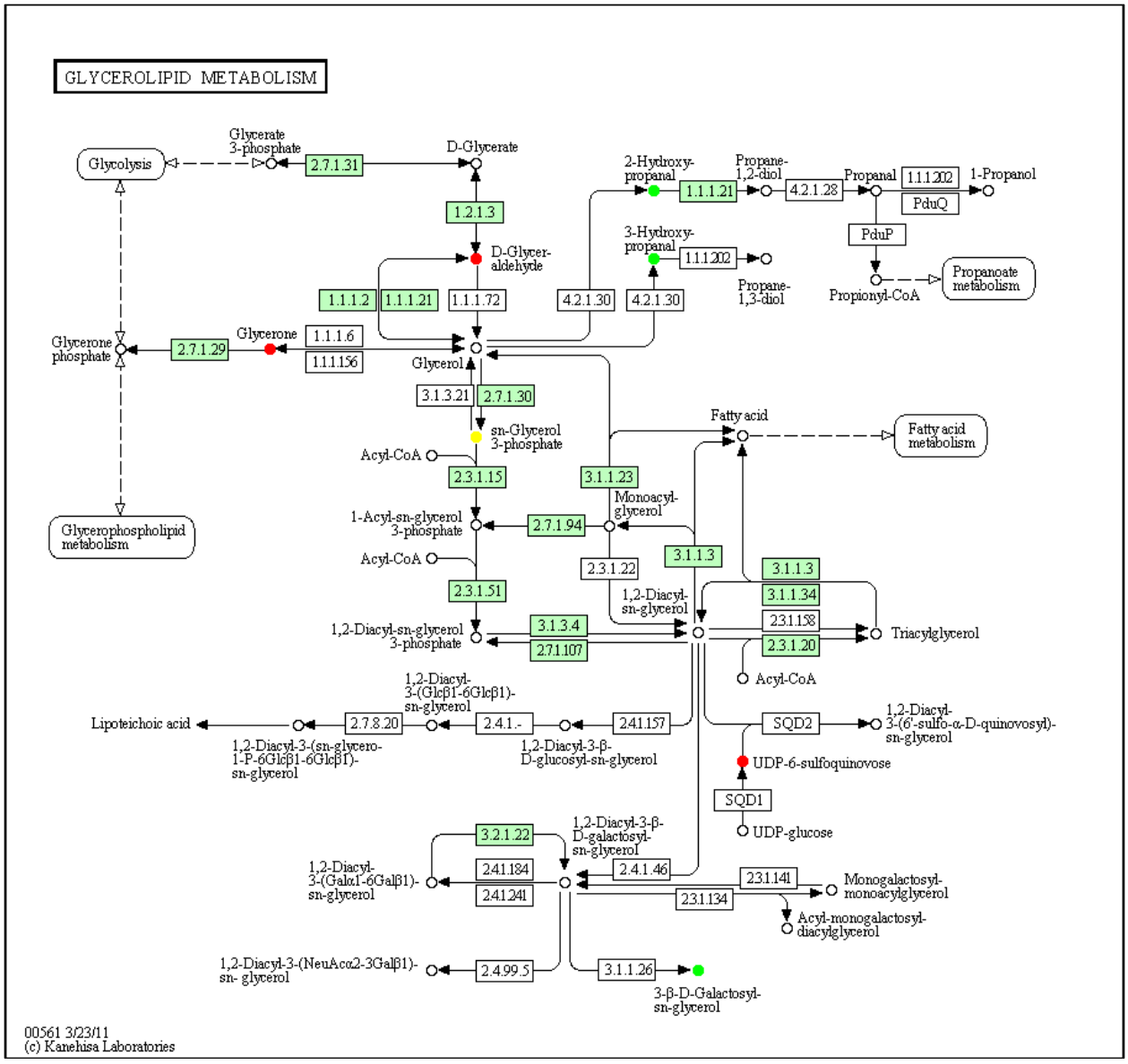


Figure E-13. Further evaluation of the glycerolipid metabolism pathway of the high dose of MPO colored by fold change (treatment vs. control) of high quality features identified with putative annotations within the pathway.

Features exhibiting abundance greater than 50% (x > 0.5) of the control are colored red, features between 50% and -50% (0.5 < x > - 0.5) are colored yellow and features with an abundance less than 50% (x < -0.5) of the control are colored green. Enzymes or enzymatic activity observed in humans are represented by green colored boxes. Putative metabolites observed in this study are represented with colored circles. Arrows represent direction of enzymatic activity.

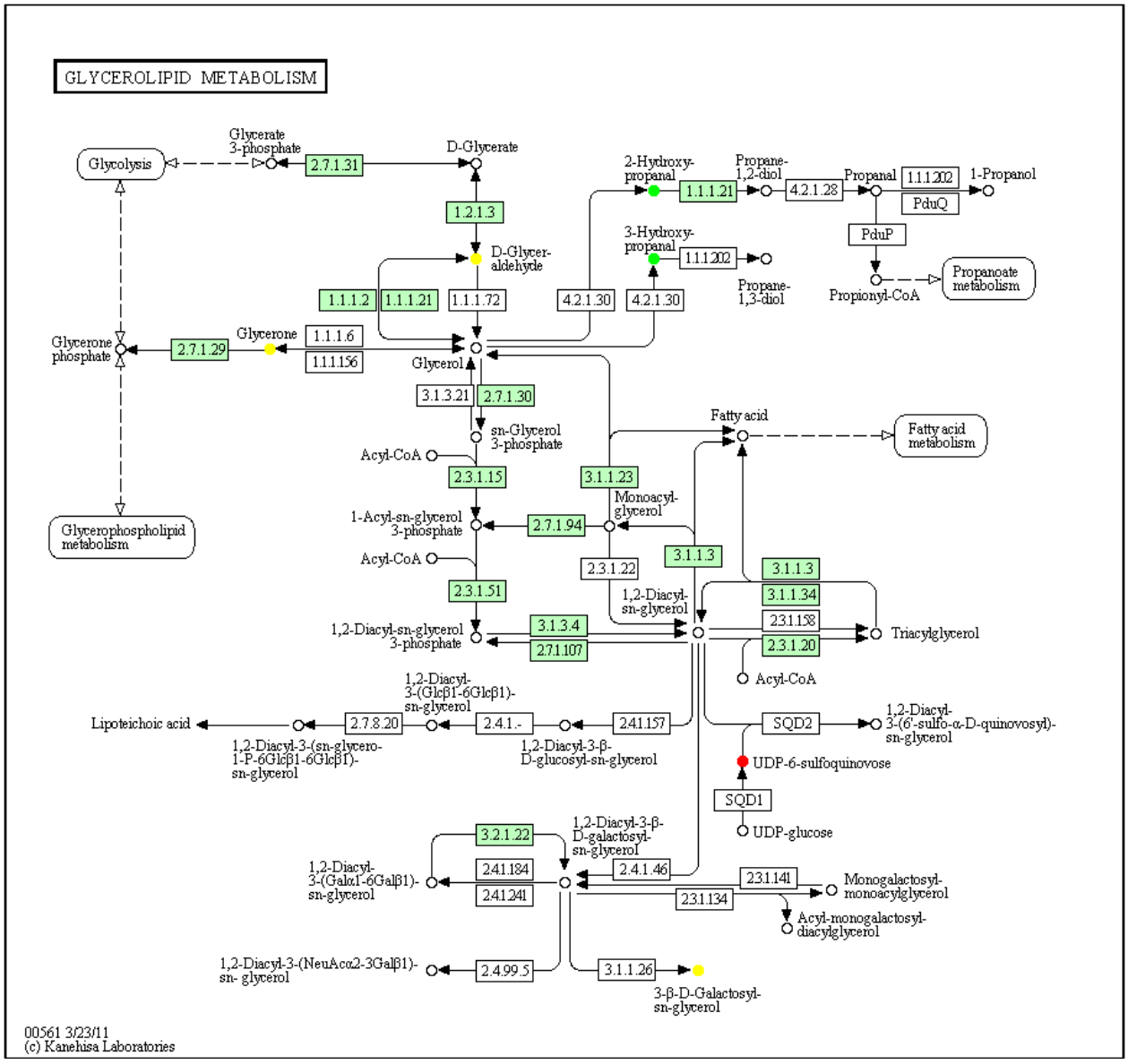


Figure E-14. Further evaluation of the glycerolipid metabolism pathway of the middle dose of MPO colored by fold change (treatment vs. control) of high quality features identified with putative annotations within the pathway.

Features exhibiting abundance greater than 50% ($x > 0.5$) of the control are colored red, features between 50% and -50% ($0.5 < x > - 0.5$) are colored yellow and features with an abundance less than 50% ($x < -0.5$) of the control are colored green. Enzymes or enzymatic activity observed in humans are represented by green colored boxes. Putative metabolites observed in this study are represented with colored circles. Arrows represent direction of enzymatic activity.

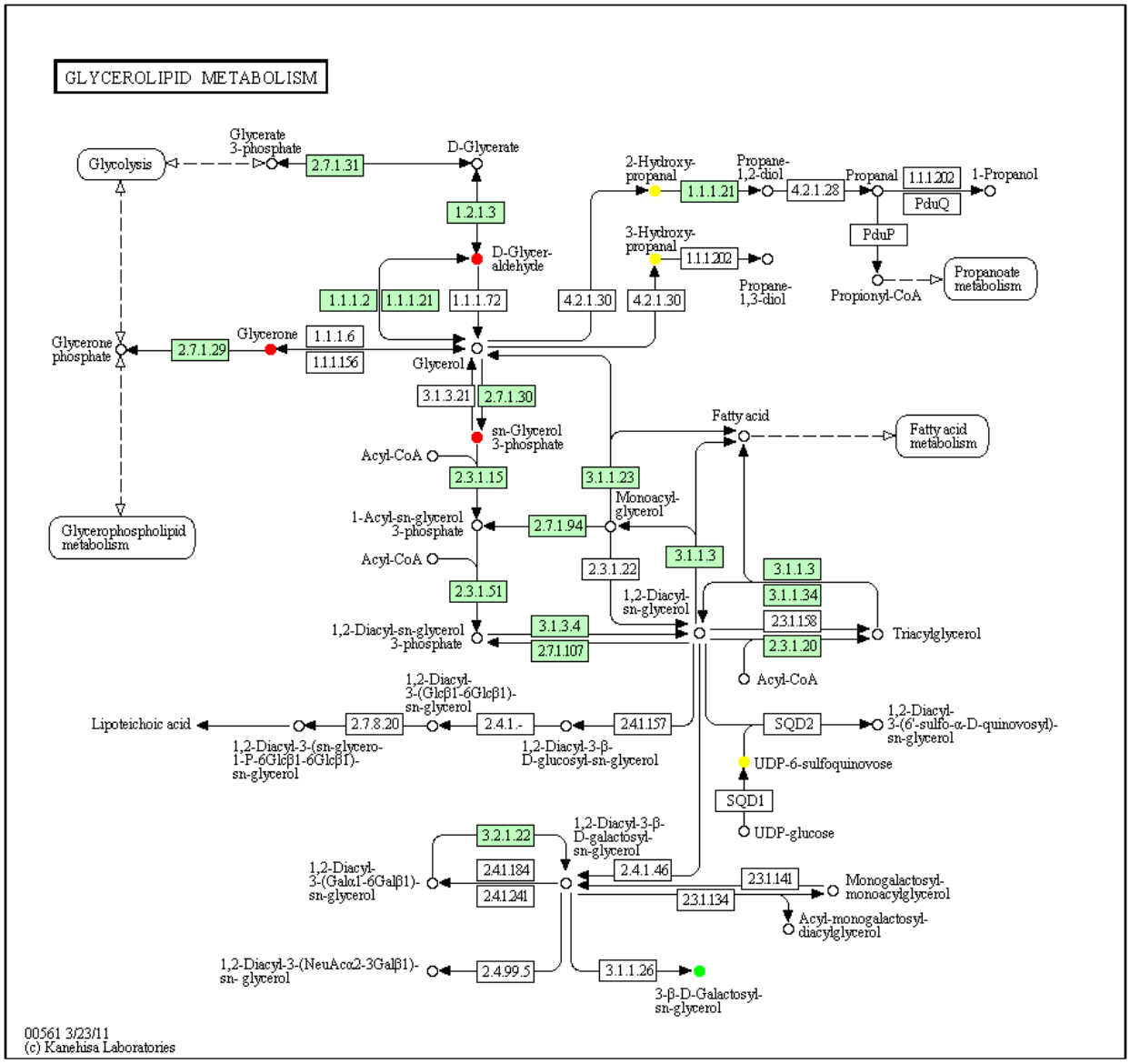


Figure E-15. Further evaluation of the glycerolipid metabolism pathway of the low dose of MPO colored by fold change (treatment vs. control) of high quality features identified with putative annotations within the pathway.

Features exhibiting abundance greater than 50% (x > 0.5) of the control are colored red, features between 50% and -50% (0.5 < x > - 0.5) are colored yellow and features with an abundance less than 50% (x < -0.5) of the control are colored green. Enzymes or enzymatic activity observed in humans are represented by green colored boxes. Putative metabolites observed in this study are represented with colored circles. Arrows represent direction of enzymatic activity.

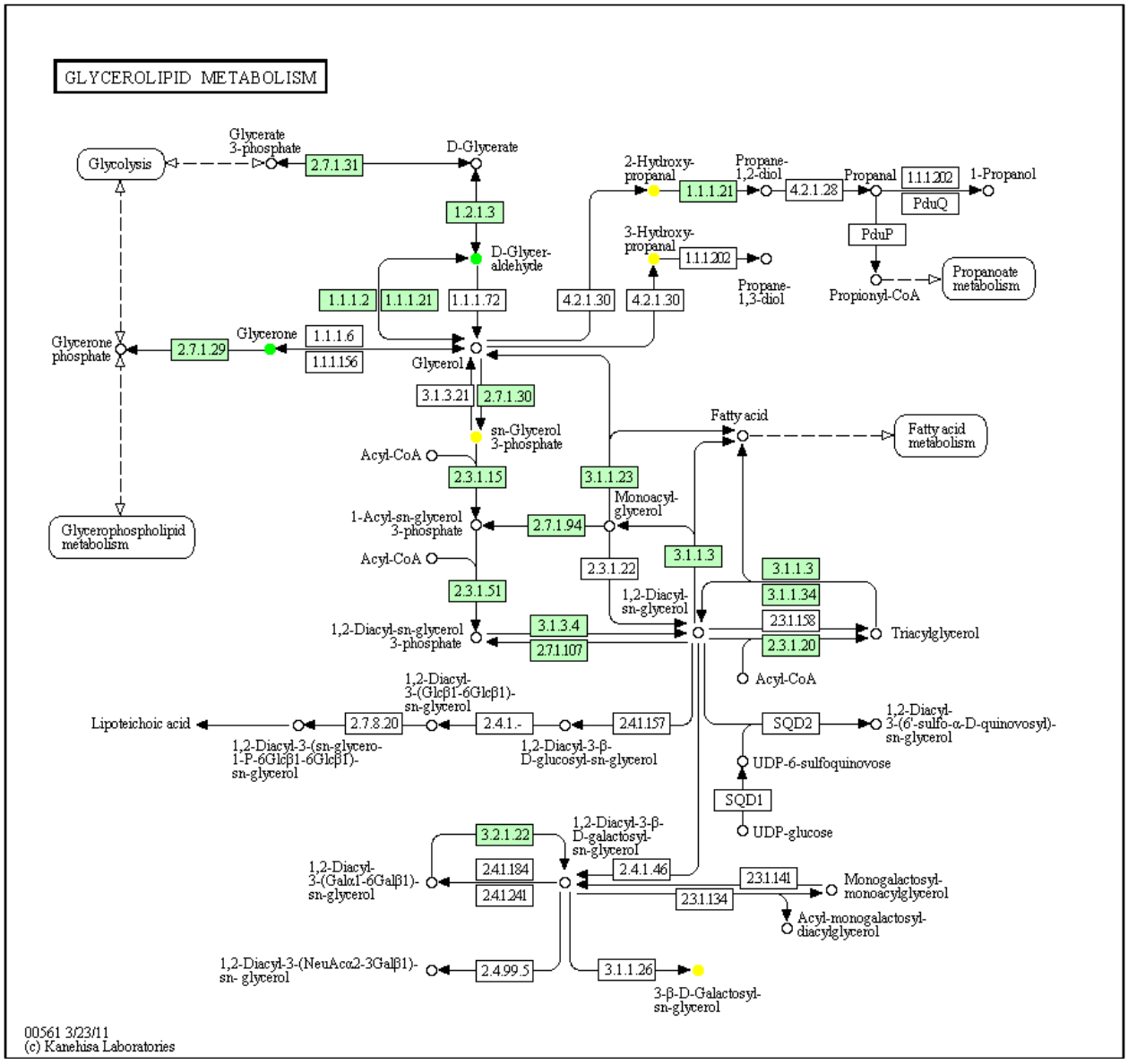


Figure E-16. Further evaluation of the glycerolipid metabolism pathway of the high dose of MP colored by fold change (treatment vs. control) of high quality features identified with putative annotations within the pathway.

Features exhibiting abundance greater than 50% (x > 0.5) of the control are colored red, features between 50% and -50% (0.5 < x > - 0.5) are colored yellow and features with an abundance less than 50% (x < -0.5) of the control are colored green. Enzymes or enzymatic activity observed in humans are represented by green colored boxes. Putative metabolites observed in this study are represented with colored circles. Arrows represent direction of enzymatic activity.

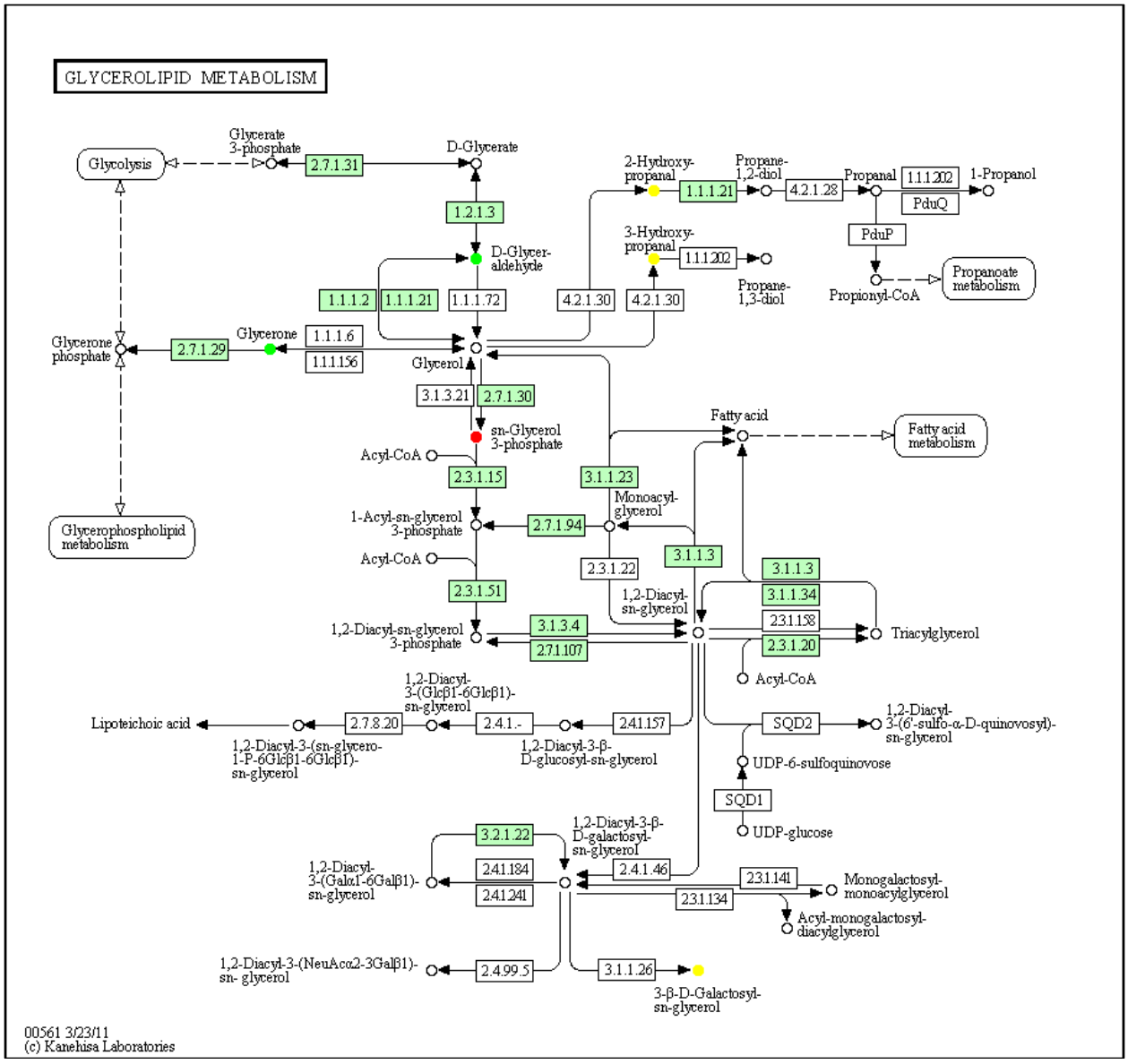


Figure E-17. Further evaluation of the glycerolipid metabolism pathway of the middle dose of MP colored by fold change (treatment vs. control) of high quality features identified with putative annotations within the pathway.

Features exhibiting abundance greater than 50% (x > 0.5) of the control are colored red, features between 50% and -50% (0.5 < x > - 0.5) are colored yellow and features with an abundance less than 50% (x < -0.5) of the control are colored green. Enzymes or enzymatic activity observed in humans are represented by green colored boxes. Putative metabolites observed in this study are represented with colored circles. Arrows represent direction of enzymatic activity.

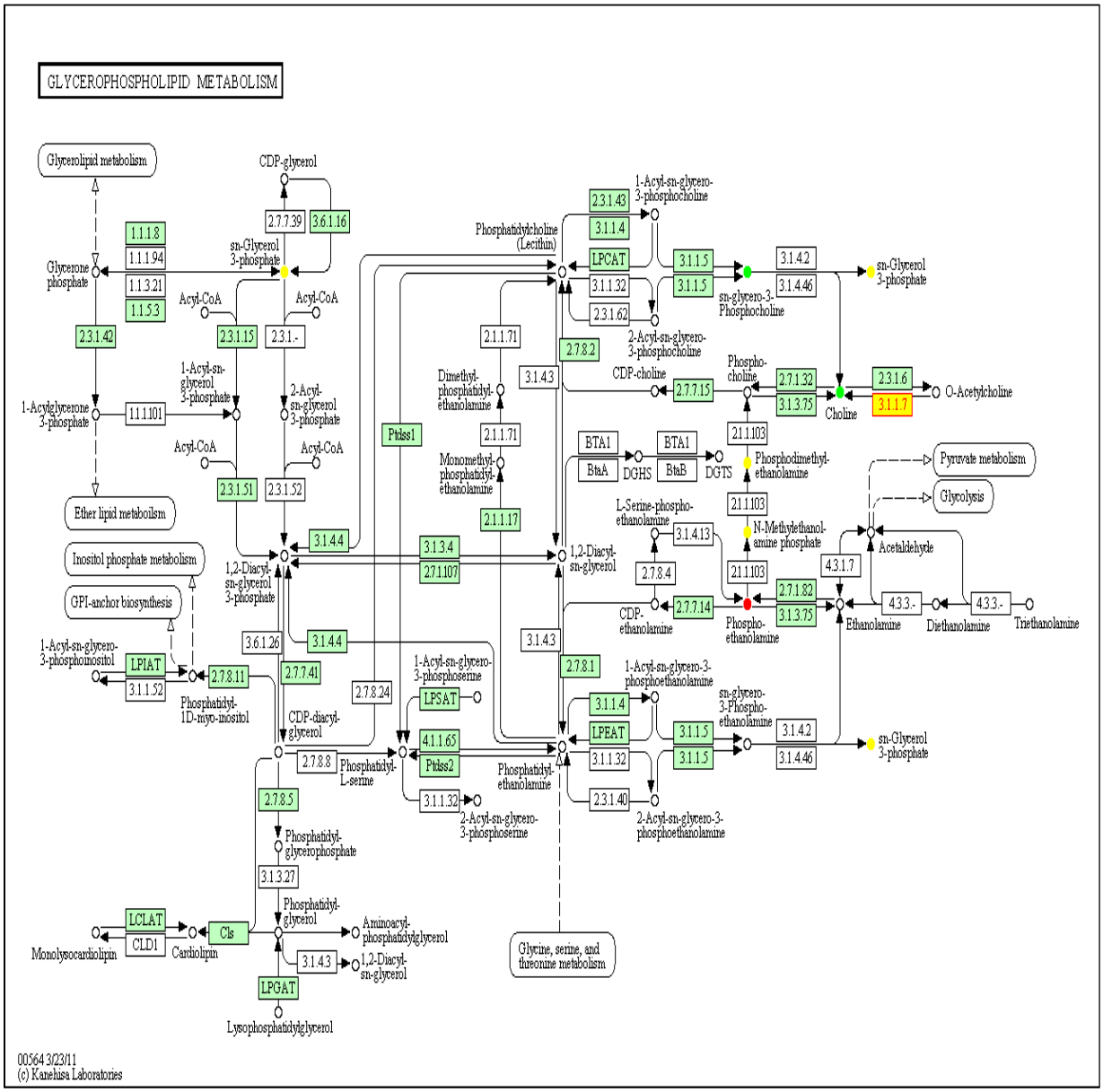


Figure E-18. Further evaluation of the glycerophospholipid metabolism pathway of the high dose of MPO colored by fold change (treatment vs. control) of high quality features identified with putative annotations within the pathway.

Features exhibiting abundance greater than 50% (x > 0.5) of the control are colored red, features between 50% and -50% (0.5 < x > -0.5) are colored yellow and features with an abundance less than 50% (x < -0.5) of the control are colored green. Enzymes or enzymatic activity observed in humans are represented by green colored boxes. Putative metabolites observed in this study are represented with colored circles. Arrows represent direction of enzymatic activity. Acetylcholinesterase, (AChE) an enzyme effected by MPO, is highlighted with a yellow box.

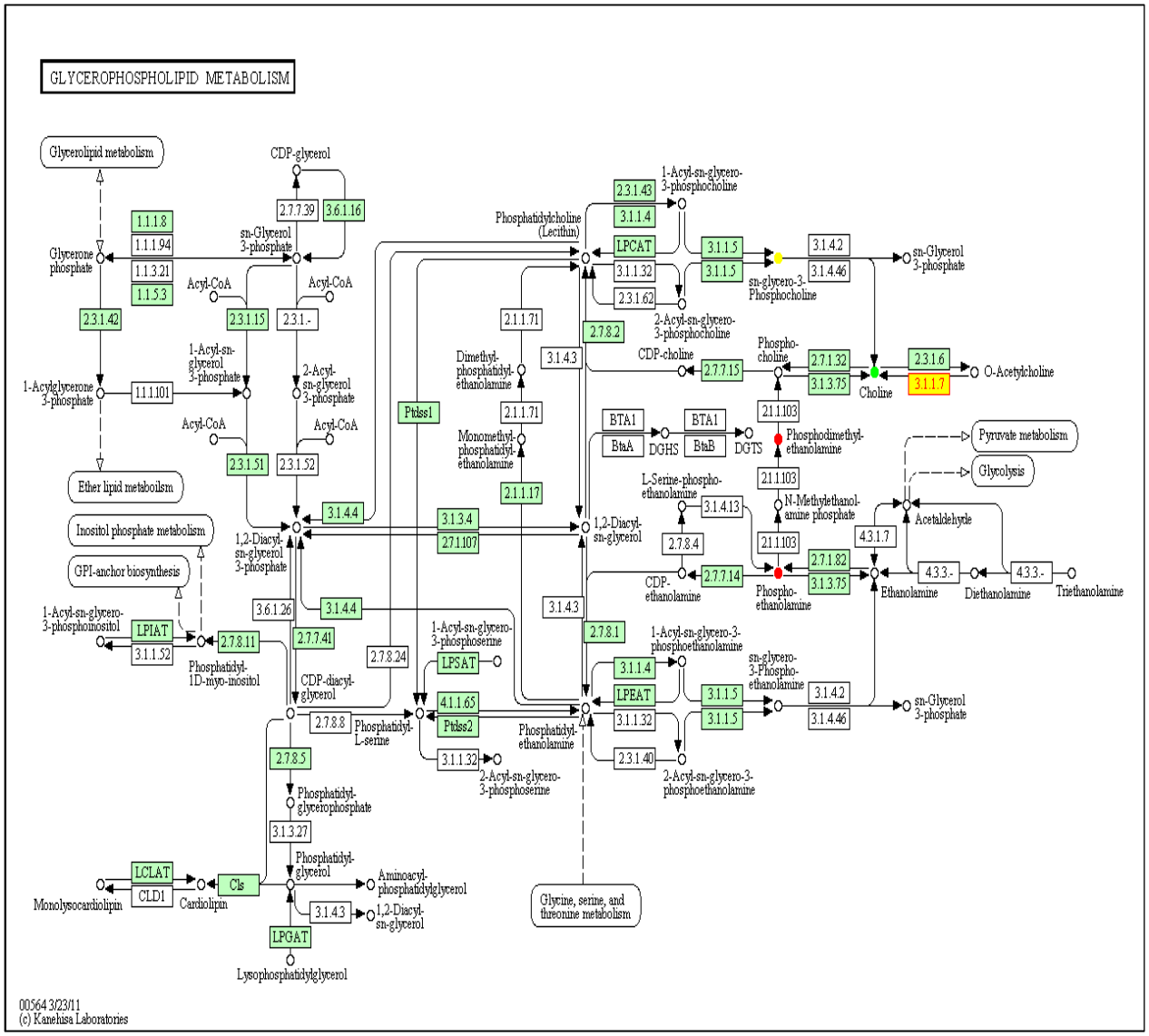


Figure E-19. Further evaluation of the glycerophospholipid metabolism pathway of the middle dose of MPO colored by fold change (treatment vs. control) of high quality features identified with putative annotations within the pathway.

Features exhibiting abundance greater than 50% (x > 0.5) of the control are colored red, features between 50% and -50% (0.5 < x > -0.5) are colored yellow and features with an abundance less than 50% (x < - 0.5) of the control are colored green. Enzymes or enzymatic activity observed in humans are represented by green colored boxes. Putative metabolites observed in this study are represented with colored circles. Arrows represent direction of enzymatic activity. AChE an enzyme effected by MPO is highlighted with a yellow box.

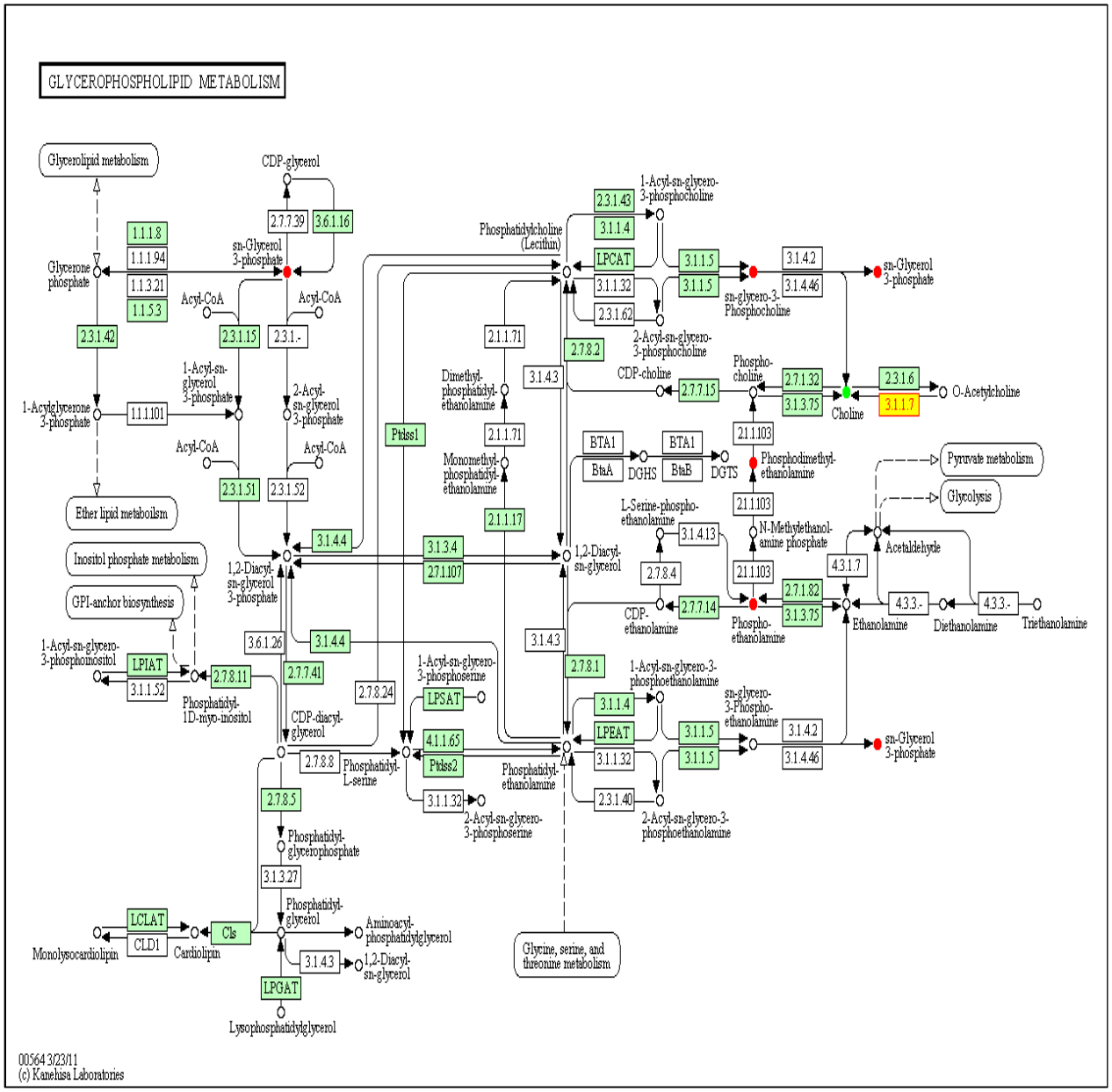


Figure E-20. Further evaluation of the glycerophospholipid metabolism pathway of the low dose of MPO colored by fold change (treatment vs. control) of high quality features identified with putative annotations within the pathway.

Features exhibiting abundance greater than 50% (x > 0.5) of the control are colored red, features between 50% and -50% (0.5 < x > -0.5) are colored yellow and features with an abundance less than 50% (x < -0.5) of the control are colored green. Enzymes or enzymatic activity observed in humans are represented by green colored boxes. Putative metabolites observed in this study are represented with colored circles. Arrows represent direction of enzymatic activity. AChE an enzyme effected by MPO is highlighted with a yellow box.

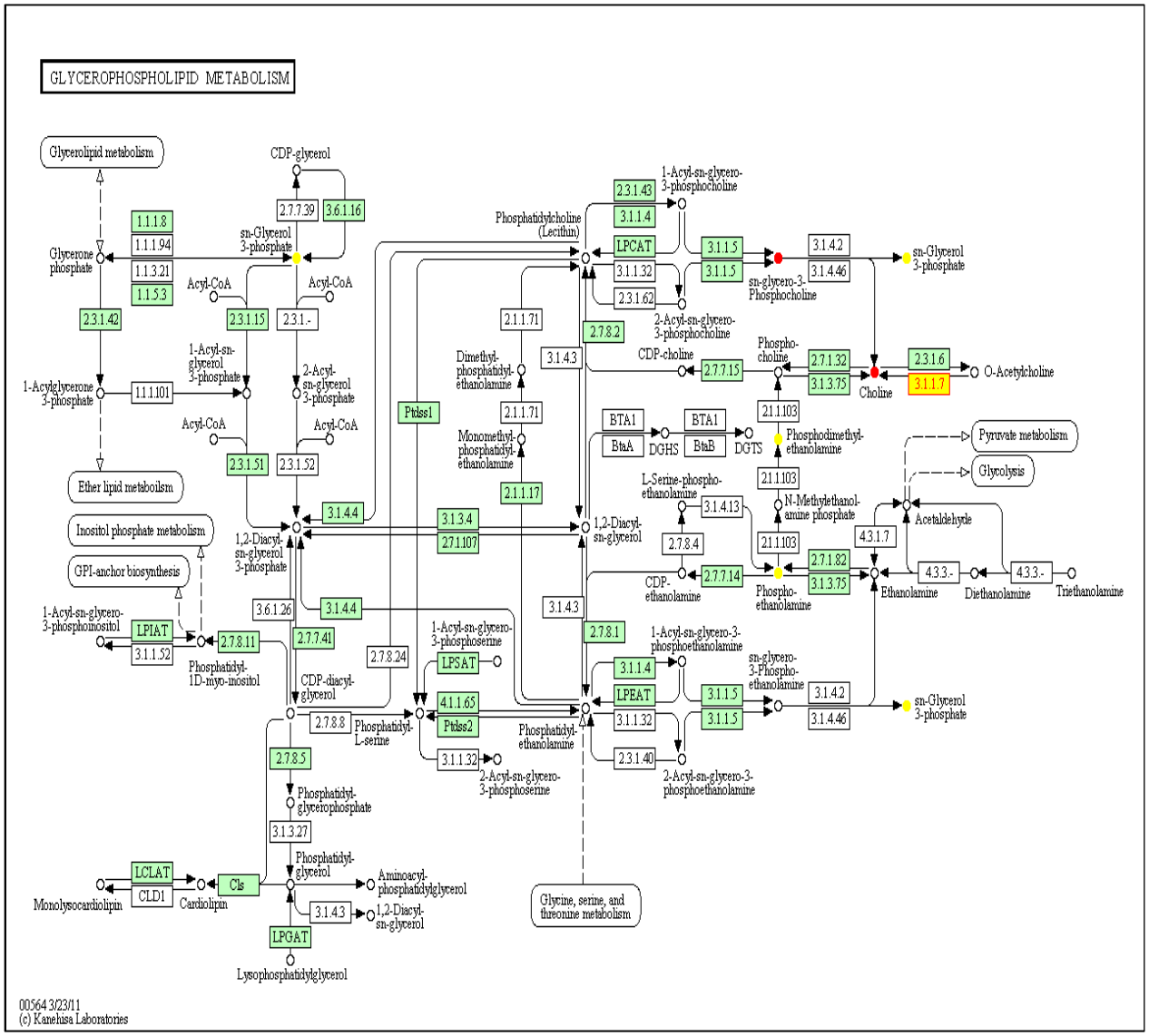


Figure E-21. Further evaluation of the glycerophospholipid metabolism pathway of the high dose of MP colored by fold change (treatment vs. control) of high quality features identified with putative annotations within the pathway.

Features exhibiting abundance greater than 50% (x > 0.5) of the control are colored red, features between 50% and -50% (0.5 < x > -0.5) are colored yellow and features with an abundance less than 50% (x < -0.5) of the control are colored green. Enzymes or enzymatic activity observed in humans are represented by green colored boxes. Putative metabolites observed in this study are represented with colored circles. Arrows represent direction of enzymatic activity. AChE an enzyme effected by MPO is highlighted with a yellow box.

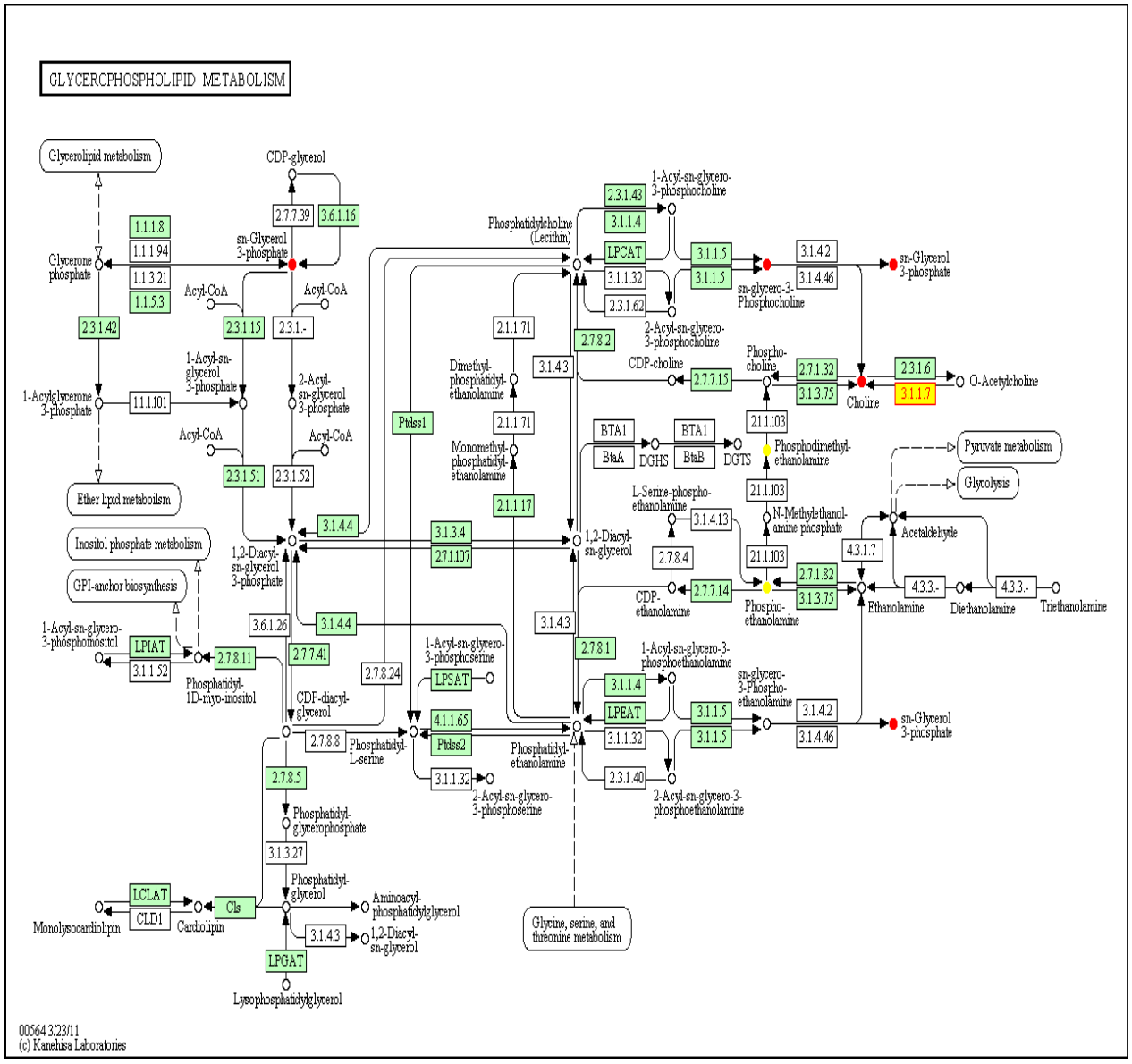


Figure E-22. Further evaluation of the glycerophospholipid metabolism pathway of the middle dose of MP colored by fold change (treatment vs. control) of high quality features identified with putative annotations within the pathway.

Features exhibiting abundance greater than 50% (x > 0.5) of the control are colored red, features between 50% and -50% (0.5 < x > -0.5) are colored yellow and features with an abundance less than 50% (x < - 0.5) of the control are colored green. Enzymes or enzymatic activity observed in humans are represented by green colored boxes. Putative metabolites observed in this study are represented with colored circles. Arrows represent direction of enzymatic activity. AChE an enzyme effected by MPO is highlighted with a yellow box.

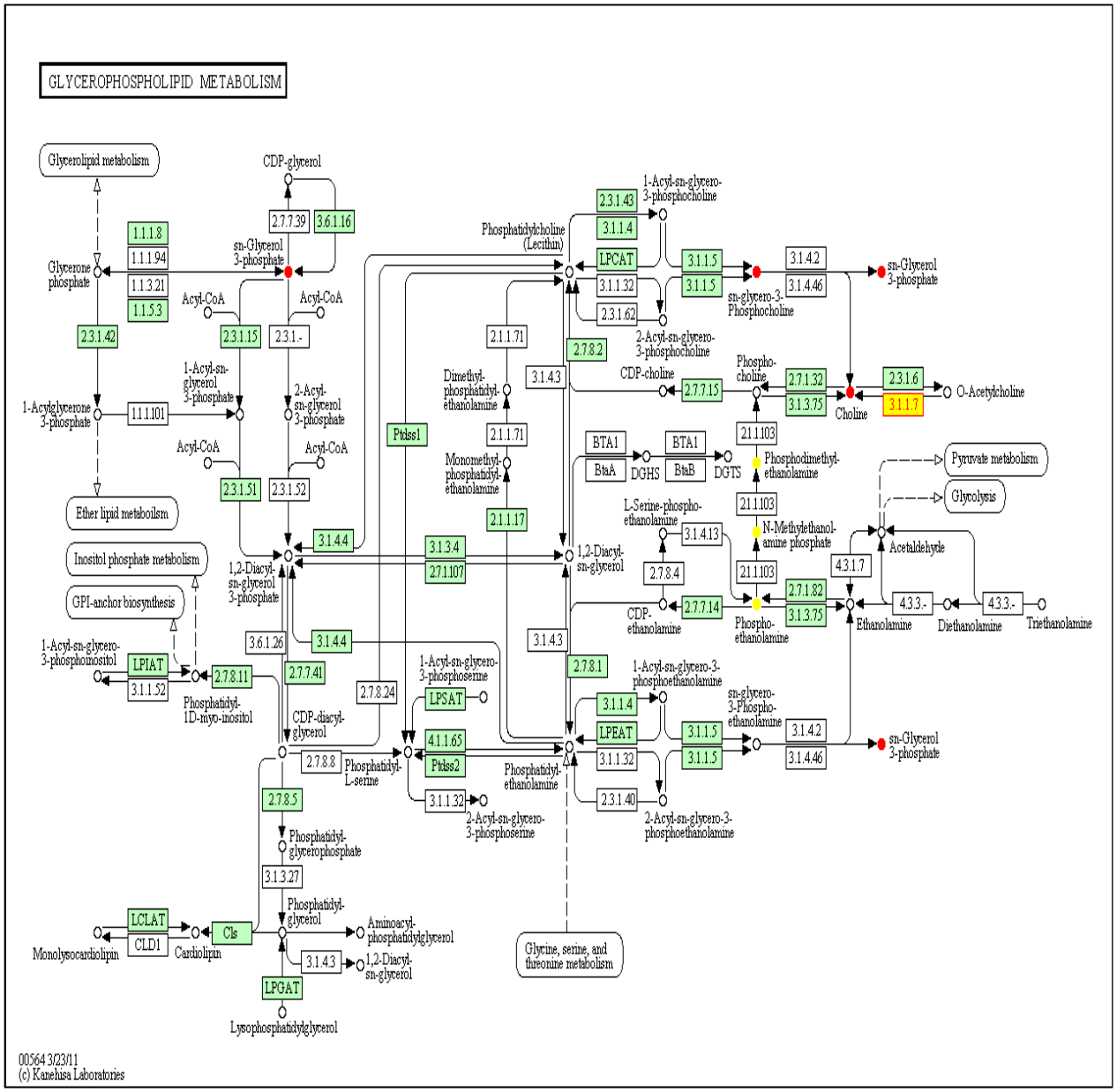


Figure E-23. Further evaluation of the glycerophospholipid metabolism pathway of the low dose of MP colored by fold change (treatment vs. control) of high quality features identified with putative annotations within the pathway.

Features exhibiting abundance greater than 50% (x > 0.5) of the control are colored red, features between 50% and -50% (0.5 < x > -0.5) are colored yellow and features with an abundance less than 50% (x < -0.5) of the control are colored green. Enzymes or enzymatic activity observed in humans are represented by green colored boxes. Putative metabolites observed in this study are represented with colored circles. Arrows represent direction of enzymatic activity. AChE an enzyme effected by MPO is highlighted with a yellow box.

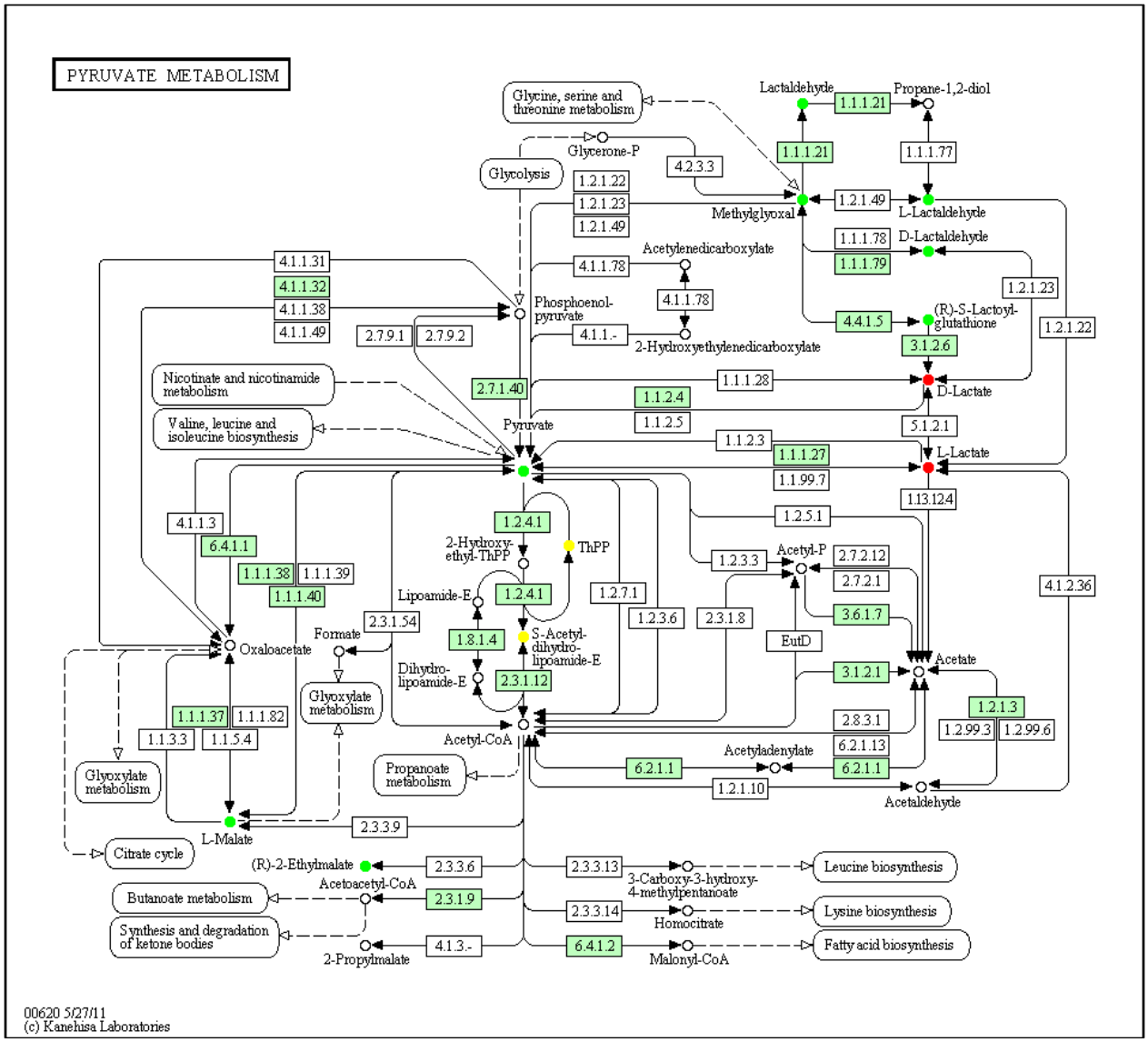


Figure E-24. Further evaluation of the pyruvate metabolism pathway of the high dose of MPO colored by fold change (treatment vs. control) of high quality features identified with putative annotations within the pathway.

Features exhibiting abundance greater than 50% (x > 0.5) of the control are colored red, features between 50% and -50% (0.5 < x > - 0.5) are colored yellow and features with an abundance less than 50% (x < -0.5) of the control are colored green. Enzymes or enzymatic activity observed in humans are represented by green colored boxes. Putative metabolites observed in this study are represented with colored circles. Arrows represent direction of enzymatic activity.

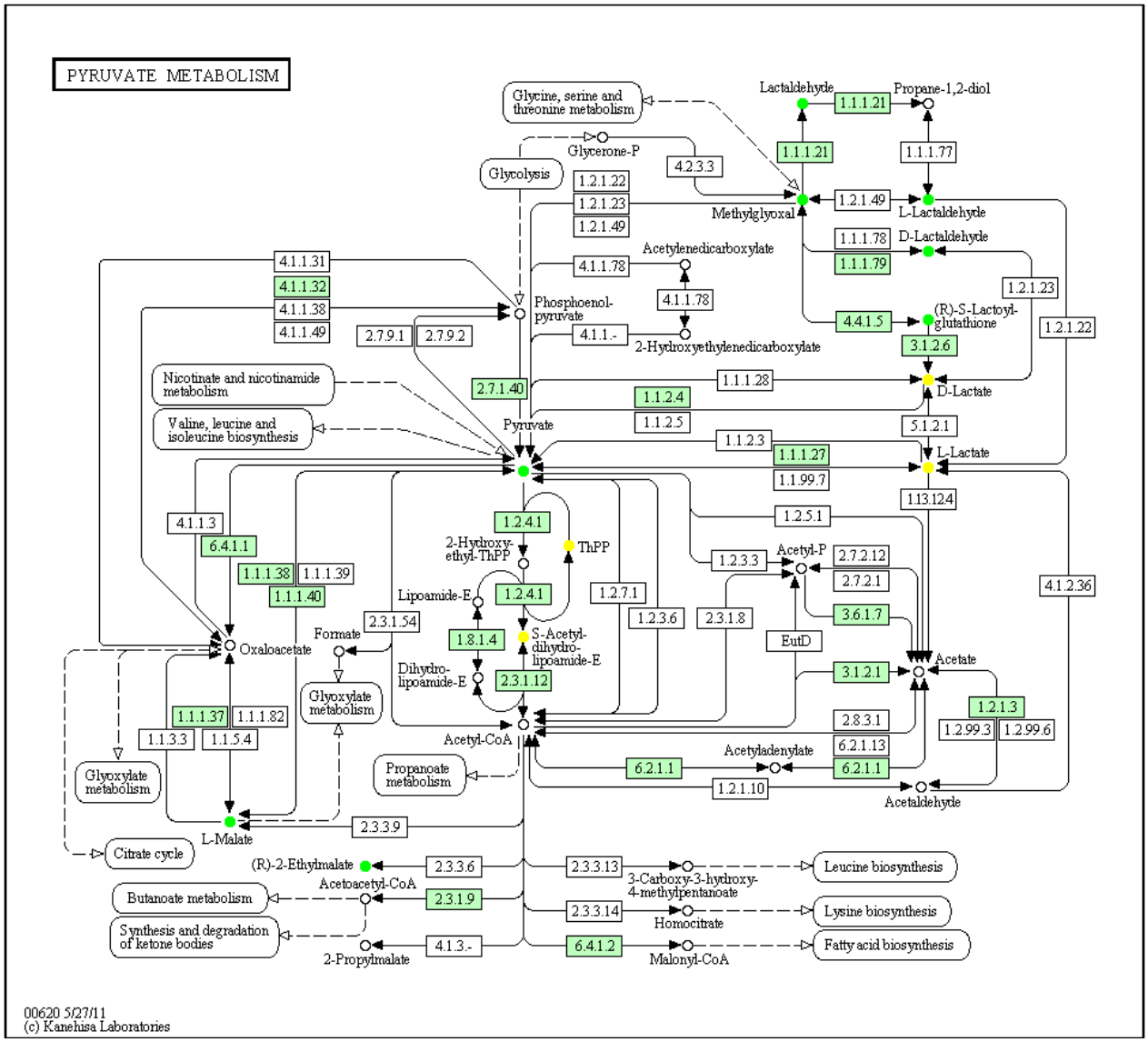


Figure E-25. Further evaluation of the pyruvate metabolism pathway of the middle dose of MPO colored by fold change (treatment vs. control) of high quality features identified with putative annotations within the pathway.

Features exhibiting abundance greater than 50% (x > 0.5) of the control are colored red, features between 50% and -50% (0.5 < x > - 0.5) are colored yellow and features with an abundance less than 50% (x < -0.5) of the control are colored green. Enzymes or enzymatic activity observed in humans are represented by green colored boxes. Putative metabolites observed in this study are represented with colored circles. Arrows represent direction of enzymatic activity.

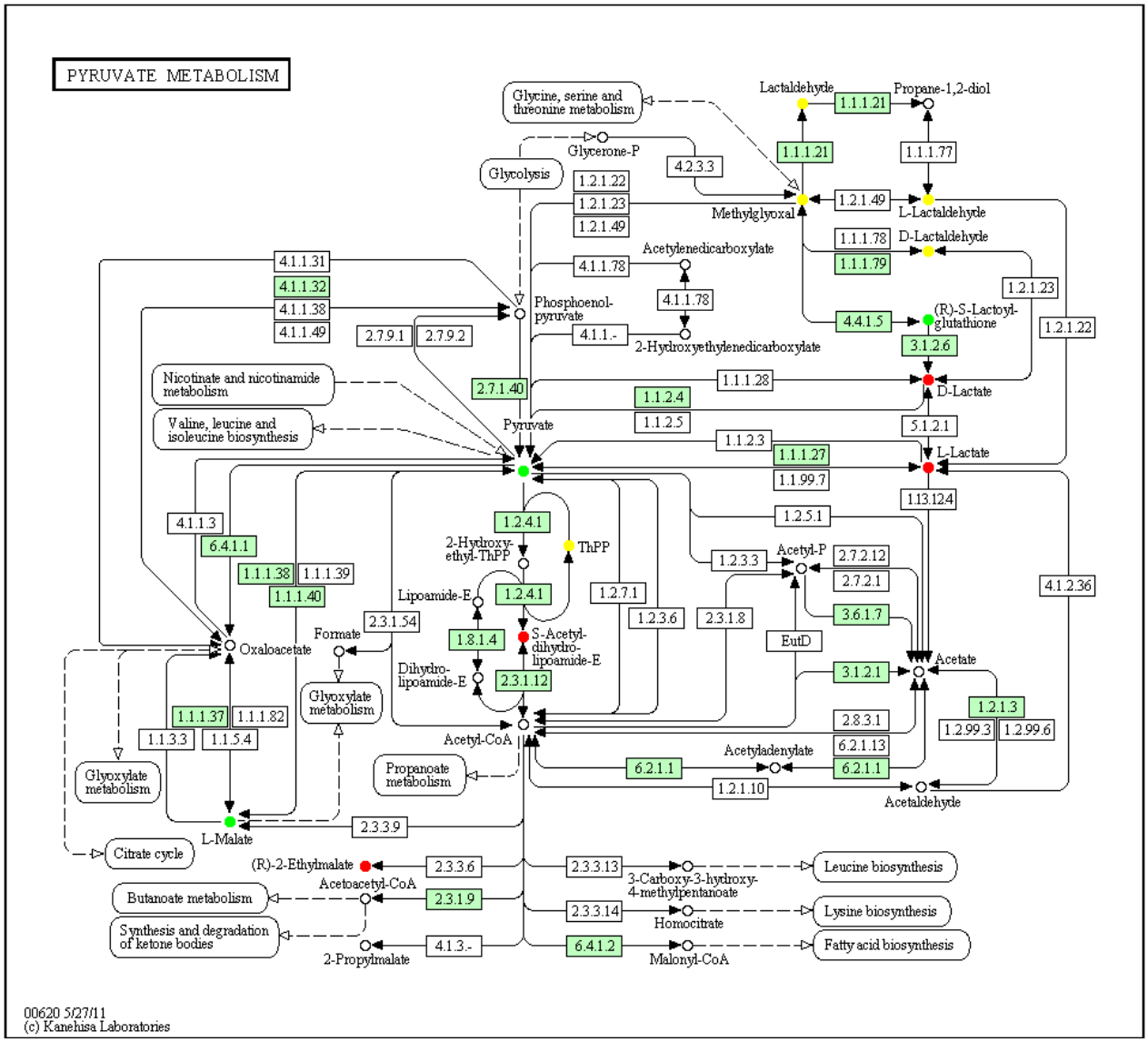


Figure E-26. Further evaluation of the pyruvate metabolism pathway of the low dose of MPO colored by fold change (treatment vs. control) of high quality features identified with putative annotations within the pathway.

Features exhibiting abundance greater than 50% (x > 0.5) of the control are colored red, features between 50% and -50% (0.5 < x > -0.5) are colored yellow and features with an abundance less than 50% (x < -0.5) of the control are colored green. Enzymes or enzymatic activity observed in humans are represented by green colored boxes. Putative metabolites observed in this study are represented with colored circles. Arrows represent direction of enzymatic activity.

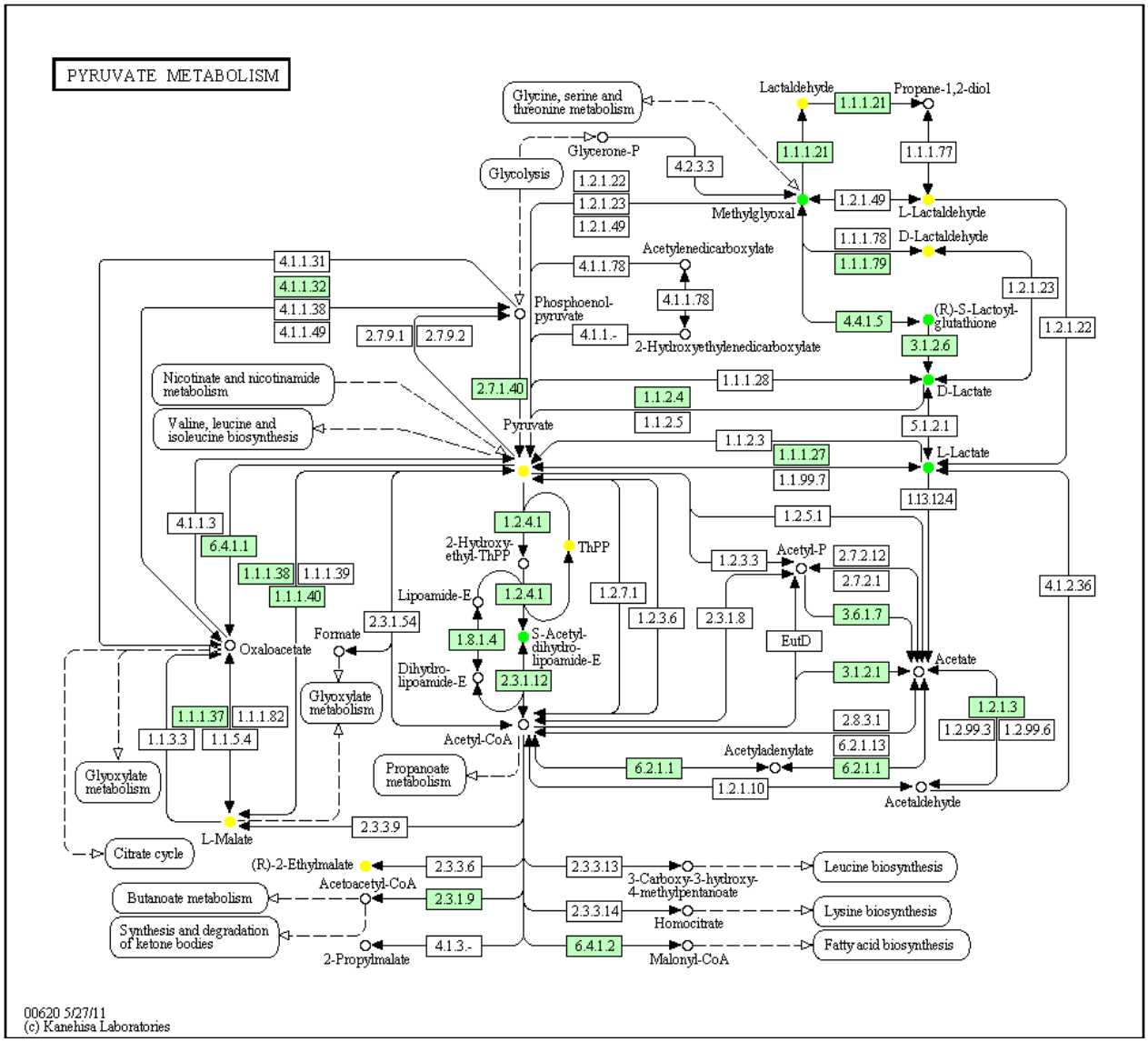


Figure E-27. Further evaluation of the pyruvate metabolism pathway of the high dose of MP colored by fold change (treatment vs. control) of high quality features identified with putative annotations within the pathway.

Features exhibiting abundance greater than 50% (x > 0.5) of the control are colored red, features between 50% and -50% (0.5 < x > -0.5) are colored yellow and features with an abundance less than 50% (x < -0.5) of the control are colored green. Enzymes or enzymatic activity observed in humans are represented by green colored boxes. Putative metabolites observed in this study are represented with colored circles. Arrows represent direction of enzymatic activity.

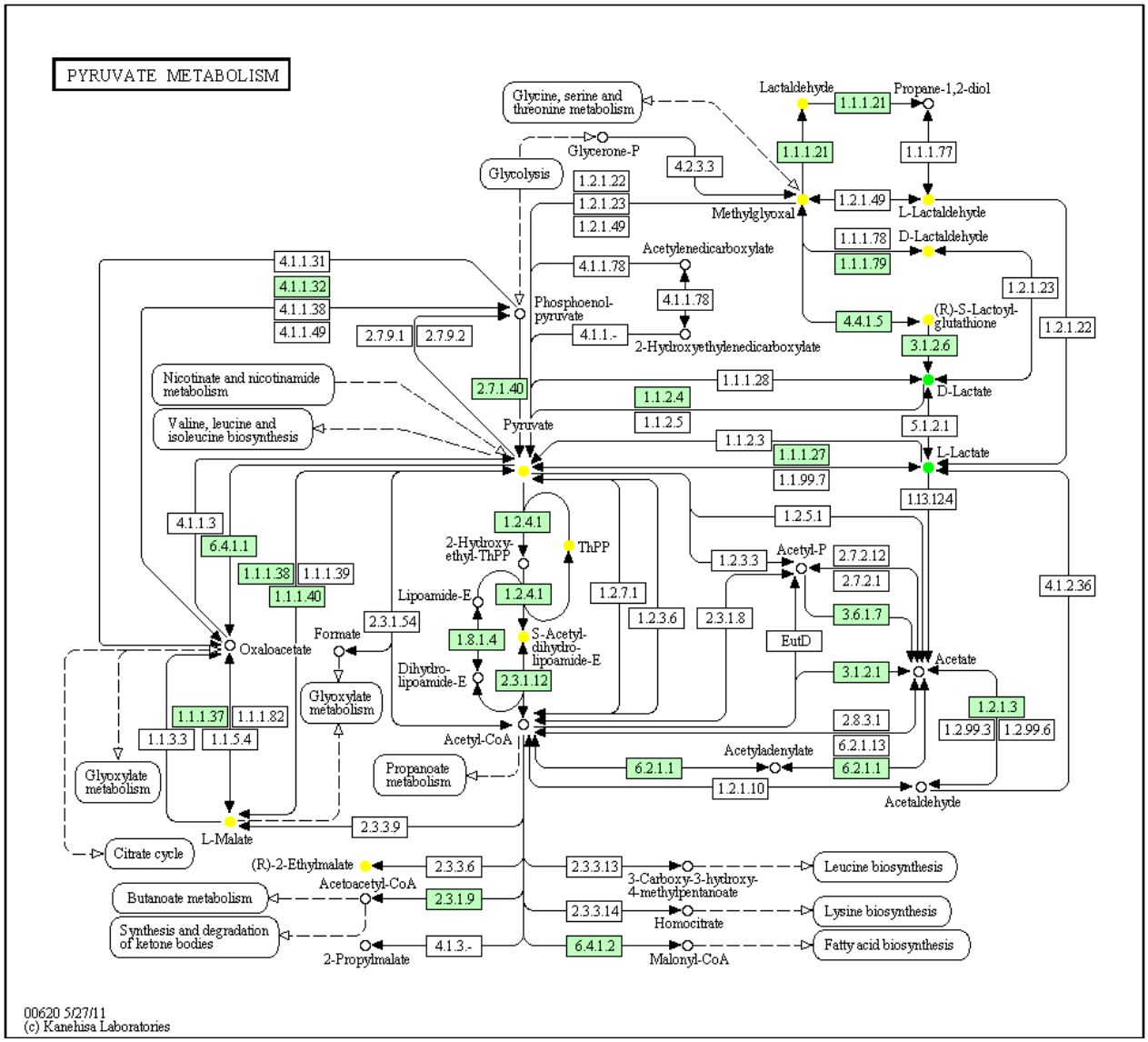


Figure E-28. Further evaluation of the pyruvate metabolism pathway of the middle dose of MP colored by fold change (treatment vs. control) of high quality features identified with putative annotations within the pathway.

Features exhibiting abundance greater than 50% (x > 0.5) of the control are colored red, features between 50% and -50% (0.5 < x > -0.5) are colored yellow and features with an abundance less than 50% (x < -0.5) of the control are colored green. Enzymes or enzymatic activity observed in humans are represented by green colored boxes. Putative metabolites observed in this study are represented with colored circles. Arrows represent direction of enzymatic activity.

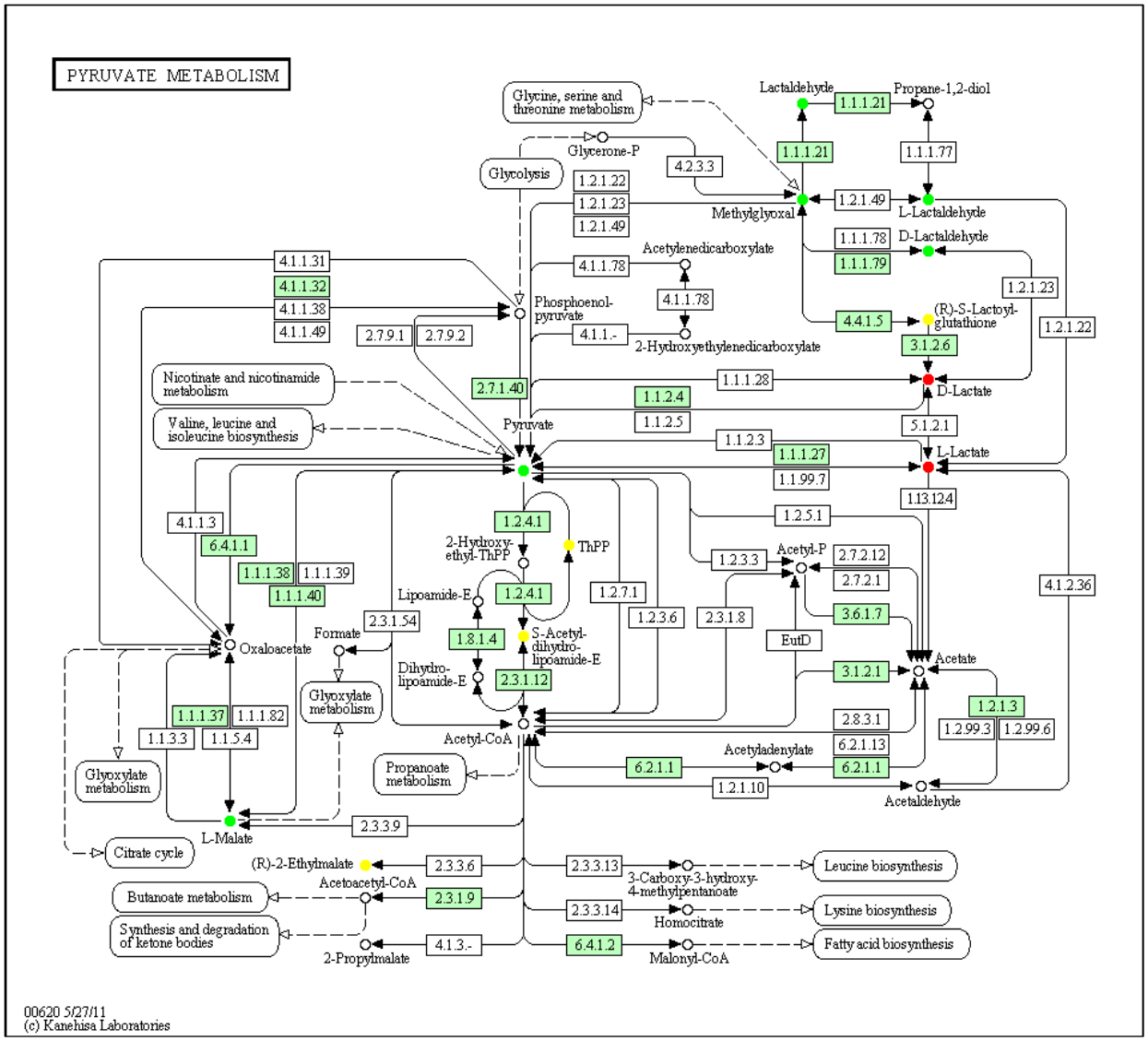


Figure E-29. Further evaluation of the pyruvate metabolism pathway of the low dose of MP colored by fold change (treatment vs. control) of high quality features identified with putative annotations within the pathway.

Features exhibiting abundance greater than 50% (x > 0.5) of the control are colored red, features between 50% and -50% (0.5 < x > -0.5) are colored yellow and features with an abundance less than 50% (x < -0.5) of the control are colored green. Enzymes or enzymatic activity observed in humans are represented by green colored boxes. Putative metabolites observed in this study are represented with colored circles. Arrows represent direction of enzymatic activity.

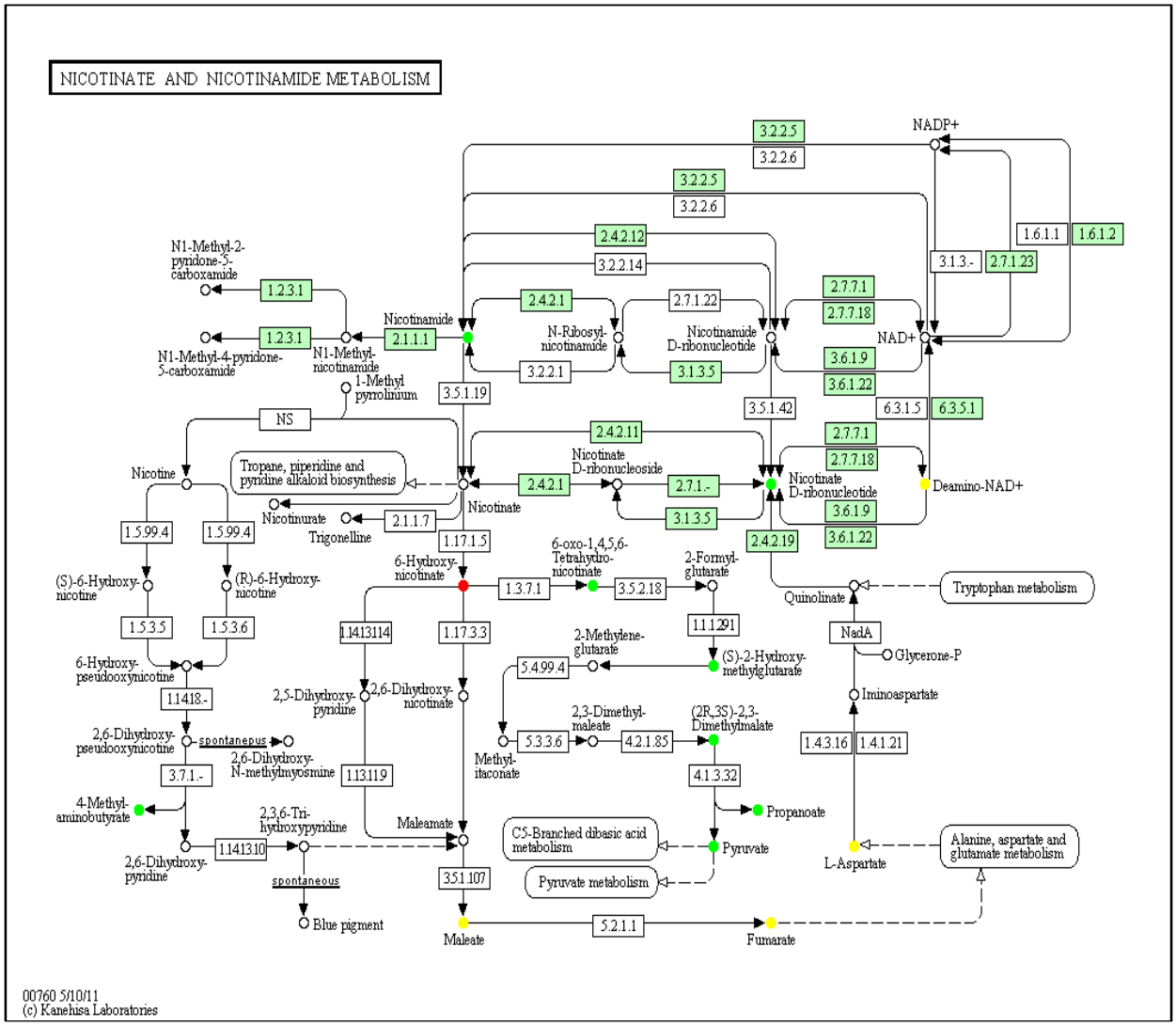


Figure E-30. Further evaluation of the nicotinate and nicotinamide metabolism pathway of the high dose of MPO colored by fold change (treatment vs. control) of high quality features identified with putative annotations within the pathway.

Features exhibiting abundance greater than 50% ($x > 0.5$) of the control are colored red, features between 50% and -50% ($0.5 < x > -0.5$) are colored yellow and features with an abundance less than 50% ($x < -0.5$) of the control are colored green. Enzymes or enzymatic activity observed in humans are represented by green colored boxes. Putative metabolites observed in this study are represented with colored circles. Arrows represent direction of enzymatic activity.

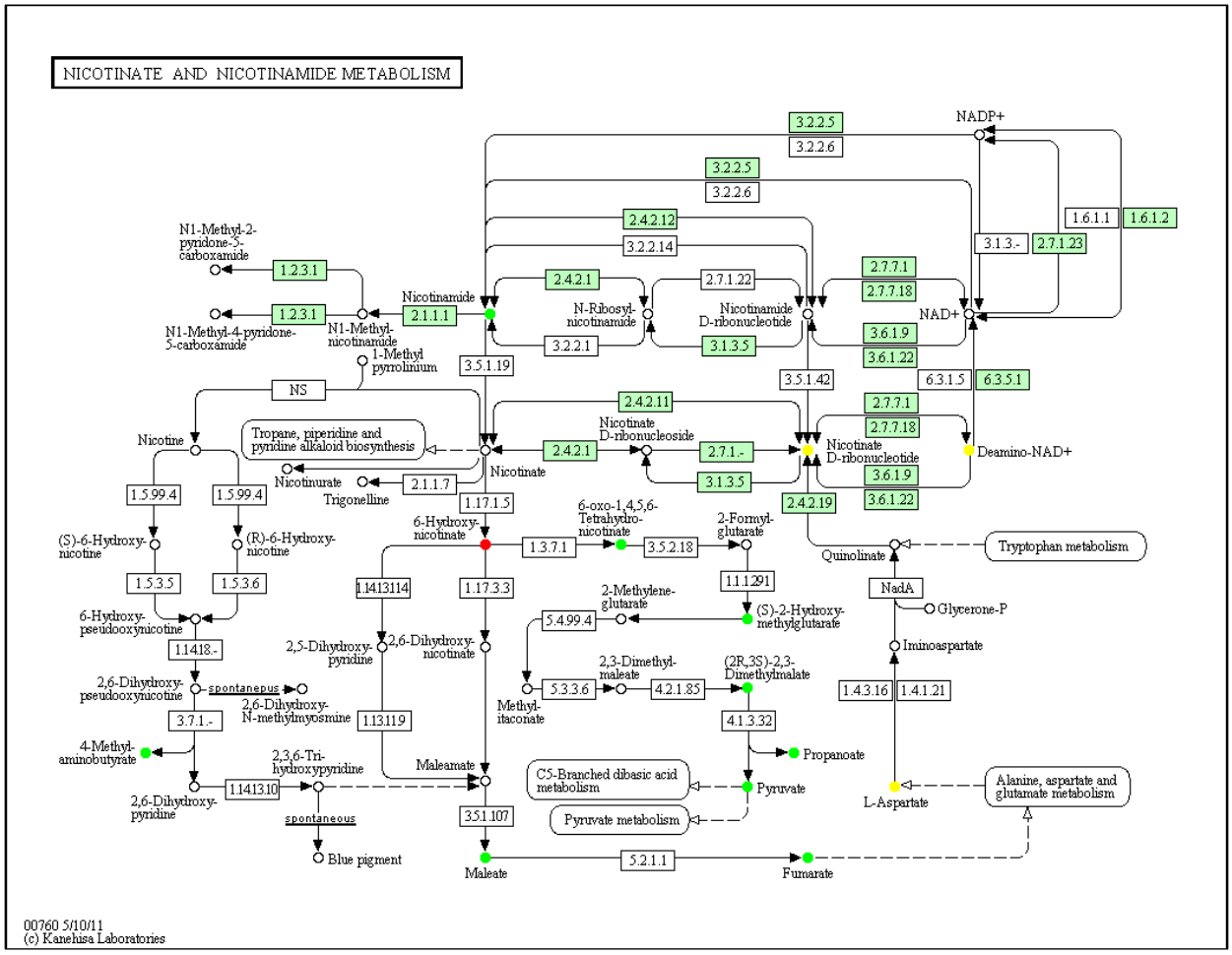


Figure E-31. Further evaluation of the nicotinate and nicotinamide metabolism pathway of the middle dose of MPO colored by fold change (treatment vs. control) of high quality features identified with putative annotations within the pathway.

Features exhibiting abundance greater than 50% (x > 0.5) of the control are colored red, features between 50% and -50% (0.5 < x > -0.5) are colored yellow and features with an abundance less than 50% (x < -0.5) of the control are colored green. Enzymes or enzymatic activity observed in humans are represented by green colored boxes. Putative metabolites observed in this study are represented with colored circles. Arrows represent direction of enzymatic activity.

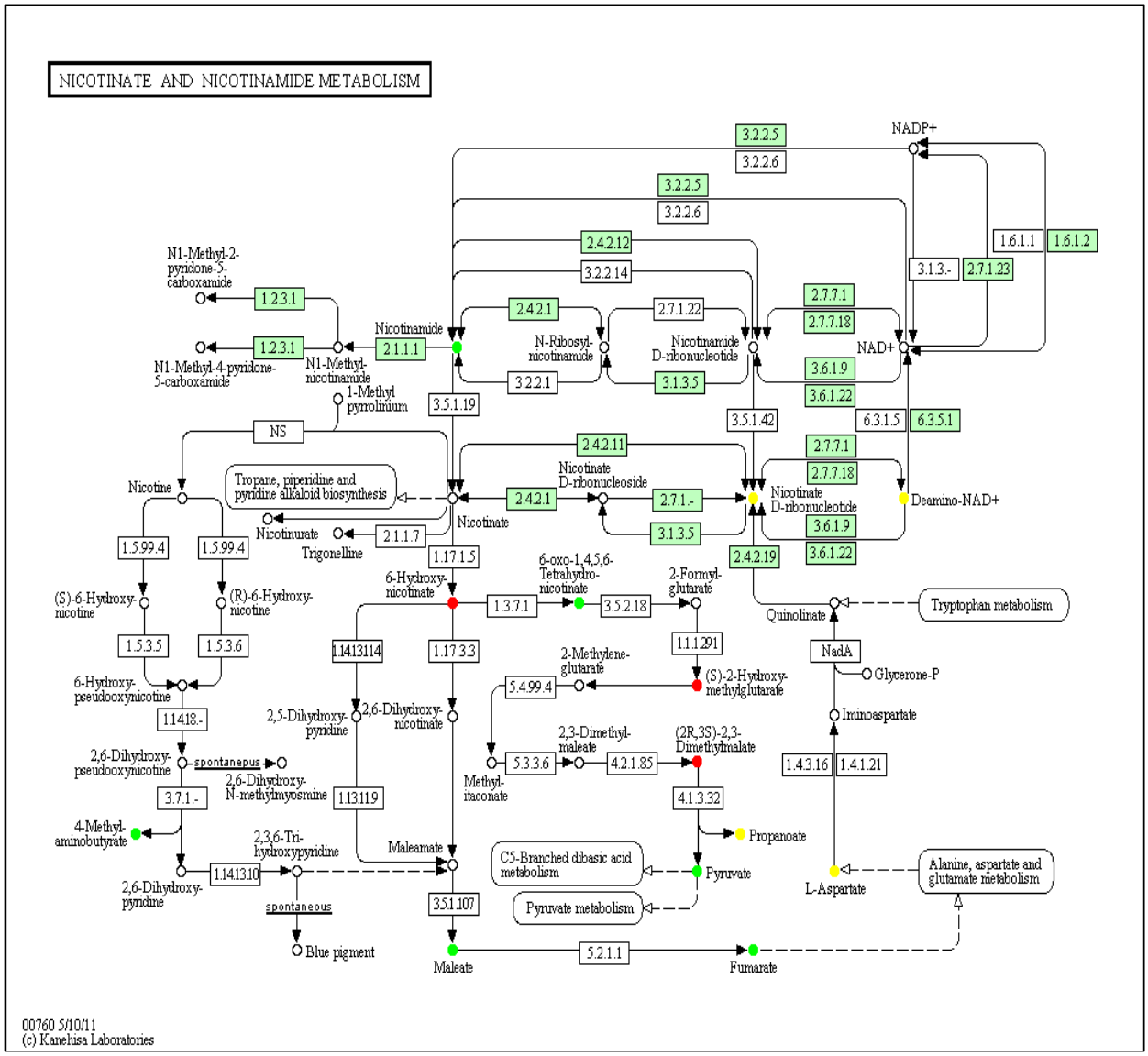


Figure E-32. Further evaluation of the nicotinate and nicotinamide metabolism pathway of the low dose of MPO colored by fold change (treatment vs. control) of high quality features identified with putative annotations within the pathway.

Features exhibiting abundance greater than 50% (x > 0.5) of the control are colored red, features between 50% and -50% (0.5 < x > -0.5) are colored yellow and features with an abundance less than 50% (x < -0.5) of the control are colored green. Enzymes or enzymatic activity observed in humans are represented by green colored boxes. Putative metabolites observed in this study are represented with colored circles. Arrows represent direction of enzymatic activity.

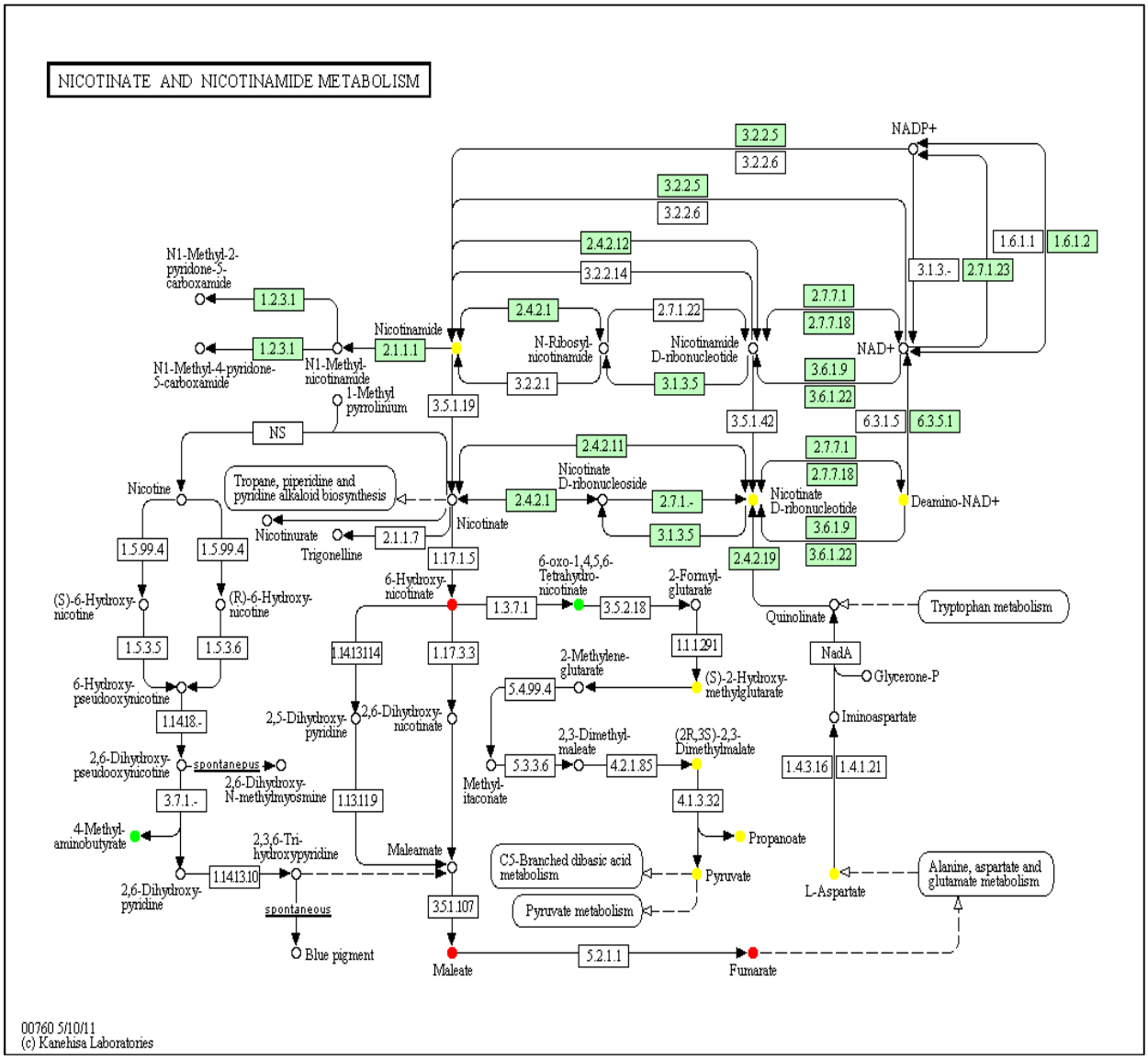


Figure E-33. Further evaluation of the nicotinate and nicotinamide metabolism pathway of the high dose of MP colored by fold change (treatment vs. control) of high quality features identified with putative annotations within the pathway.

Features exhibiting abundance greater than 50% (x > 0.5) of the control are colored red, features between 50% and -50% (0.5 < x > -0.5) are colored yellow and features with an abundance less than 50% (x < -0.5) of the control are colored green. Enzymes or enzymatic activity observed in humans are represented by green colored boxes. Putative metabolites observed in this study are represented with colored circles. Arrows represent direction of enzymatic activity.

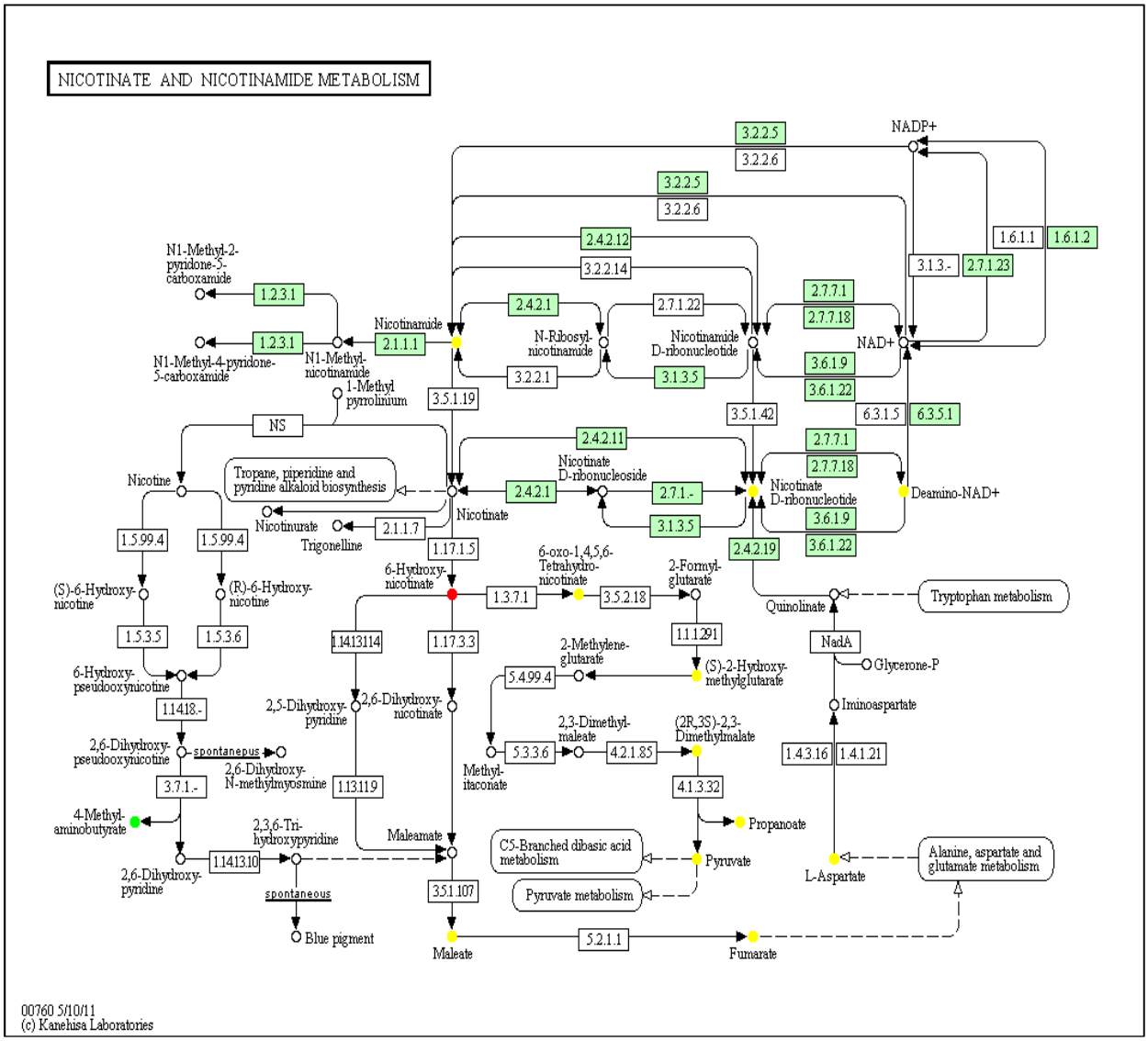


Figure E-34. Further evaluation of the nicotinate and nicotinamide metabolism pathway of the middle dose of MP colored by fold change (treatment vs. control) of high quality features identified with putative annotations within the pathway.

Features exhibiting abundance greater than 50% (x > 0.5) of the control are colored red, features between 50% and -50% (0.5 < x > -0.5) are colored yellow and features with an abundance less than 50% (x < -0.5) of the control are colored green. Enzymes or enzymatic activity observed in humans are represented by green colored boxes. Putative metabolites observed in this study are represented with colored circles. Arrows represent direction of enzymatic activity.

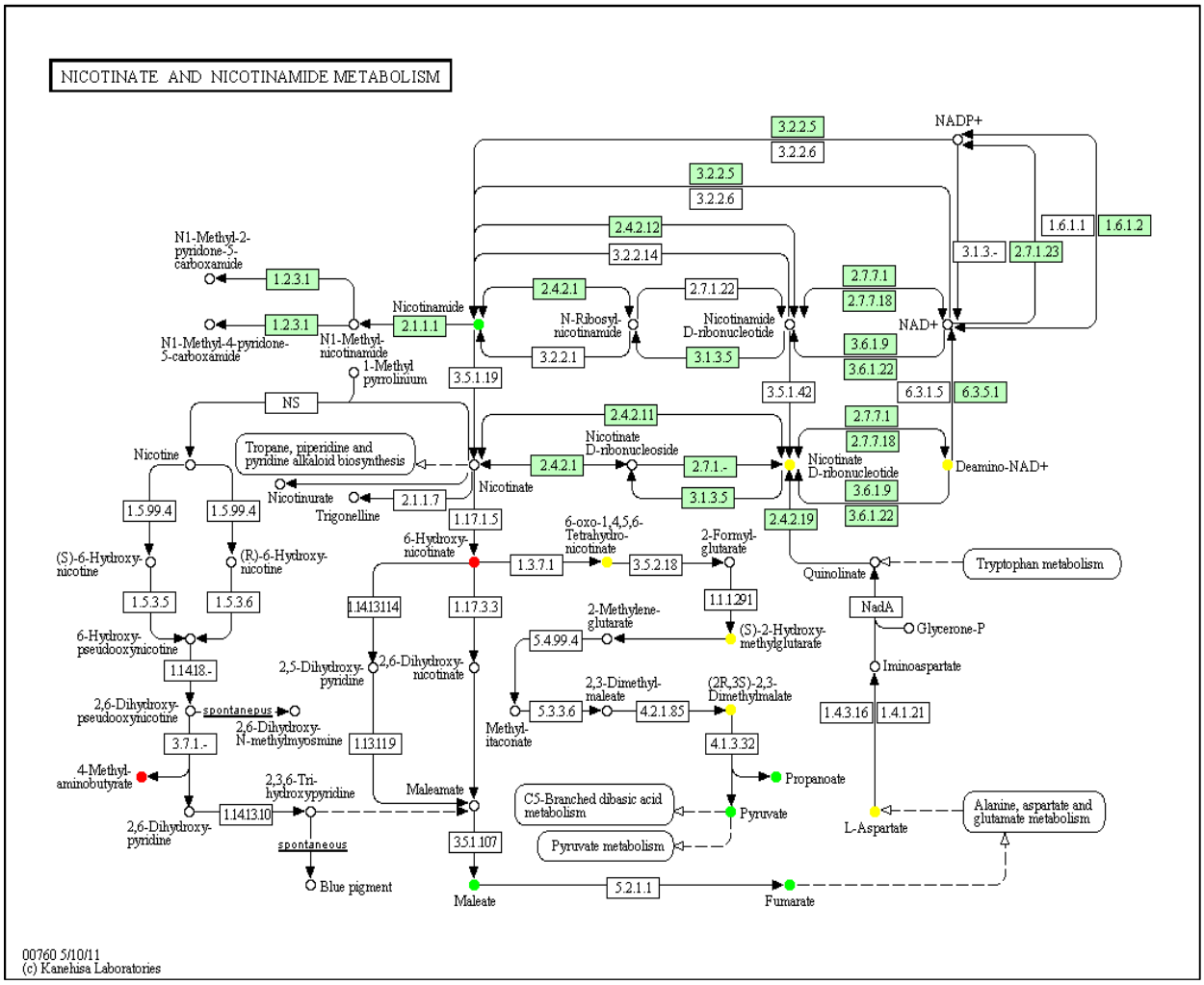


Figure E-35. Further evaluation of the nicotinate and nicotinamide metabolism pathway of the low dose of MP colored by fold change (treatment vs. control) of high quality features identified with putative annotations within the pathway.

Features exhibiting abundance greater than 50% ($x > 0.5$) of the control are colored red, features between 50% and -50% ($0.5 < x > -0.5$) are colored yellow and features with an abundance less than 50% ($x < -0.5$) of the control are colored green. Enzymes or enzymatic activity observed in humans are represented by green colored boxes. Putative metabolites observed in this study are represented with colored circles. Arrows represent direction of enzymatic activity.

**Blank**

APPENDIX F

Enriched Pathways Colored by Dose Level Exhibiting Statistically Significant Fold Change

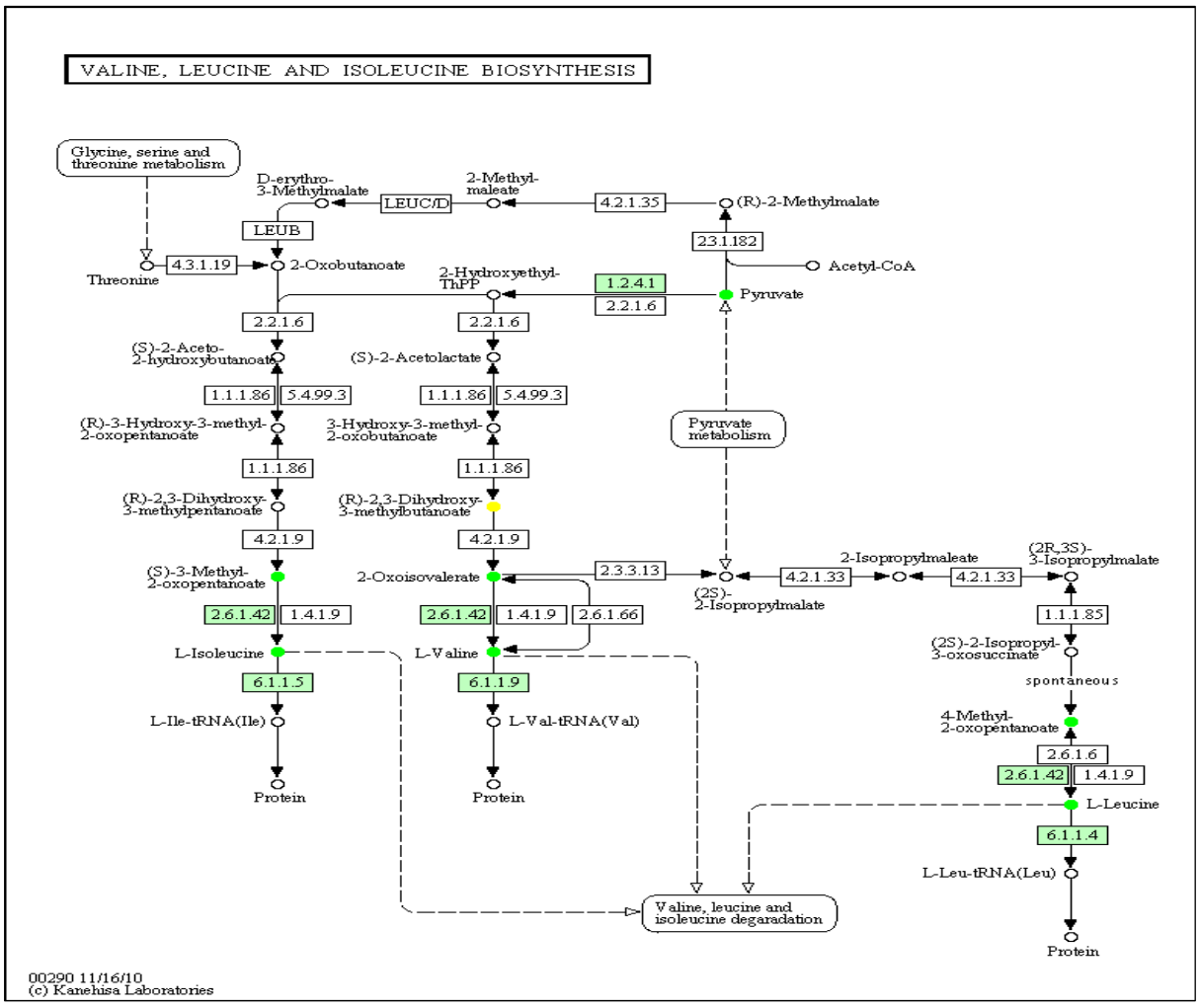


Figure F-1. Kyoto Encyclopedia of Genes and Genomes (KEGG) pathway diagram of the high quality features in the valine, leucine and isoleucine biosynthesis pathway that were putatively annotated with KEGG identifications (ID)s and identified as significant in the pathways enrichment analysis of methyl paraoxon (MPO).

Metabolites within the pathways are colored according to the combination of dose levels where a statistically significant fold change was observed. A feature exhibiting a statistically significant fold change at each dose level is colored black, at the middle and highest dose colored green, at the middle dose only yellow, at the low dose only magenta, and the high dose only light blue. Enzymes or enzymatic activity observed in humans are colored green colored boxes. Putative metabolites observed in this study are represented with colored circles. Arrows represent direction of enzymatic activity.

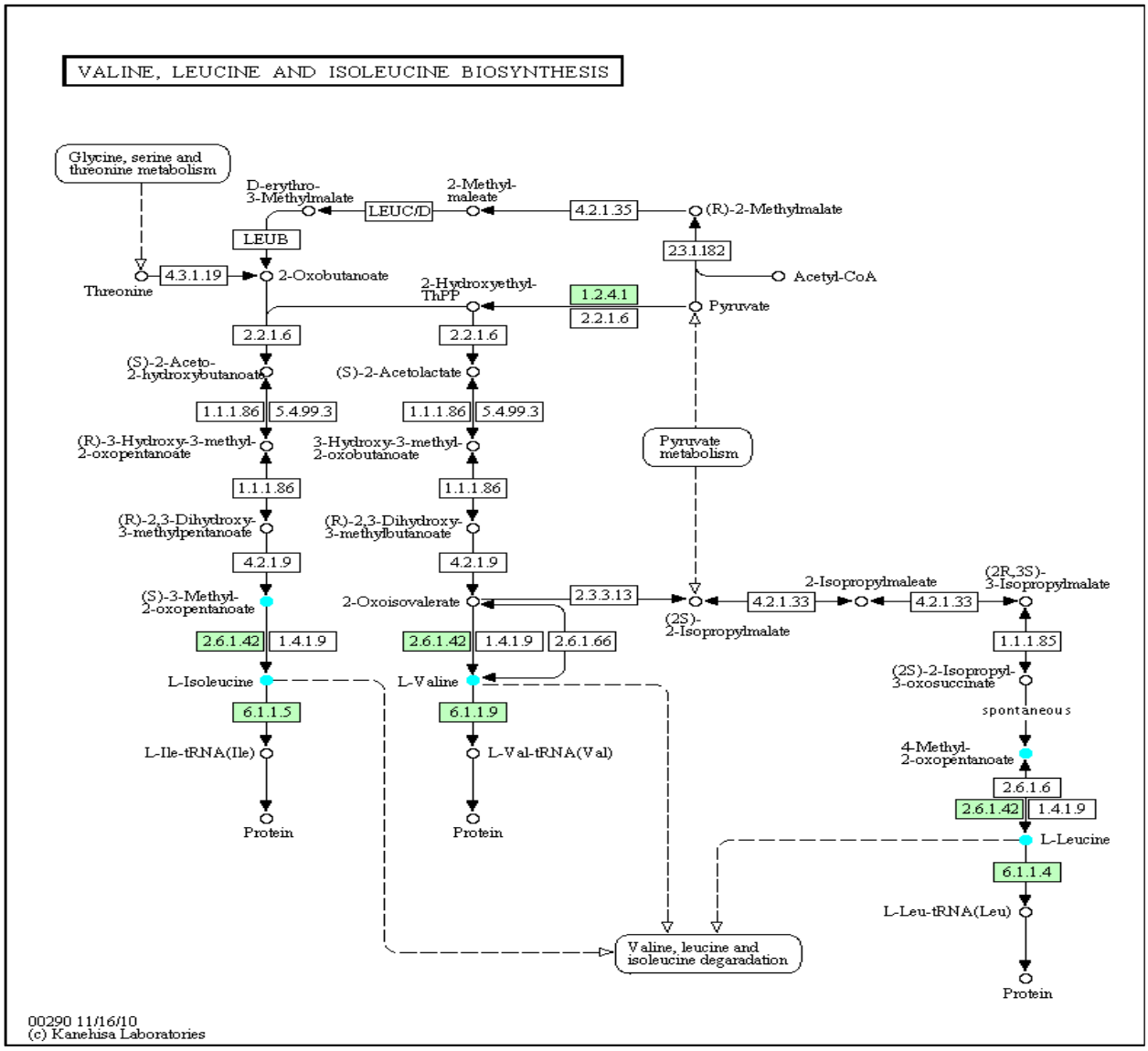


Figure F-2. KEGG pathway diagram of the high quality features in the valine, leucine and isoleucine biosynthesis pathway that were putatively annotated with KEGG ID's and identified as significant in the pathways enrichment analysis of methyl parathion (MP).

Metabolites within the pathways are colored according to the combination of dose levels where a statistically significant fold change was observed. A feature exhibiting a statistically significant fold change at each dose level is colored black, at the middle and highest dose colored green, at the middle dose only yellow, at the low dose only magenta, and the high dose only light blue. Enzymes or enzymatic activity observed in humans are colored green colored boxes. Putative metabolites observed in this study are represented with colored circles. Arrows represent direction of enzymatic activity.

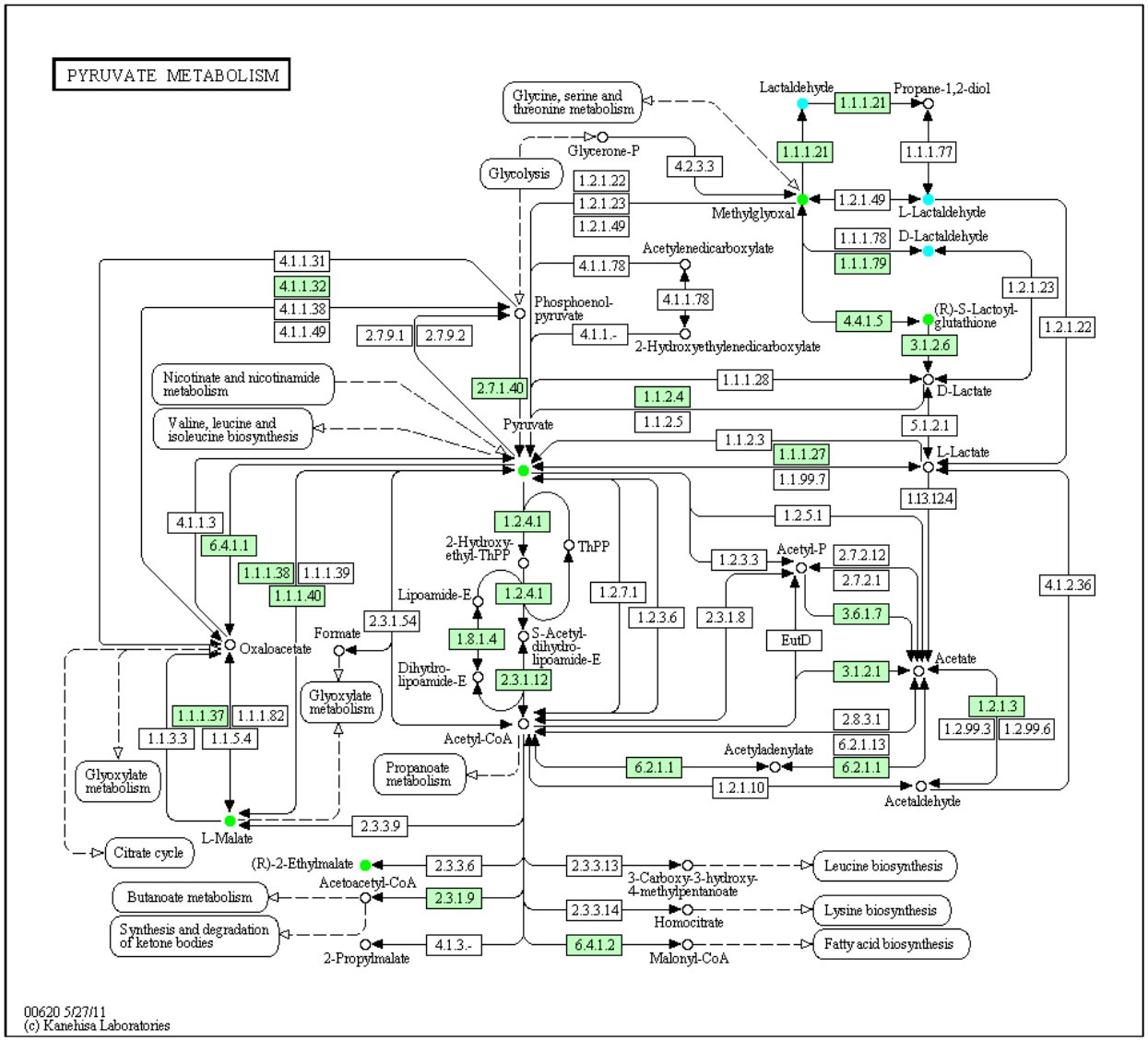


Figure F-3. KEGG pathway diagram of the high quality features in the pyruvate metabolism pathway that were putatively annotated with KEGG ID's and identified as significant in the pathways enrichment analysis of MPO.

Metabolites within the pathways are colored according to the combination of dose levels where a statistically significant fold change was observed. A feature exhibiting a statistically significant fold change at each dose level is colored black, at the middle and highest dose colored green, at the middle dose only yellow, at the low dose only magenta, and the high dose only light blue. Enzymes or enzymatic activity observed in humans are colored green colored boxes. Putative metabolites observed in this study are represented with colored circles. Arrows represent direction of enzymatic activity.

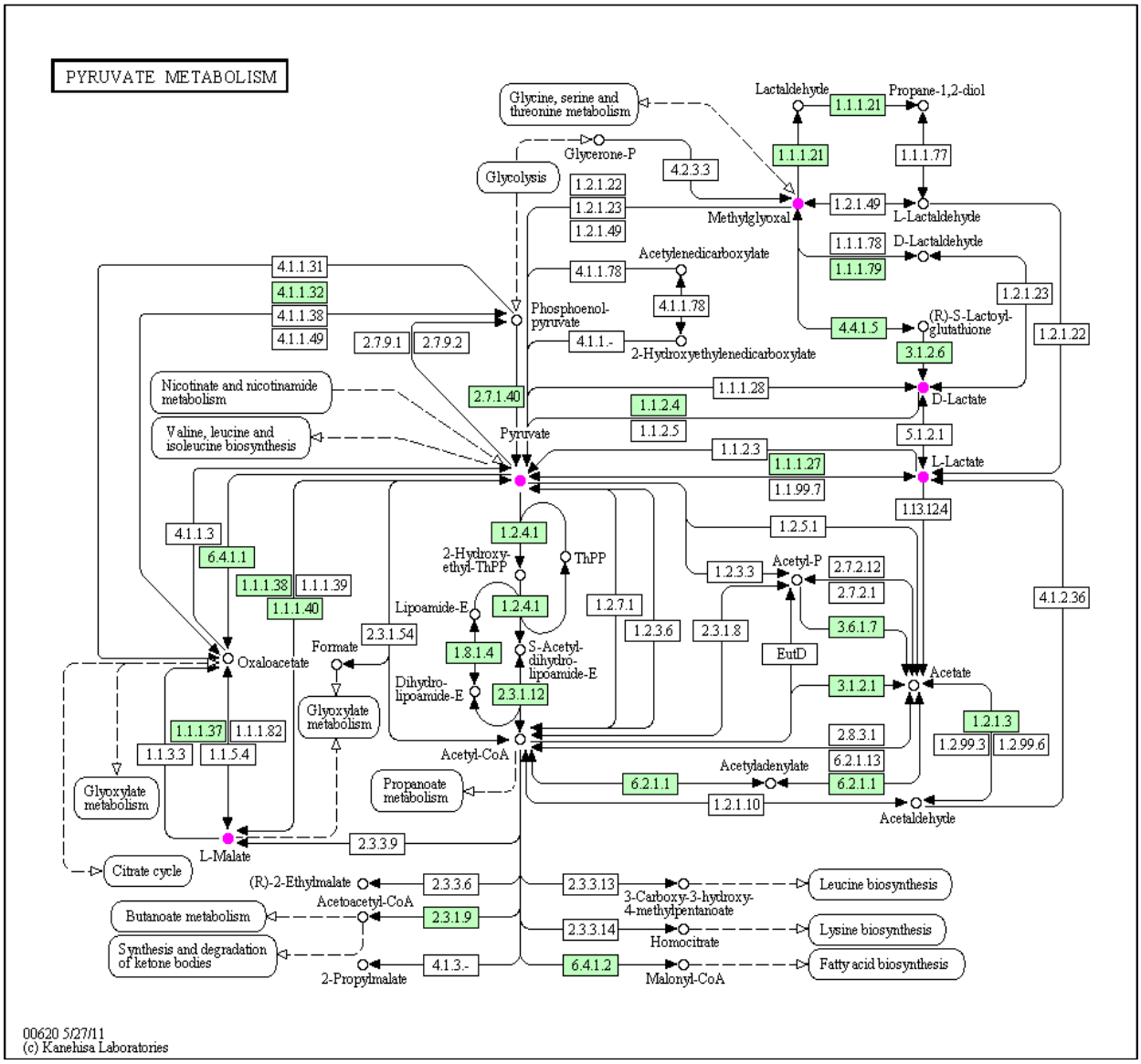


Figure F-4. KEGG pathway diagram of the high quality features in the pyruvate metabolism pathway that were putatively annotated with KEGG ID's and identified as significant in the pathways enrichment analysis of MP.

Metabolites within the pathways are colored according to the combination of dose levels where a statistically significant fold change was observed. A feature exhibiting a statistically significant fold change at each dose level is colored black, at the middle and highest dose colored green, at the middle dose only yellow, at the low dose only magenta, and the high dose only light blue. Enzymes or enzymatic activity observed in humans are colored green colored boxes. Putative metabolites observed in this study are represented with colored circles. Arrows represent direction of enzymatic activity.

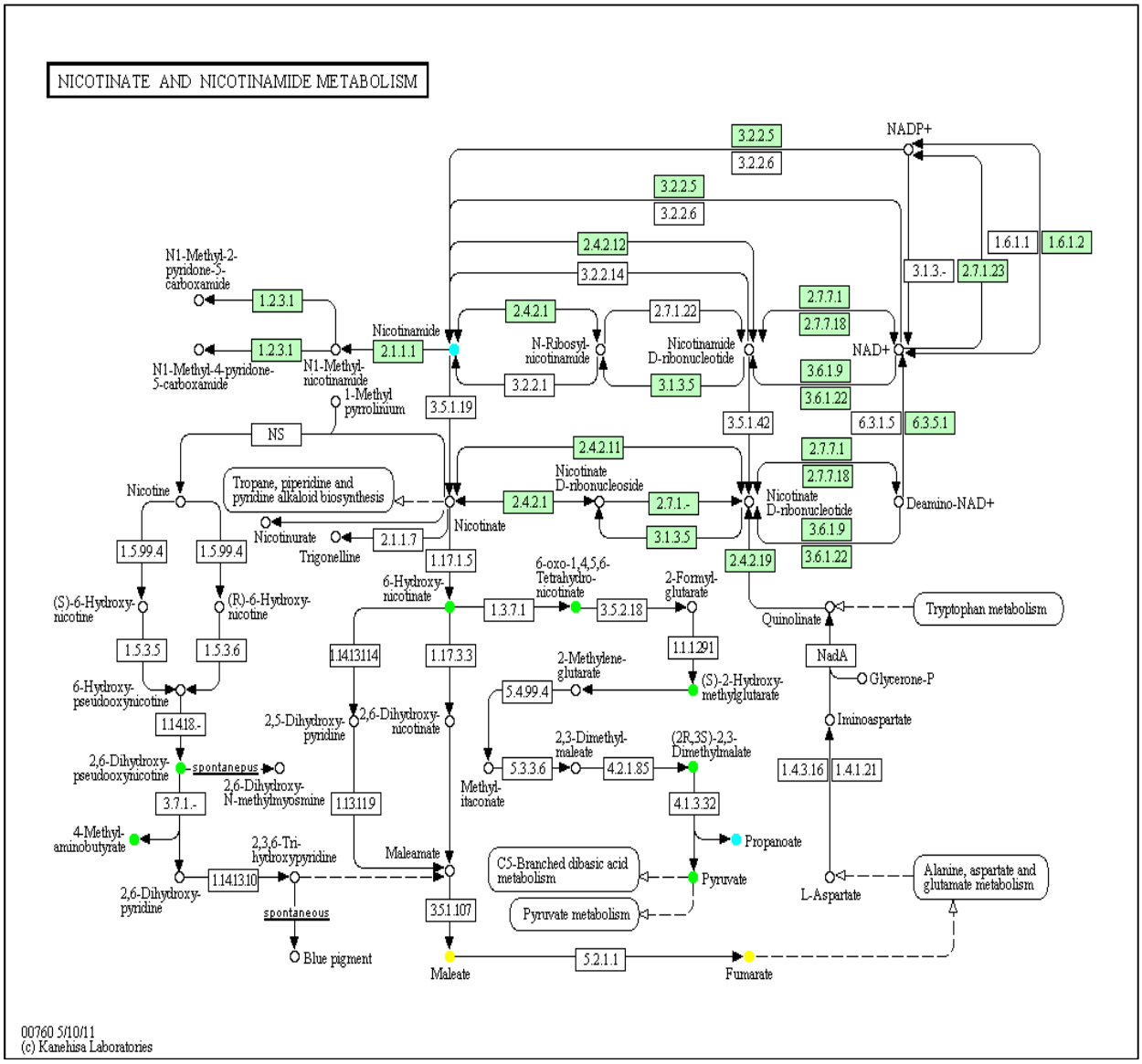


Figure F-5. KEGG pathway diagram of the high quality features in the nicotinate and nicotinamide metabolism pathway that were putatively annotated with KEGG ID's and identified as significant in the pathways enrichment analysis of MPO.

Metabolites within the pathways are colored according to the combination of dose levels where a statistically significant fold change was observed. A feature exhibiting a statistically significant fold change at each dose level is colored black, at the middle and highest dose colored green, at the middle dose only yellow, at the low dose only magenta, and the high dose only light blue. Enzymes or enzymatic activity observed in humans are colored green colored boxes. Putative metabolites observed in this study are represented with colored circles. Arrows represent direction of enzymatic activity.

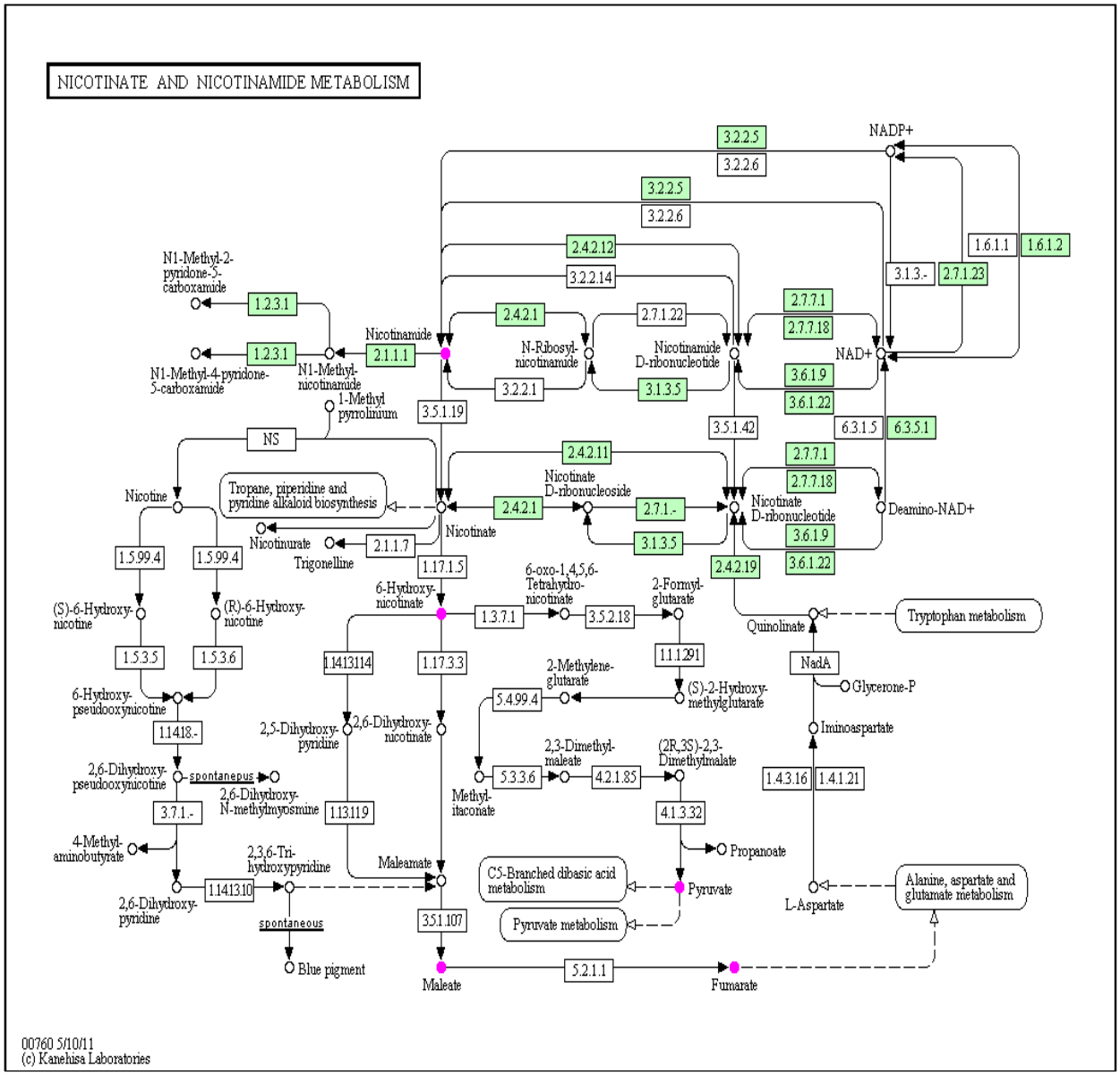


Figure F-6. KEGG pathway diagram of the high quality features in the nicotinate and nicotinamide metabolism pathway that were putatively annotated with KEGG ID's and identified as significant in the pathways enrichment analysis of MP.

Metabolites within the pathways are colored according to the combination of dose levels where a statistically significant fold change was observed. A feature exhibiting a statistically significant fold change at each dose level is colored black, at the middle and highest dose colored green, at the middle dose only yellow, at the low dose only magenta, and the high dose only light blue. Enzymes or enzymatic activity observed in humans are colored green colored boxes. Putative metabolites observed in this study are represented with colored circles. Arrows represent direction of enzymatic activity.

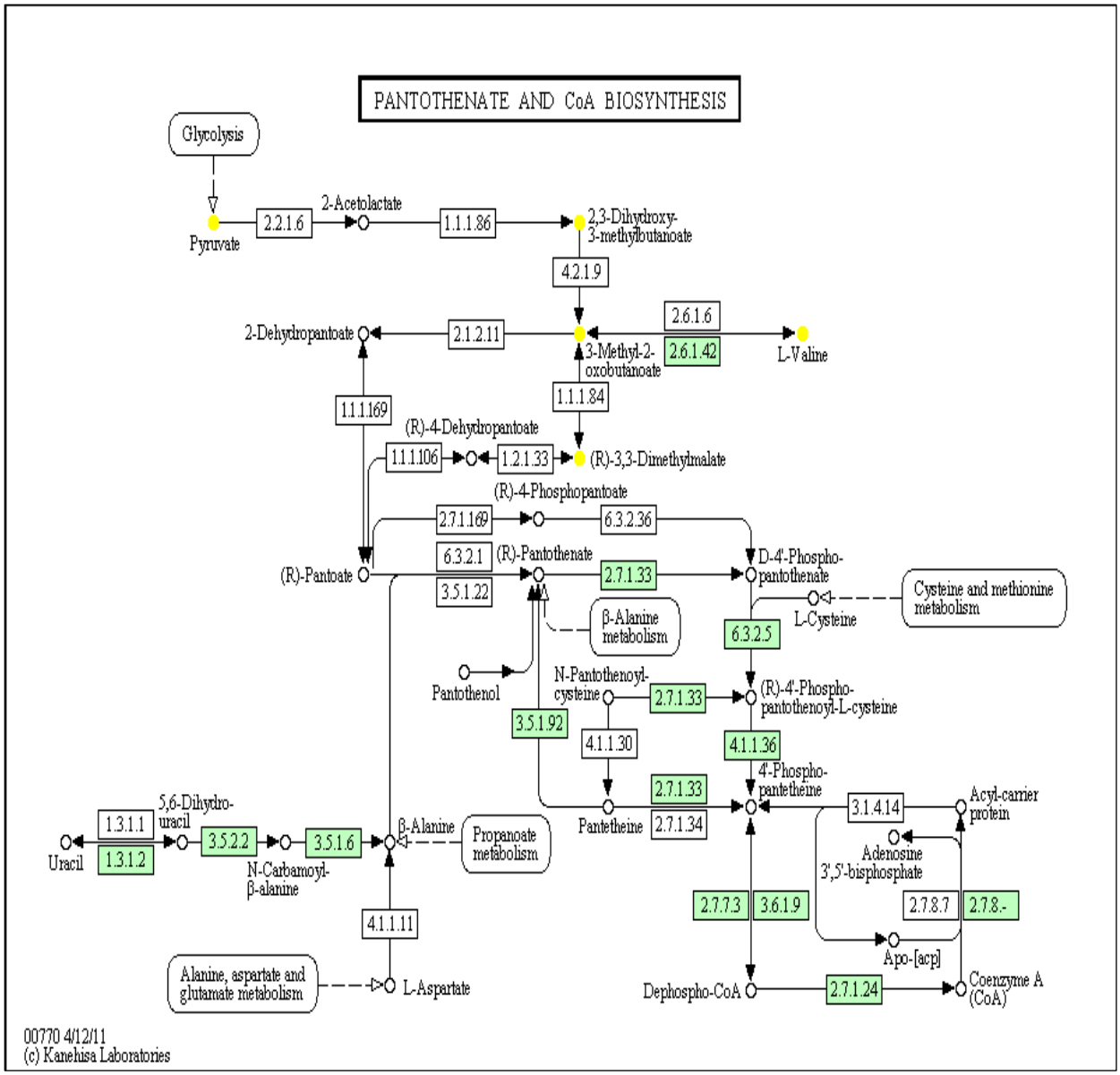


Figure F-7. KEGG pathway diagram of the high quality features in the pantothenate and coenzyme A (CoA) biosynthesis pathway that were putatively annotated with KEGG ID's and identified as significant in the pathways enrichment analysis of MPO.

Metabolites within the pathways are colored according to the combination of dose levels where a statistically significant fold change was observed. A feature exhibiting a statistically significant fold change at each dose level is colored black, at the middle and highest dose colored green, at the middle dose only yellow, at the low dose only magenta, and the high dose only light blue. Enzymes or enzymatic activity observed in humans are colored green colored boxes. Putative metabolites observed in this study are represented with colored circles. Arrows represent direction of enzymatic activity.

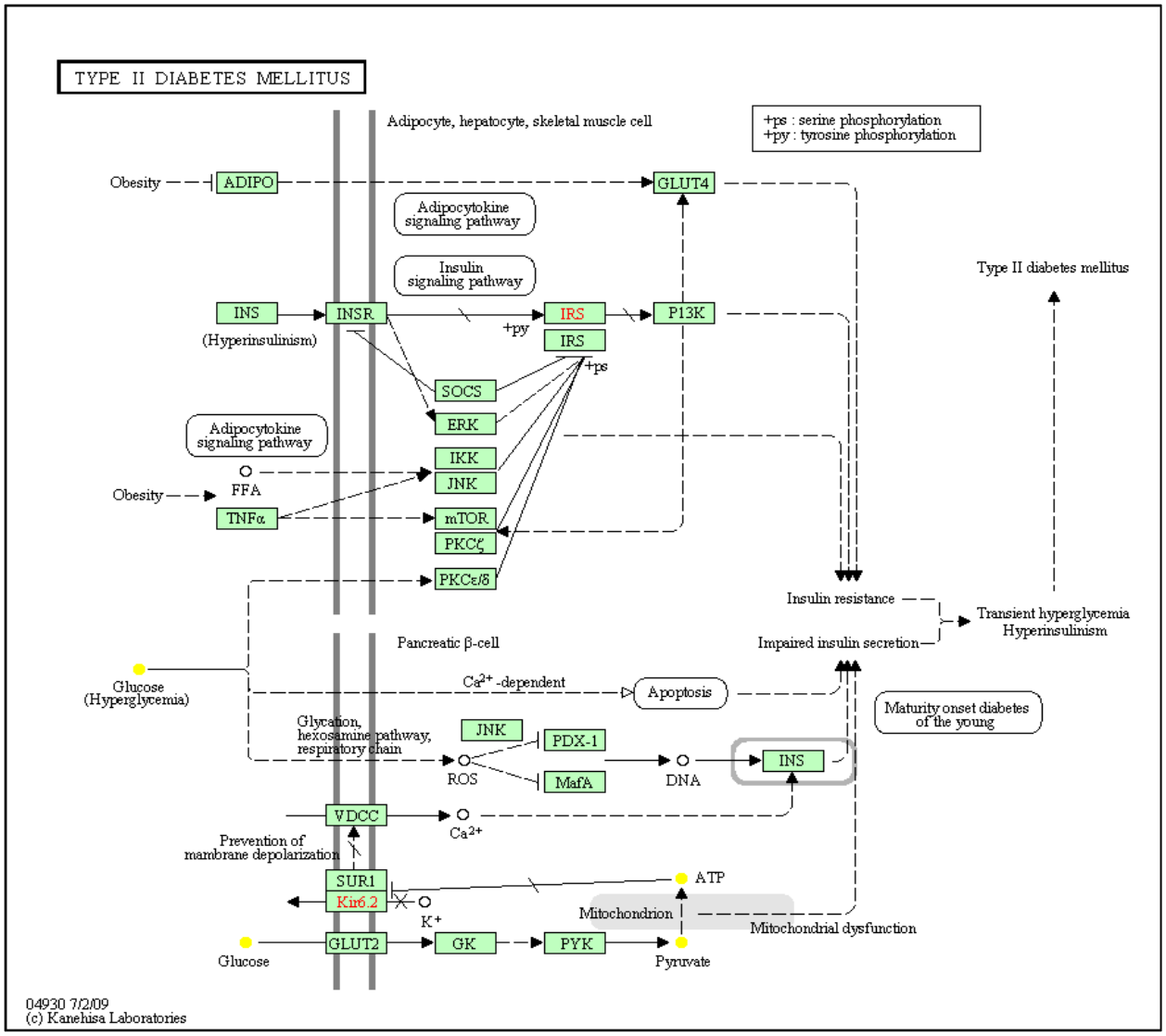


Figure F-8. KEGG pathway diagram of the high quality features in the Type II diabetes mellitus pathway that were putatively annotated with KEGG ID's and identified as significant in the pathways enrichment analysis of MPO.

Metabolites within the pathways are colored according to the combination of dose levels where a statistically significant fold change was observed. A feature exhibiting a statistically significant fold change at each dose level is colored black, at the middle and highest dose colored green, at the middle dose only yellow, at the low dose only magenta, and the high dose only light blue. Enzymes or enzymatic activity observed in humans are colored green colored boxes. Putative metabolites observed in this study are represented with colored circles. Arrows represent direction of enzymatic activity.

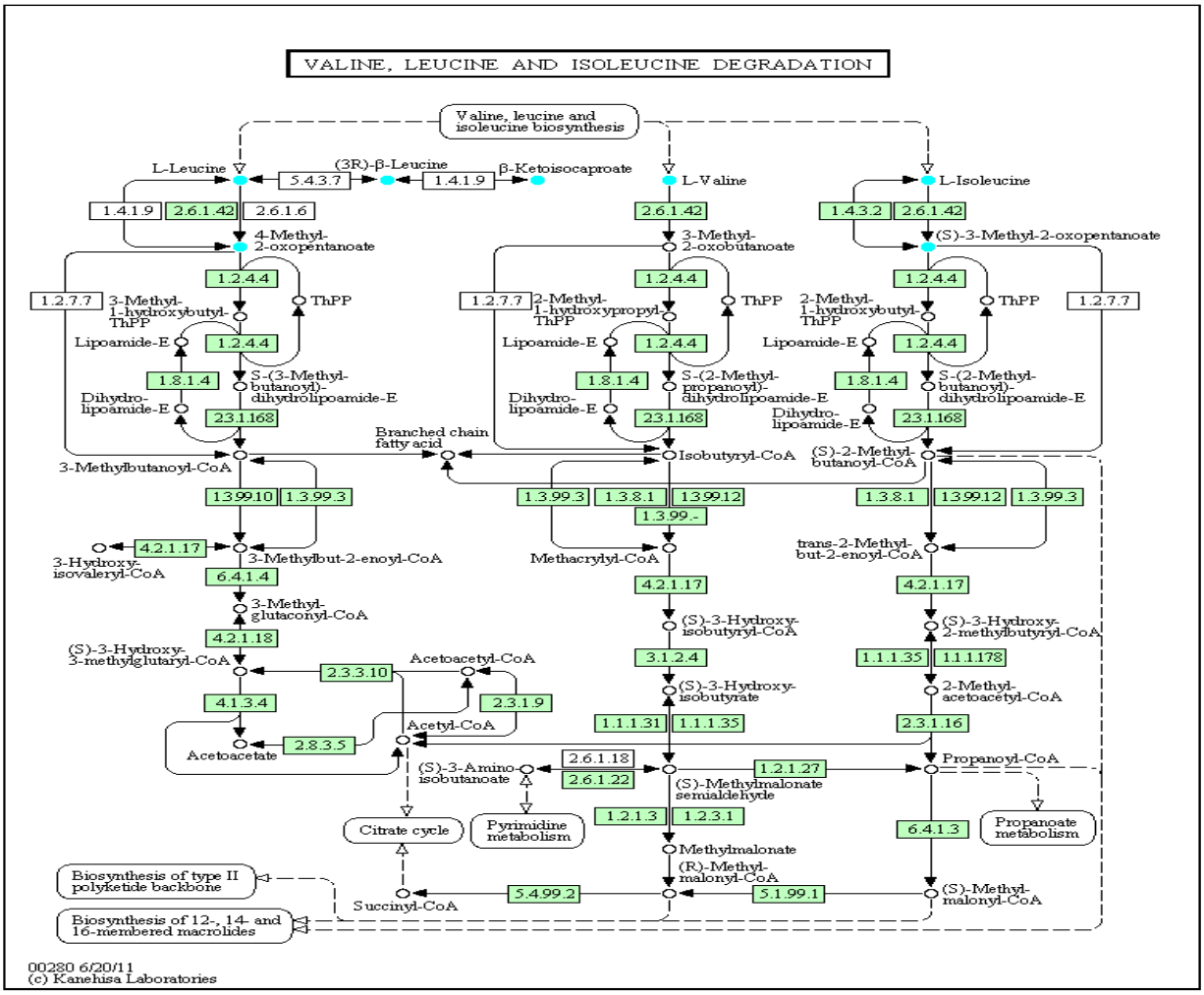


Figure F-9. KEGG pathway diagram of the high quality features in the valine, leucine and isoleucine degredation pathway that were putatively annotated with KEGG ID's and identified as significant in the pathways enrichment analysis of MP.

Metabolites within the pathways are colored according to the combination of dose levels where a statistically significant fold change was observed. A feature exhibiting a statistically significant fold change at each dose level is colored black, at the middle and highest dose colored green, at the middle dose only yellow, at the low dose only magenta, and the high dose only light blue. Enzymes or enzymatic activity observed in humans are colored green colored boxes. Putative metabolites observed in this study are represented with colored circles. Arrows represent direction of enzymatic activity.

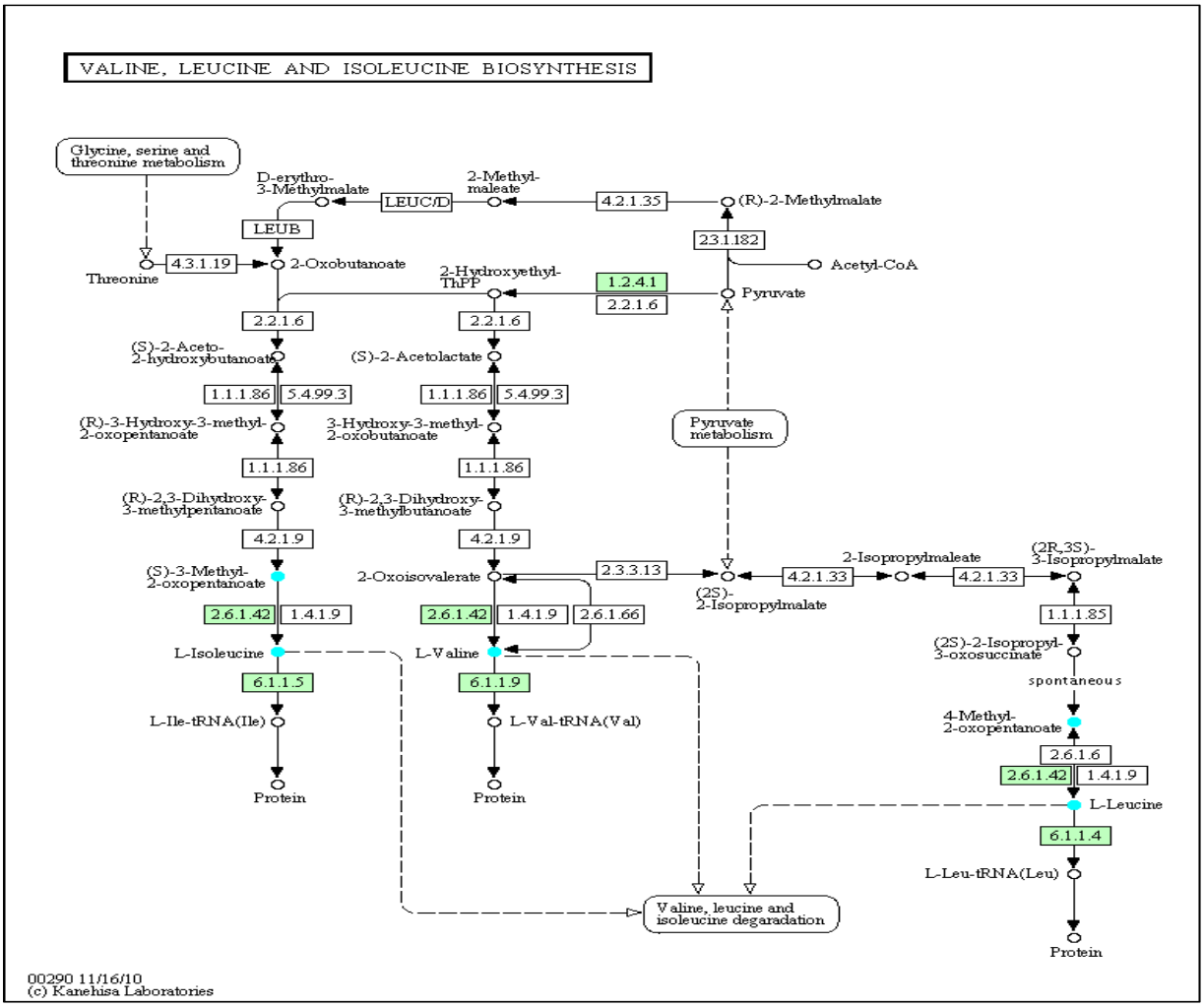


Figure F-10. KEGG pathway diagram of the high quality features in the valine, leucine and isoleucine biosynthesis pathway that were putatively annotated with KEGG ID's andand identified as significant in the pathways enrichment analysis of MP.

Metabolites within the pathways are colored according to the combination of dose levels where a statistically significant fold change was observed. A feature exhibiting a statistically significant fold change at each dose level is colored black, at the middle and highest dose colored green, at the middle dose only yellow, at the low dose only magenta, and the high dose only light blue. Enzymes or enzymatic activity observed in humans are colored green colored boxes. Putative metabolites observed in this study are represented with colored circles. Arrows represent direction of enzymatic activity.

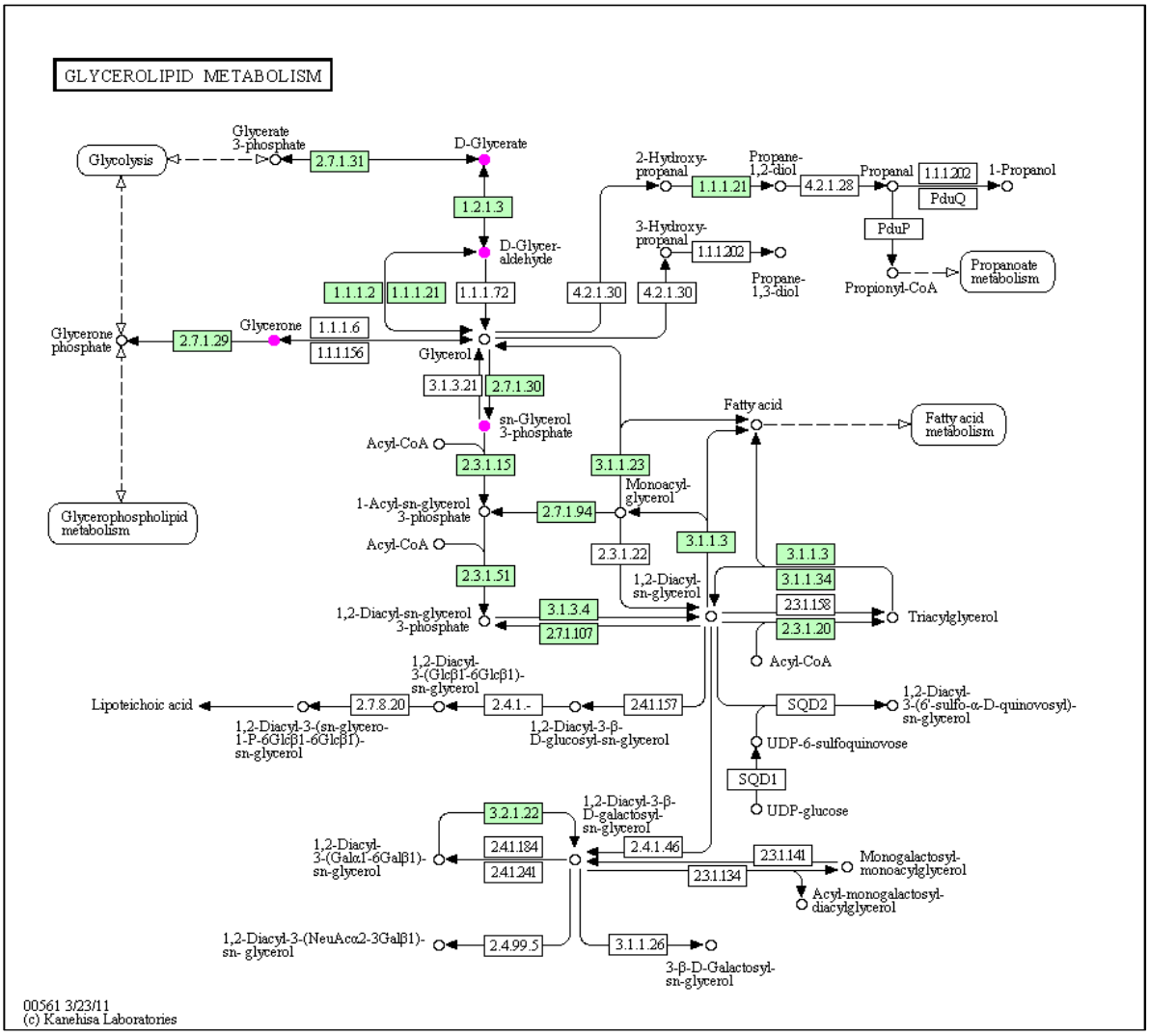


Figure F-11. KEGG pathway diagram of the high quality features in the glycerolipid metabolism pathway that were putatively annotated with KEGG ID's and identified as significant in the pathways enrichment analysis of MP.

Metabolites within the pathways are colored according to the combination of dose levels where a statistically significant fold change was observed. A feature exhibiting a statistically significant fold change at each dose level is colored black, at the middle and highest dose colored green, at the middle dose only yellow, at the low dose only magenta, and the high dose only light blue. Enzymes or enzymatic activity observed in humans are colored green colored boxes. Putative metabolites observed in this study are represented with colored circles. Arrows represent direction of enzymatic activity.

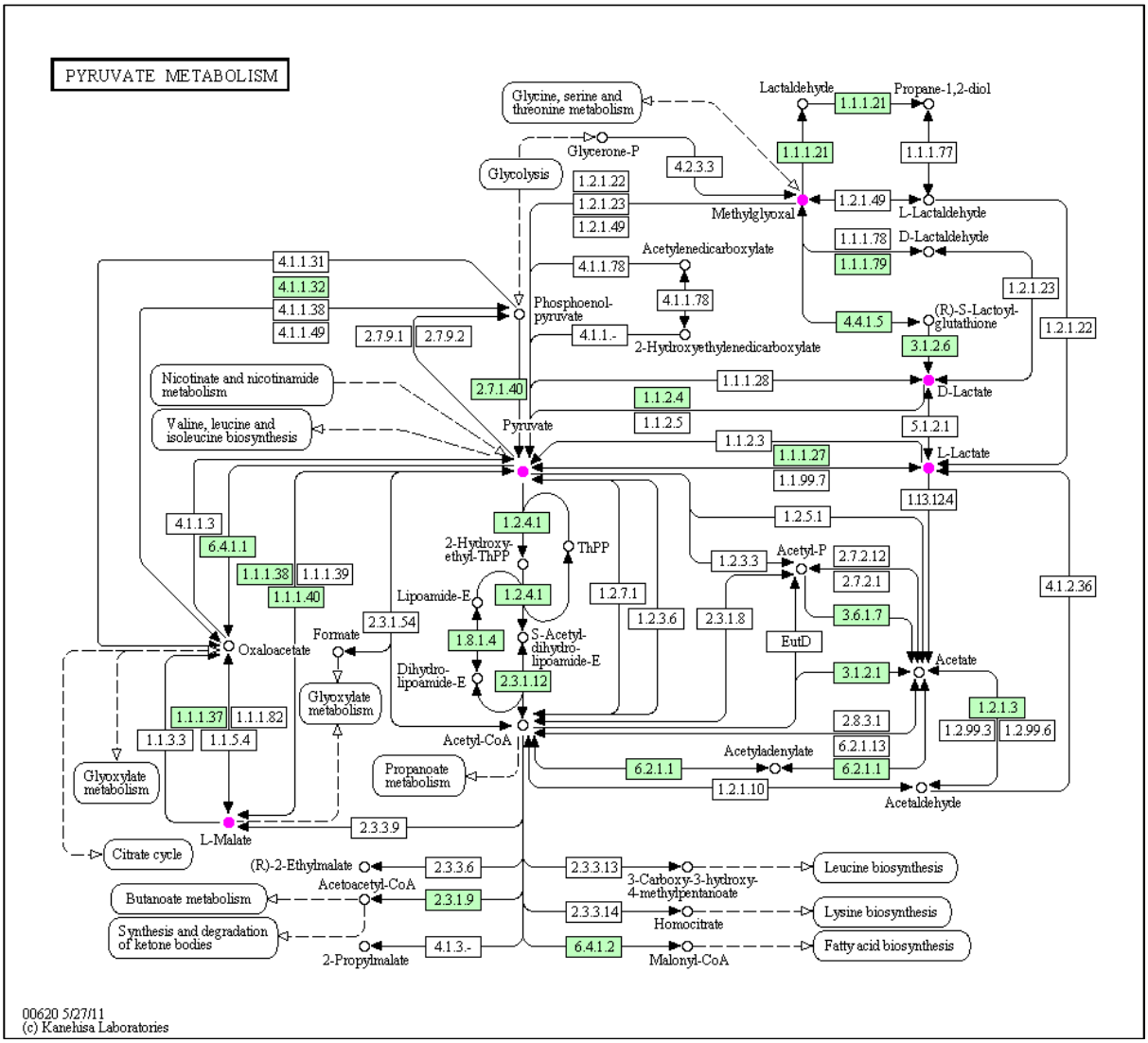


Figure F-12. KEGG pathway diagram of the high quality features in the pyruvate metabolism pathway that were putatively annotated with KEGG ID's and identified as significant in the pathways enrichment analysis of MP.

Metabolites within the pathways are colored according to the combination of dose levels where a statistically significant fold change was observed. A feature exhibiting a statistically significant fold change at each dose level is colored black, at the middle and highest dose colored green, at the middle dose only yellow, at the low dose only magenta, and the high dose only light blue. Enzymes or enzymatic activity observed in humans are colored green colored boxes. Putative metabolites observed in this study are represented with colored circles. Arrows represent direction of enzymatic activity.


EDGEWOOD CHEMICAL BIOLOGICAL CENTER
A U.S. Army RDECOM Laboratory